# Limitations on Gain in Rare-Earth Doped Fiber Amplifiers due to Amplified Spontaneous Emission

Andrew Miskowiec and Thomas Max Roberts

Advisor: Prof. Richard S. Quimby

May 1, 2009

# 1 Abstract

The purpose of this project was to develop a numerical model in MATLAB of the limitation on signal gain in ytterbium and neodymium doped fiber amplifiers due to amplified spontaneous emission (ASE). It was shown that significant signal gain was achievable in ytterbium devices near 1023 nm despite the ASE limitation. Furthermore, without the inclusion of diffraction gratings to limit ASE near 1060 nm, it was shown to be impossible to obtain significant gain in the 1400 nm range for neodymium doped devices. Other possible signal wavelengths for these dopants were also investigated. Validity of the Equivalent Bandwidth approximation method was also examined, proving to be sufficient in several applications, but in some cases generally misrepresenting the spectra significantly.

# Contents

# 2 Introduction

Fiber optic amplifiers are devices which take an incoming signal and directly increase the power of that signal, while preserving the information therein. The uses of such an amplifier are extensive. In fiber optic cable, a signal is transmitted by the propagation of certain modes of light. Over long distances this signal can be significantly weakened due to a number of attenuating factors such as absorption, scattering, or bending losses. [1] The signal needs to be restored in a manner that keeps its structure identical, such that after being transmitted, the receiver observes the intended signal shape. This could be done by decoupling the light from the fiber, converting it into a digital format, and recoupling it back into a fiber at a stronger power. This is a slow and costly method, as it requires an external apparatus to be place directly into the system. A more efficient method is to implement an inline fiber amplifier and amplify the signal as it is traveling. This allows for faster transmission and lower expenses.[2] In some circumstances, a laser which doesn't produce a very powerful signal can be implemented as a "seed" laser, providing an initial signal waveform . By having this initial waveform go immediately into an amplifier, the power of the signal can be boosted to more usable levels.

The optical properties of triply ionized rare-earth atoms can provide the necessary optical characteristics to achieve signal amplification. We are particularly interested in neodymium and ytterbium doped fiber amplifiers. The host glass of these fibers can be pure silica or fluoride, but sometimes using mixed glasses can prove to yield certain desirable features. Shifts can occur in spectra that allow for more amplification at some wavelengths and less at others. [3] This will prove to be useful later.

Our main focus is for telecommunication purposes; therefore our wavelength range of interest is in the visible red to infrared. The two dopants we are considering (ytterbium and neodymium), each have particular ranges where amplification can occur. These ranges coin-

cide with the wavelengths frequently used in modern telecommunications devices; therefore, Nd and Yb doping can provide a means of amplifying signals at these wavelengths.

There are several problems with using doped fiber optics cable as a method of signal amplification that must be addressed. A naturally occurring process of an excited ion is the random emission of energy, which involves the release of a photon, known as spontaneous emission. If a spontaneous photon is emitted in a direction with a sufficiently small angle with respect to the direction of the fiber axis, it can be trapped within the fiber by total internal reflection. Once trapped within the fiber, the photon can, through stimulated emission with other excited ions, become amplified. This process, known as Amplified Spontaneous Emission (ASE), decreases the potential of the amplifier to boost the actual signal. Because the ASE becomes amplified by stimulated emission, the ions in the excited state that are added to the ASE light cannot be added to the signal. In many situations, ASE can be a limiting factor on the effectiveness of a fiber amplifier. We will determine under which circumstances ASE is a significant factor as a limitation on signal gain and explore methods for reducing ASE.

From the physical principles involved and basic fiber parameters, we design a numerical model which simulates actual fiber amplifier behavior under varied conditions. With this model, we can experiment by modifying conditions in the amplifier and even the actual parameters of the fiber itself. In doing so, we gain a better understanding of the complexities and limitations of the amplifier.

# 3 Fundamental Physical Principles Involved in Fiber Optics

## 3.1 Total Internal Reflection

Fiber-optic communication is made possible by the phenomenon of total internal reflection. TIR occurs when a beam of light is incident on a transparent surface at an angle greater than the critical angle, which is defined by Snell's law for the condition that the reflected angle is 90 degrees:

$$\theta_c = \arcsin(\frac{n_2}{n_1}) \text{ (Snell's Law for TIR)} \tag{1}$$

where $n_2$ and $n_1$ are the indices of the cladding and core glass respectively. The relative indices of the core and cladding glass are also important for the coupling of light into the fiber. A greater difference in index will allow a greater fraction of light to be trapped within the fiber when coupling the initial signal.

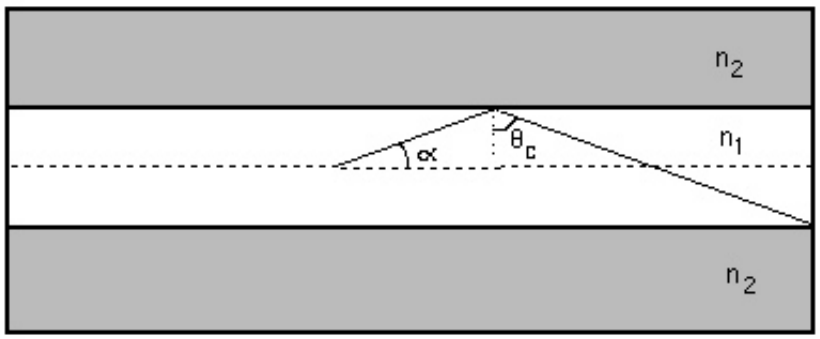


Figure 1: Total Internal Reflection in a fiber

## 3.2 Fiber Parameters

In practical use of fiber amplifiers, many different methods of pumping and fiber geometry can be used. A common method that is frequently used is cladding pumping. In this technique, the fiber core is surrounded by an additional layer of glass with similar index of refraction. This layer is called the inner cladding. Surrounding the inner cladding is a third layer, the outer cladding. The difference in index between the outer and inner cladding is generally much larger than the difference in index between the inner cladding and the core. A diagram of this configuration is show in Figure 2

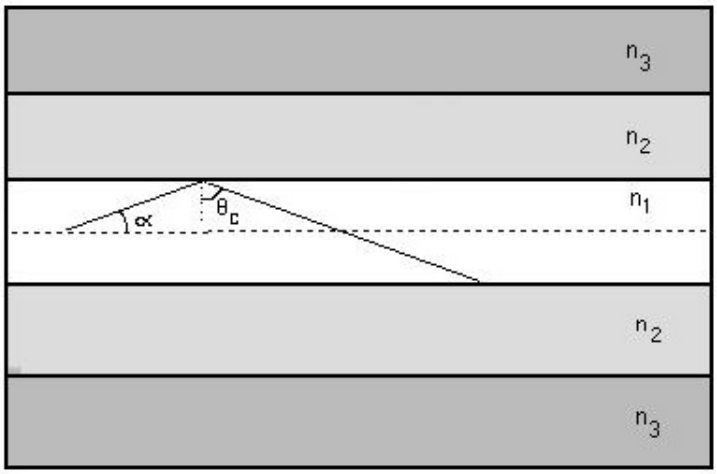


Figure 2: Double Cladding Fiber

A major advantage of cladding pumping is that the greater difference in index between the inner and outer cladding allows a greater amount of light to be trapped within the fiber. This allows more powerful lasers devices to be used as light sources than in the case of normal core pumping.

Also, a wide variety of core and cladding radii may be used. Commercially available fibers can also be purchased with a large spread in numerical aperture, which relates the acceptance angle to the indices of refraction of the core and cladding glass. In our model, we maintain constant values for fiber core and cladding radii: 3.4 $\mu$m for the core radius and

43 $\mu$m for the cladding radius. The core index in this configuration is 1.5, with a numerical aperture of 0.15. We will also make use of the cladding pumping method described above. Because of this, we must define a second numerical aperture at the inner and outer cladding boundaries. In our case, this value will be 0.53.

Fiber designers can also choose the method of pumping. Pump lasers can be used as either a "continuous wave" (cw) or in "pulsed" (Q-switched) mode. [1] The pulsed mode provides a time-dependent output power, whereas the continuous wave method provides constant, time-independent light. In our model, we have chosen the approximation of time-independent conditions throughout. Therefore, our pump beams will be modeled by the cw method instead of the Q-switched mode.

## 3.3 Multiplets and Energy Levels

Every atom, whether it is a rare-earth element or not, can be excited by a photon to a higher energy level. The process through which this occurs is known as photon absorption. The exact physical mechanism responsible for this will be discussed in the next section. Here, we will explain the different energy levels and multiplets in which electrons can reside within an atomic energy well. An electron in its ground state is in its lowest possible energy and orbits closely to the host nucleus. An incoming photon can excite this electron to a higher energy level. The energy levels available to electrons are discretized, however, so only photons of specific energies can be absorbed. If a photon has enough energy, it can eject the electron completely from the electromagnetic potential created by the protons in the nucleus. This process is called ionization, and the photon energies required for this process are generally on the order of 10 electron-Volts. For instance, in neutral hydrogen, the energy required to ionize the atom is 13.6 eV. The wavelength of a photon of this energy is around 22 nm. The wavelengths we are interested in are between 700 and 1400 nm, well beyond this range.

If the electron becomes excited by a photon with an energy less than the ionization energy,

it will reside in a higher level than the ground state. This is what is meant by energy levels of an atom. Each electron also possesses an innate spin and angular momentum. These, too, are discretized. The electron can have a ranges of values of angular momentum. The energy an electron has by virtue of its angular momentum is subtracted from the potential caused by the protons in the nucleus. The energy of angular momentum is typically much smaller than the spacing between energy levels. This effectively causes a splitting of the energy levels: the electron can reside in any one of these separated levels. Also, for each energy level, there are many sublevels that are available. When an atom is in a lattice, the interactions between the atom and its neighbors can create additional sublevels, known as Stark levels. This means that photons of energy that are not exactly equal to the energy gap can be absorbed as well. Because of all these factors, there are actually a large number of energy levels available to an electron in an excited state. These sublevels comprise what is known as a multiplet.

We have seen that electrons in an atom can be in any one of a large number of energy levels. When a photon is incident on an electron in an atom, its energy determines whether it can be absorbed or not. If we plot the probability of photon absorption versus incident photon energy, we can see sharp peaks at the wavelengths corresponding to the energy differences between levels that are available to the electron. Because of the splitting of energy levels due to electronic angular momentum, spin, and lattice interactions, these peaks will not be at a single wavelength; instead, the peaks will be spread over a range of similar wavelengths. The probability of photon absorption just mentioned is proportional to what is called the cross section for absorption. We will see how the cross sections of the two elements we are interested in, ytterbium and neodymium, can allow for signal amplification.

## 3.4 Radiative Processes

As mentioned before, fiber amplifiers can be used to increase the strength of an incident signal. Understanding how this occurs requires some knowledge of atomic physics. When an electron in an atom becomes excited, it is promoted to a higher orbital. This excitation occurs in the case of fiber amplifiers through the absorption of a photon. The excited state has a finite lifetime which, depending on the state, can range from picoseconds to seconds for exotic, fluorescent material. The excited state lifetime represents the average time required for an excited electron to transition back to a lower energy level in one of several radiative and nonradiative processes. For an atom in free-space, the only possible decay method is through spontaneous emission of a photon of energy equal to the difference in the energy of the electronic orbitals. When the atom is in a lattice, the transition can also occur non-radiatively in the form of a phonon, or lattice vibrations. As this process relates to our model, the radiative lifetime for the upper level of ytterbium is 720 ms. In neodymium, this value is 309 $\mu$s

For the purpose of fiber amplifiers, neither of these transitions are desirable. A third and more dynamic transition known as stimulated emission is responsible for photon amplification. In this process an incoming photon interacts with an already excited atom. The electric field of the incoming photon oscillates the atom, inciting it to emit a photon of equal frequency and direction as that of the incident photon. One could imagine how this process after many occurrences could take a low intensity signal and amplify it significantly. This process, although the source of amplification for the signal, also creates one of the limiting factors in overall possible amplification. While there is a chance that an excited ion will encounter a signal photon, it is also possible that a pump or ASE photon will encounter the ion. Because of this, the ASE can grow in a manner identical to the signal. An immediate result is that an ion that may have potentially been used to amplify the signal has been removed from the excited state; however, this phenomenon has deeper reaching consequences

as we will see later.

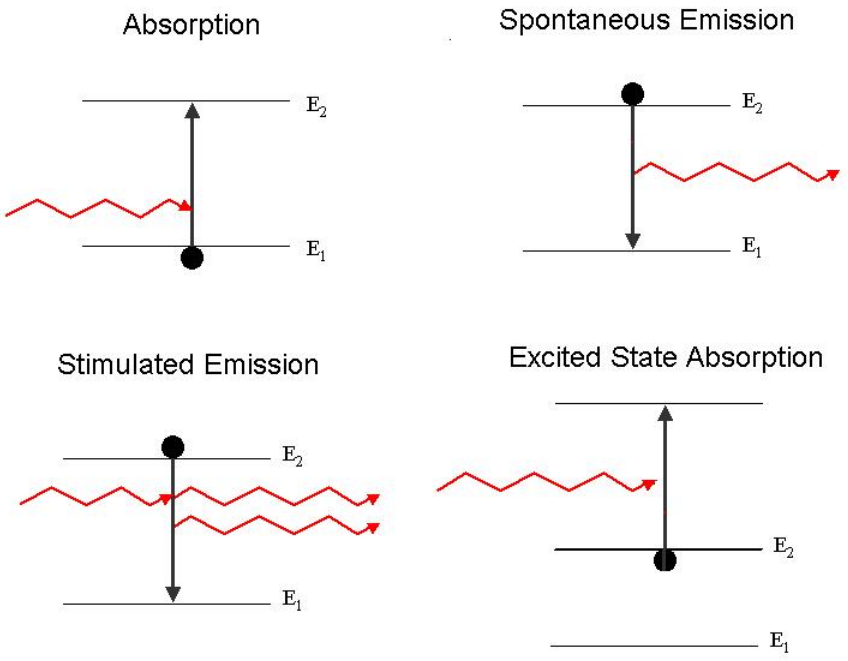


Figure 3: Radiative Processes

The excitations we have just discussed occur through the process of photon absorption. In this process, an electron in one of the outer shells absorbs a photon and is excited to a higher energy level. The likelihood of a transition at a particular energy is given by the cross section. The cross sections are different depending on the dopant and host material and will be discussed at greater length later. In the wavelength range we are considering for telecommunication (700-1500 nm), there are several significant transitions of the ions we will be looking at. First, neodymium has three main emission transitions at around 900 nm, 1060 nm and 1300 nm. These all start from the ${}^4F_{3/2}$ state down and emit to the ${}^4I_{9/2}$, ${}^4I_{11/2}$ and ${}^4I_{13/2}$ respectively. In ytterbium, the there exists only one transition in this range, from the ${}^2F_{7/2}$ to the ${}^2F_{5/2}$. [2] These transitions are shown in Figure 4.

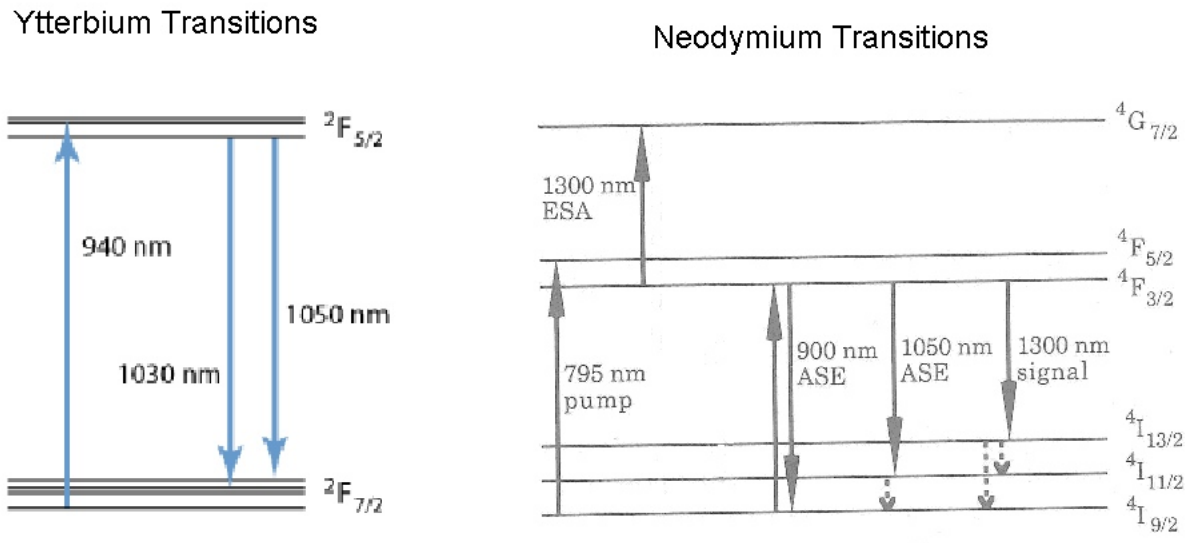


Figure 4: Nd and Yb transition

## 3.5 Gain in Optical Amplifiers

In order to keep the ions of an optical amplifier in the excited state, somehow energy must be put into the system. This is generally done through pumping the fiber with a light source independent from the signal. This pump light has a wavelength which corresponds to a transition of energy larger than that of the signal. Therefore the ions have enough energy in their excited electrons to undergo stimulated emission when they interact with the signal photons. Another condition on the pump light is that the cross section for absorption must be relatively large such that a significant proportion will be absorbed by the dopant ions, while it is desirable for the emission cross section to be small to prevent reemission back into the pump beam. With these conditions in mind, we chose a pump wavelength based on the absorption cross section. Obviously, this wavelength must lie in the lower portion of our range of interest as it must have larger energy than the signal (in exotic cases such as up-conversion, pump light can be at a lower energy than signal light). Pumping of light into

a fiber is usually done from one end. As the light can be rapidly absorbed, in some cases pumping from both ends is an implemented option.

In order for there to be continuous gain in a fiber even where there is substantial emission, the upper-state must be maintained at a certain population compared with that of the lower state. The pump beam excites ions to the upper state, where the signal photons can interact with these ions and elicit them to release a photon via stimulated emission. This is how the signal beam becomes amplified. As we shall see, it is also possible for the spontaneously emitted photons to become amplified in this manner, resulting in the phenomenon of amplified spontaneous emission.

We can define a gain coefficient, $\gamma$, which will represent the coefficient of fractional change in signal power in a unit length, as given by the equation

$$\frac{dP}{dz} = \gamma P(z) \tag{2}$$

If $\gamma$ is a positive quantity, the power will become amplified in a given length of fiber; on the other hand, if $\gamma$ is negative, power will be lost instead. Equation 2 is valid for all light, whether it is pump, signal or ASE light. We shall see that additional subtleties arise in the case of ASE later.

As mentioned, light becomes amplified by the process of stimulated emission. Stimulated emission requires ions to be in the excited state. In the case of the signal, where it is desired to achieve amplification, a higher upper state population is advantageous. The amount of amplification is related, therefore, to the number of ions in the upper state population.

$$\text{Cross sectional area of excited ions} = N_2 \sigma_{\text{emission}}(\lambda_{signal}) \tag{3}$$

The above equation requires explaining. Physically, each excited ion has an area of space adjacent to it in which an incident photon can elicit a stimulated emission. If we multiply

by the upper state ion density, $N_2$, we arrive at an expression for the total cross sectional area in a given length element that incident photons can be within to elicit a stimulated emission. Intuitively, it is desired that this area be large, as a given signal photon will be more likely to elicit a stimulated emission as it travels down the fiber. The other term in the equation, $\sigma_{\text{emission}}$ can be interpreted as the probability that any given excited ion will emit a stimulated photon in the presence of light. This term is a property of the ion itself, but varies with wavelength of incident photons. When choosing a signal wavelength, it is desirable that this number be high as well. The above expression represents, in some sense, the amount of amplification that can be achieved with a given signal wavelength (which influences the term $\sigma_{\text{emission}}$) and amplifier state (which is described by the number of ions in the upper state, $N_2$).

In addition to the number of photons that can be added to the beam, we must also consider the number of ions that can be absorbed into the upper state by the light as well. This number is related to the number of ions in the lower state (instead of the upper state), as well as the cross section for absorption, which is defined analogously to the cross section for emission.

$$\text{Cross sectional area of lower state ions} = N_1 \sigma_{\text{absorption}}(\lambda_{signal}) \tag{4}$$

For signal light, we require this number to be relatively low to achieve maximum gain, because a large value will imply that many signal photons will be absorbed. On the other hand, the purpose of the pump light is to excite ions to the upper state from the lower state and so a large number for this term is desired. If we are considering the pump light instead, the argument of the term $\sigma_{\text{absorption}}$ will be replaced by the pump wavelength instead (this is also true in Equation 3).

We have calculated the cross sectional area of all upper and lower state ions, and com-

bining these terms results in the definition for $\gamma$ from above.

$$\gamma = -N_1\sigma_{\text{absorption}}(\lambda) + N_2\sigma_{\text{emission}}(\lambda) \tag{5}$$

where the cross section terms are evaluated at the wavelength of the light term which is being considered (whether it is pump, signal, or ASE light). The negative sign in front of the first term represents that photons are lost to the fiber, whereas the positive term can be interpreted as indicating that photons are added to the beam. If we consider the signal beam, and recall that a positive value for $\gamma$ indicates signal growth (whereas negative values indicate signal depletion), it is clear that a higher value of $N_2$ is desirable.

Since the cross sections in the above equation are constant, $\gamma$ is only dependent on the energy level populations. Let us determine the minimum value for upper state population that is required for signal gain. To do this, we set $\gamma$ to zero, as this will indicate that the signal is neither growing nor shrinking.

$$0 = -N_1\sigma_{\text{absorption}} + N_2\sigma_{\text{emission}} \text{ (Minimum condition for signal gain)} \tag{6}$$

We have dropped the argument on the cross sections as it is implicit that they should be evaluated at the signal wavelength. Now we note that the total number of ions in the fiber (denoted by $N$) is constant, so the condition $N = N_1 + N_2$ is true. Rearranging the above expression with $N_1 = N - N_2$:

$$(N - N_2)\sigma_{\text{absorption}} = N_2\sigma_{\text{emission}} \tag{7}$$

$$N\sigma_{\text{absorption}} = N_2(\sigma_{\text{emission}} + \sigma_{\text{absorption}}) \tag{8}$$

Finally, solving for the fraction of ions in the upper state, $N_2/N$

$$\frac{N_2}{N} = \frac{1}{\frac{\sigma_{\text{emission}}}{\sigma_{\text{absorption}}} + 1} \tag{9}$$

where we have done a small amount of algebraic simplification. We can see from this expression that the upper state population required for gain is related to the cross sections at the signal wavelength.

In this section we have defined the gain coefficient, $\gamma$, and shown how it is related to the state population levels and the cross sections. Furthermore, we have derived an expression for the minimum upper state population required to achieve signal gain in terms of the cross sections. We have demonstrated the importance of high upper state population and proper choice of signal wavelength (which determines the cross sections) in achieving signal gain.

Of particular interest in optical communication is the 1400 nm wavelength band. The ${}^4F_{3/2}$ to ${}^4I_{13/2}$ transition in neodymium-doped silica fiber has an energy gap with an associated wavelength of 1400 nm. In the recent past, praseodymium doped fiber amplifiers had been used in conjunction with a 1300 nm signal and have been shown to provide gain in this wavelength region. [3] Previous work has been done with Nd fibers in the shorter wavelengths used in telecommunication, especially in the area of 1300 nm. [18] Using techniques implemented to solve the problems at 1300 nm, we hope to determine if optical amplification with Nd-doped fibers is viable at 1400 nm. There are two major problems with amplification at 1400 nm. The first is gain limitation, or saturation, due to the build up of amplified spontaneous emission. When spontaneous emission occurs with large cross sections, such as the ${}^4F_{3/2}$ to ${}^4I_{11/2}$ transition at 1060 nm, the emission is propagated and amplified significantly. This results in depopulation of the excited state and less potential gain for the signal. The second problem is the phenomenon of excited state absorption, or ESA, which we will discuss at greater length later.

## 3.6 Fiber Loss

There are a number of sources of loss in fiber materials. A few examples of sources of loss are related to geometry (bending losses), Rayleigh scattering, and Raman scattering. [1] Each of these can contribute to an overall absorption coefficient, $\alpha$, with units of inverse length which impacts the signal power via Beer's law:

$$P_{out} = P_{in}e^{-\alpha L} \text{ (Beer's Law)} \tag{10}$$

where $L$ is the fiber length of interest. The net effect of these losses is to simply reduce the power of the signal by a factor in a length of fiber. Typically, losses are measured in $\frac{dB}{km}$. In units of decibels, the loss is related to the coefficient $\alpha$ by the following expression

$$(\frac{P_{\text{out}}}{P_{\text{in}}})_{\text{dB}} = 4.34\alpha Ł \tag{11}$$

As an example, the absorption coefficient associated with Rayleigh scattering can be approximated by the relation

$$\alpha_{Rayleigh} = (.8)(\frac{1\mu m}{\lambda})^4 \frac{dB}{km} \text{ (Rayleigh scattering in silica fiber)} \tag{12}$$

In the case of Ytterbium doped silica glass with signal wavelength of 1023 nm, $\alpha_{Rayleigh}$ is equal to about $0.73\frac{dB}{km}$. All fibers modeled in this report are less than 50 m in length, with a typical length of 10 m. For a 10 m fiber with Rayleigh loss coefficient equal to $0.73\frac{dB}{km}$, the value $\frac{P_{\text{out}}}{P_{\text{in}}}$ is 0.0317. In other words, 97% of the input power will be preserved at the end of the fiber. Other losses are of comparable magnitude; therefore, our model has ignored this subtlety. The results of ignoring these losses are an approximately 3% error in the worst cases, and less than 1% error in the average case (most significant results in this paper occur for fiber lengths of $1 - 5$ m).

# 4 Rate Equation Approach to Gain Coefficient

In order to determine the change in signal power as a function of distance it is convenient to define the gain coefficient as

$$\gamma(\nu) = N_2(t)\sigma_e(\nu) - N_1(t)\sigma_a(\nu) \text{ (gain coefficient)} \tag{13}$$

In the above equation, the terms $N_2(t)$ and $N_1(t)$ represent the upper and lower state populations. State population is, in general, a function of time; however, in our model we are assuming a time constant upper state population. This assumption is extremely valid for most situations.

The upper state population can be modeled by considering the number of ions excited into the upper state and the number of ions removed from the upper state. First, we must find an expression for the number of ions that each beam adds to the upper state per unit time. We will derive this expression by considering the number of photons included in each beam and the probability that a single photon will excite an ion. To begin, only the pump beam will be analyzed. The power of the pump light can also be described by the number of photons within that beam, multiplied by the energy of each of these photons, that propagate per unit time. In other words,

$$\text{number of photons in pump beam per unit time} = \frac{P_p}{E_p} \tag{14}$$

where $E_p$ is the energy of a pump photon. Next, we must find the number of photons in a particular cross sectional area. Since the area we are concerned with is the core area, we divide by this value. The value $\frac{P_p}{A_{core}}$ is the pump intensity. However, the pump light is spread across the entire cladding area. Only the pump light that is within the core can be absorbed by the ions (since the ions are confined to the core volume). Therefore, we must

multiply by the extra factor eta, which is the ratio of the core area to the cladding area.

$$\text{number of photons in the core per unit time} = \frac{P_p \eta}{E_p A_{core}} \tag{15}$$

Finally, each ion in the core has a chance to be absorbed by a pump photon. This probability is defined as the cross section for absorption. Each wavelength has a specific absorption cross section; therefore, this value is a function of frequency.

$$\text{probability of a single ion being excited into the upper state} = \frac{P_p \eta \sigma_{abs}(\nu_{pump})}{E_p A_{core}} \tag{16}$$

At this point, we will drop the subscript 'core' on the factor $A_{core}$, as it will be assumed that all light (other than the pump) will be confined to the core area. Moreover, we will drop the dependence of $\sigma_{abs}$ on frequency, as it will also be assumed that the frequency of interest is the same as the frequency of the light we are writing the rate for. We will call this factor in the above expression the pump rate and assign the variable $R_{12}$

$$R_{12} = \frac{P_p \eta \sigma_{\text{abs}}}{E_p A} \text{ (Pump Rate)} \tag{17}$$

We can define identical terms for the signal and ASE light. For these terms, we simply define the term $\eta$ to be 1, as these terms propagate exclusively in the core.

$$W_{12} = \frac{P_{signal} \sigma_{abs}}{E_s A} \text{ (Signal Absorption Rate)} \tag{18}$$

$$Q_{12} = \frac{P_{ASE} \sigma_a bs}{E_{ASE} A} \text{ (ASE Absorption Rate)} \tag{19}$$

If we multiply each of these terms by the lower state population, we will know the total

number of ions being absorbed into the upper state per unit time.

$$\text{Total number of ions excited into upper state per unit time} = N_1(R_{12} + W_{12} + Q_{12}) \quad (20)$$

In general, the pump rate is much higher than the signal or ASE absorption rates. This is not by accident: the pump wavelength is chosen at a value which has a much higher absorption cross section than at other wavelengths. In contrast, the signal wavelength is chosen so that there is low absorption (so that the signal does not become reabsorbed by the fiber).

In addition to the number of ions being pumped into the upper state, we must also consider the number of ions removed from the upper state. In order to do this, we simply change the rates to include the emission cross section instead of the absorption cross section.

$$R_{21} = \frac{P_p \eta \sigma_{\text{ems}}}{E_p A} \text{ (Pump Emission Rate)} \quad (21)$$

$$W_{21} = \frac{P_s \sigma_{\text{ems}}}{E_s A} \text{ (Signal Emission Rate)} \quad (22)$$

$$Q_{21} = \frac{P_{ASE} \sigma_{\text{ems}}}{E_{ASE} A} \text{ (ASE Emission Rate)} \quad (23)$$

In most cases, these terms represent almost all of the downwards transitions from the upper state. However, spontaneous emission also contributes to the depletion of the upper state. The rate for spontaneous emission is defined as the inverse of the radiative lifetime of the upper state.

$$A_{21} = \frac{1}{\tau_{21}} \text{ (Spontaneous Emission Rate)} \quad (24)$$

Once again, multiplying each of these terms by the total number of ions in the upper state yields the number of ions removed from the upper state.

Total number of ions removed from upper state per unit time $= N_2(R_{21} + W_{21} + Q_{21} + A_{21})$ (25)

We have found the rate at which ions are excited into and removed from the upper state. The sum of these terms gives the rate of change of upper state population.

$$\frac{dN_2}{dt} = N_1(R_{12} + W_{12} + Q_{12}) - N_2(R_{21} + W_{21} + Q_{21} + A_{21}) \tag{26}$$

Figure 5 shows how each of these rates interact with the energy levels in a typical system.

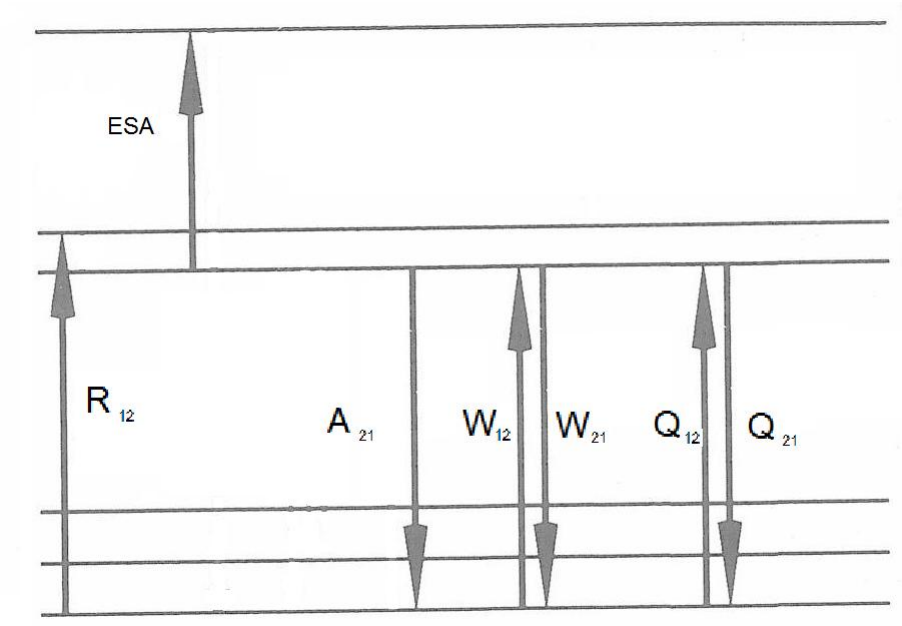


Figure 5: Transitions between Energy Levels

In this model, an extremely effective approximation that greatly simplifies the calculations is the condition for time independent upper state, otherwise called the steady state.

The steady state will be defined intuitively as

$$\frac{dN_2(t)}{dt} = 0 \text{ (steady state condition)} \tag{27}$$

At this point we can find an expression for $N_2$, given the assumption that the steady state condition is true. This can be derived by using the two relations

$$n_1 + n_2 = 1 \tag{28}$$

$$n_1(R_{12} + W_{12} + Q_{12}) - n_2(R_{21} + W_{21} + A_{21} + Q_{21}) = 0 \tag{29}$$

Here $n_1$ and $n_2$ will represent the fraction of the total ions in each state, defined as $N_1/N$ and $N_2/N$ respectively, with $N$ as the total ion concentration in units of ions per unit volume. The first equation represents the fact that each ion must either be in the upper ($N_2$) or lower ($N_1$) state. In a three level system, such as Ytterbium, these are the only populated energy levels. In four level systems there is an additional energy level to consider; however, this level is also assumed to be depopulated because of fast phonon transitions from the lower laser level to the ground state. The second equation represents that the rate of transition from the ground state to the excited state is the same as the rate of transition from the excited state to the ground state. This is found simply by setting Equation 26 to zero and rearranging. The second equation is only true in the case of steady state, which we have assumed to be true. Rearranging the above equations yields

$$n_1 = 1 - n_2 = n_2 \frac{R_{21} + W_{21} + A_{21} + Q_{21}}{R_{12} + W_{12} + Q_{12}} \tag{30}$$

Add $n_2$ to the previous expression and using the identity $n_1 + n_2 = 1$

$$n_1 + n_2 = 1 = n_2[1 + \frac{R_{21} + W_{21} + A_{21} + Q_{21}}{R_{12} + W_{12} + Q_{12}}] \tag{31}$$

Next we algebraically simplify the right hand side to arrive at

$$n_2 \frac{R_{12} + W_{12} + Q_{12} + R_{21} + W_{21} + A_{21} + Q_{21}}{R_{12} + W_{12} + Q_{12}} = 1 \tag{32}$$

And rearrange to get our final result:

$$n_2 = \frac{R_{12} + W_{12} + Q_{12}}{R_{12} + W_{12} + Q_{12} + R_{21} + W_{21} + A_{21} + Q_{21}} \tag{33}$$

This result can be expressed as a total number of ions simply by multiplying by the ion density, N:

$$N_2 = N \frac{R_{12} + W_{12} + Q_{12}}{R_{12} + W_{12} + Q_{12} + R_{21} + W_{21} + A_{21} + Q_{21}} \tag{34}$$

At this point we can use this relation in our expression for the gain coefficient, noting that $N_1$ can still be written as $N_1 = N - N_2$. The gain coefficient, $\gamma$, is related to the change in power by

$$\frac{dP}{dz} = \gamma(\nu, z)P(z) \text{ (fractional change in power per unit length)} \tag{35}$$

If it is desired to find the total gain of an amplifier over a given length of fiber, the previous equation must be integrated over the distance parameter $z$. However, the upper state fraction is in general a function of position along the fiber and therefore the integration is non-trivial. For numerical modeling, the integration is performed iteratively by taking a proper step size, $dz$, and repeating the calculation of $N_2$, $\gamma(\nu)$, and $dP$ a fixed number of times. In general, smaller choices of $dz$ will give more accurate calculations of final signal powers; however, even if the choice of $dz$ is larger than optimal, it is possible to improve

accuracy by repeating the iteration process with results from the previous pass as initial values.

# 5 Excited State Absorption

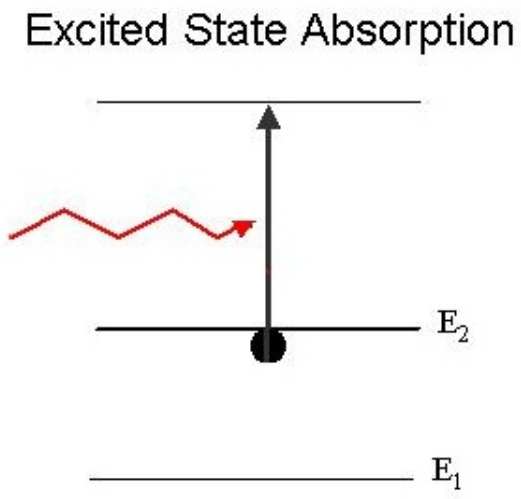


Figure 6: Excited State Absorption

In neodymium, there is an additional radiative process known as excited state absorption. This is a phenomenon where a photon is incident on an ion in an excited state. Instead of inducing the ion to undergo a stimulated emission, the ion absorbs the photon, further raising its energy level. Generally, the ion decays back down in a non-radiative manner relatively rapidly. The result of this entire process results is no change in population level, but does in fact remove a signal photon from the beam, limiting overall gain. In neodymium, this process occurs near the 1300 nm transition. As the excited ions are mostly in the ${}^4F_{3/2}$ multiplet, when 1300 nm signal photon are absorbed, the ion transitions upward to the ${}^4G_{7/2}$, where it rapidly decays in the form of phonon release.

This newly introduced type of absorption turns out to be a relatively significant source

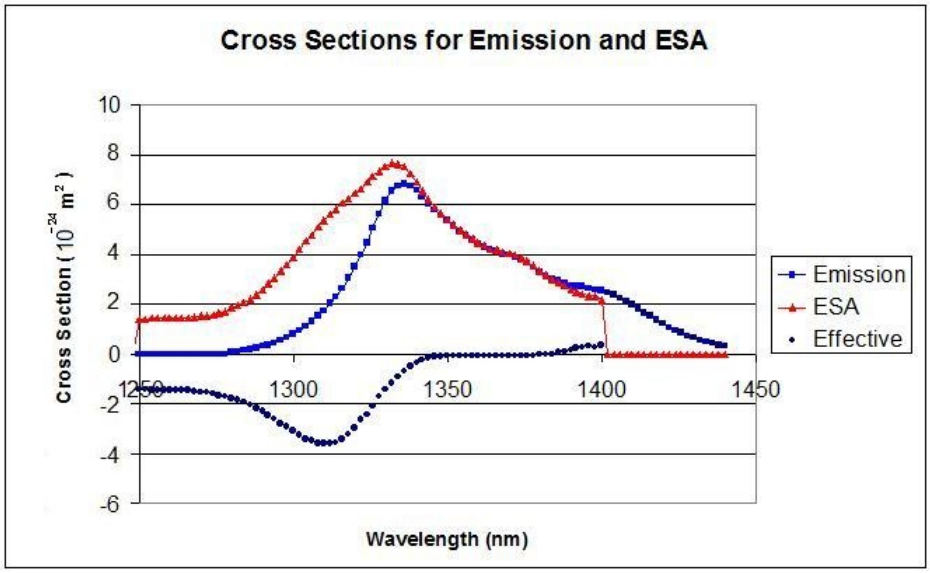


Figure 7: Effective Cross Section Due to ESA, Neodymium Doped in Silica Host Glass

of gain limitation. We are particularly interested in achieving gain at 1400 nm, and while there is little to no absorption at the lower laser level, in turns out that the upper level experiences significant absorption when compared to emission. Figure 7 shows the cross sections for both emission and ESA at the 1300 nm transition, as well as the effective cross section for neodymium in silica. Notice how well the two cross sections begin to overlap after 1330 nm. This results in an effective cross section of zero for these wavelengths, which would result in no signal gain. Also notice the lack of ESA data after 1400 nm; this was due to a lack of available data past this point, but if one simply extrapolates this trend further, it would seem that gain at 1400 nm would be impossible. ESA is a fundamental property of the ion in the host glass; therefore no type of filter would remove this issue.

Although it seems that achieving signal gain at 1400 nm is unlikely, there is another way to get around the issue of ESA. Changing the host glass in which the neodymium ions are doped, while changing the cross section spectra for emission and ground state absorption, also changes the ESA. As can be seen in Figure 8, by using a fluoride based host glass as in

ZBLAN fibers, we can shift the ESA spectra to shorter wavelengths. This has the potential for removing the limitation imposed by ESA. Due to this shift, and the completely limiting nature gain experiences without it, we modeled the fiber excluding ESA considerations. As such, this keeps with our original task of simply observing the gain limitations imposed by ASE.

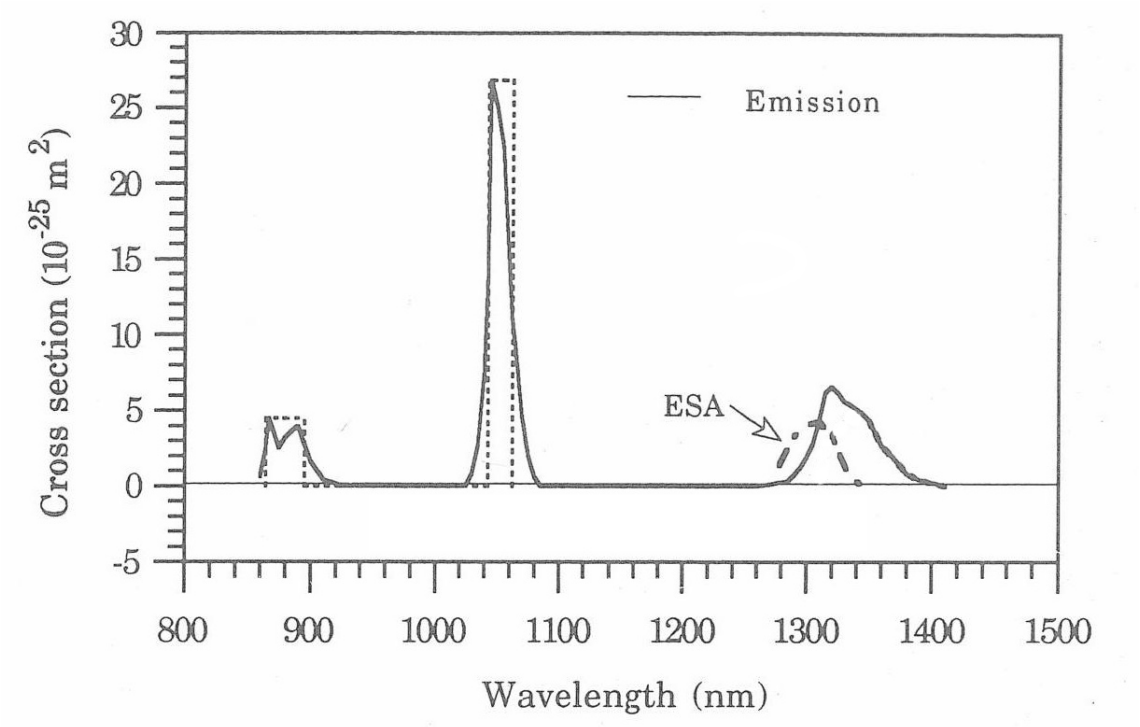


Figure 8: ESA Spectrum Shifted Relative to Spectrum in Silica, shown in Fluoride Host Glass.

# 6 Experimental and Theoretical Results

Recent advances in telecommunications research have spurred interest in fiber amplification as supplemental devices in fiber optic systems. Of particular interest to these applications is the 1300 nm wavelength band, as many of the fiber optic systems already in use rely on

this as a signal wavelength. The earliest demonstration of the potential amplification of 1300 nm light was shown by Miniscalco in 1988. [18] This result was shown in neodymium doped fluoride based glass. Fluoride based glass has the advantage that the considerable ESA that is present in silica is shifted to shorter wavelengths. Unfortunately, despite the shifting of ESA in fluoride glass, this effect and the effect of ASE at 1060 nm have limited the effectiveness of this configuration. It was demonstrated by Sugawa and also by Ohishi that the maximum achievable signal gain was approximately 10 dB.[20] [21] However, this was a major breakthrough and sparked further research into improving the rare earth doped fiber amplifier operating near 1300 nm. To date, it has yet to be shown that a high gain Nd doped fiber amplifier can be used in any host glass to boost signal power near 1300 nm; however, the potential seems to exist for other similar devices. [12]

## 6.1 The Praseodymium Doped Fiber Amplifier

We have mentioned the importance of the 1300 - 1400 nm wavelength band in optical telecommunications. The Nd doped fiber amplifier has many problems that may be insurmountable. Here we will investigate alternatives to the NDFA for amplification in this band. One choice that has been shown to provide significant amplification near 1300 nm is the praseodymium doped fiber amplifier. This amplifier was developed in 1990 by Sugawa. [20] A major advantage of this amplifier is that the range of wavelengths that can be amplified extends across the entire 1300 nm telecommunications window (1290 to 1330 nm). Ohishi demonstrated signal gain of 30 dB with a fluoride based host glass (much higher than the maximum gain shown in NDFAs). [21] The emission and absorption spectra of praseodymium also display characteristics that allow amplification at longer wavelengths around 1400 and 1650 nm. Finally, it was shown by Ohishi that the choice of effective pump wavelengths can be quite broad: extending over 70 nm between 980 and 1050 nm with commercially available laser devices.[21]

Of note is the strong dependence of signal gain on fiber length for the PDFA. [24] For signal near 1300 nm, the absorption of the signal at long fiber lengths is significant. Therefore, it is important to choose the proper length for this device. The optimal length for the PDFA, as it happens, is longer than the optimal length for most of the ytterbium doped fiber amplifier and the neodymium doped fiber amplifier configurations that we model in this report. Also, the signal gain is also highly dependent on temperature. [23] This is due to the increased possibility of multi-phonon relaxation processes (essentially, the lifetime of upper state levels is decreased by this process). Therefore, it is suggested that improved performance can be achieved by choosing glass hosts with lower phonon energy. [21]

## 6.2 Rate and Propagation Equation Modeling

In this section we will explore the techniques used in theoretically modeling optical amplifiers. In particular, much of the focus of this section will be devoted to erbium doped fiber amplifiers, as this configuration has elicited much of the theoretical research. We will begin by presenting the equations that are used to describe the propagation of light within a fiber, as well as the equations governing the upper state population. Morkel and Laming use a rate equation approach for upper state population that was used to model signal gain in erbium doped fiber amplifiers. [11]

$$\frac{dN_2(z)}{dt} = W_p(z)[N_{tot} - N_2(z)] - W_s(z)[(1 + \frac{\sigma_{12}}{\sigma_{21}})N_2(z) - \frac{\sigma_{12}}{\sigma_{21}}N_{tot}] - \frac{N_2(z)}{\tau_{21}} \qquad (36)$$

where $W_p(z)$ is the pump rate and the $W_s(z)$ is the stimulated emission rate. $\sigma_{12}$ and $\sigma_{21}$ are the absorption and stimulated emission cross sections respectively. $\tau_{21}$ is the radiative lifetime between levels 2 and 1. The authors couple this equation with the propagation equations:

$$\frac{dP_p^+(z)}{dz} = -P_p^+(z)\sigma_{abs}[N_{tot} - N_2(z)] - P_p^+(z)\sigma_{ESA}N_2(z) \tag{37}$$

$$\frac{dP_s^\pm(z)}{dz} = P_s^\pm(z)\gamma(z) \tag{38}$$

$$\frac{dP_f^\pm(z)}{dz} = \mu(z)h\nu\Delta\nu\gamma(z) + P_f^\pm(z)\gamma(z) \tag{39}$$

Where $\gamma(z)$ is the local gain coefficient

$$\gamma(z) = \eta_s\sigma_{21}[(1 + \frac{\sigma_{12}}{\sigma_{21}})N_2(z) - \frac{\sigma_{12}}{\sigma_{21}}N_{tot}] \tag{40}$$

And $\mu(z)$ is given by

$$\mu(z) = \frac{N_2(z)}{(1 + \frac{\sigma_{12}}{\sigma_{21}})N_2(z) - \frac{\sigma_{12}}{\sigma_{21}}N_{tot}} \tag{41}$$

Here, $P_f^\pm$ is the forward and backwards going ASE respectively and $\eta_s$ is the percent of the signal power propagating within the core itself. In equilibrium, the upper state population is constant in time, so that $\frac{dN_2(z)}{dt} = 0$. The authors solve the upper state equation with this condition as

$$N_2(z) = N_{tot}\frac{W_p(z) + \frac{\sigma_{12}}{\sigma_{21}}W_s(z)}{W_p(z) + (1 + \frac{\sigma_{12}}{\sigma_{21}})W_s(z) + \frac{1}{\tau_f}} \tag{42}$$

With the rates given by

$$W_s(z) = \frac{(P_s^\pm(z) + P_f^\pm(z))\sigma_{21}\eta_s}{h\nu_s a} \tag{43}$$

$$W_p(z) = \frac{P_p^+(z)\sigma_{abs}\eta_p}{h\nu_p a} \tag{44}$$

a is the core area of the fiber. In this analysis, both the signal and ASE terms are assumed to have both forwards and backwards propagating components. The approach taken to model ASE in this method is to assume an ASE bandwidth of 2 nm ion the basis that ASE-induced saturation is experimentally observed to occur when the ASE spectrum has narrowed to approximately 2 nm. The authors justify this approach by noting that it encompasses the more important limit of ASE, when it is large enough to limit the signal gain. While this analysis is concerned with erbium doped fibers, it is also applicable to neodymium and ytterbium doped fibers. In this model, we first notice that the rate Equation 42 is in similar form to Equation 26 derived earlier. Furthermore, the propagation equations are also identical, with the additional assumption that there is no stimulated emission at the pump wavelength.

As another example, Digonnet models three and four level transitions with the following solution for upper and lower state populations: [10]

$$\frac{N_1}{N_0} = \frac{W_e + \frac{1}{\tau_2}}{W_a + W_e + \frac{1}{\tau_2} + R_{13}} \tag{45}$$

$$\frac{N_2}{N_0} = \frac{W_a + R_{13}}{W_a + W_e + \frac{1}{\tau_2} + R_{13}} \tag{46}$$

With the rate terms defined as

$$R_{13} = \sigma_p \frac{I_p}{h\nu_p} \tag{47}$$

$$W_a = \sigma_a \frac{I_s}{h\nu_s} \tag{48}$$

$$W_e = \sigma_e \frac{I_s}{h\nu_s} \tag{49}$$

Where the terms $I_p$ and $I_s$ are the intensities

$$I_p = \frac{E_p}{A} \tag{50}$$

$$I_s = \frac{E_s}{A} \tag{51}$$

For core area A. The propagation equations Digonnet uses are

$$\frac{dI_p}{dz} = -I_p(\sigma_p N_1 - \sigma_{p'} N_2) \tag{52}$$

where $\sigma_p$ is the pump absorption cross section and $\sigma'_p$ is the pump emission cross section.

$$\frac{dI_s}{dz} = I_s(\sigma_e N_2 - \sigma_a N_1) \tag{53}$$

As can be seen, these equations are similar to those used by and Morkel and Laming. The purpose of comparing these articles is to show that whether the situation being modeled is erbium or neodymium doped fiber amplifiers the equations that model the upper state population and the propagation equations are identical. Moreover, it is common practice to model ASE using a number of independent terms each with width described by $\Delta\lambda$.

## 6.3 Numerical Modeling of ASE

In this section we will continue the discussion of methods of modeling ASE with more in depth analysis of the published literature. We will begin with an alternative to the general method of ASE modeling developed by Bjarklev called the equivalent bandwidth approximation. [3]

In this method, the propagation equation is modeled by

$$\frac{dP^{\pm}_{ASE}(z)}{dz} = \pm g_s(z)P^{\pm}_{ASE}(z) \pm Bh\nu_s\sigma_e(\nu_s)N_2 \tag{54}$$

Where $g_s(z)$ is given by

$$g_s(z) = \sigma_e(\nu_s)N_2 - \sigma_a(\nu_s)N_1 \tag{55}$$

And B is defined as

$$B = \frac{\int_{-\infty}^{\infty}\sigma_e(\nu)d\nu}{\sigma_e(\nu_s)} \tag{56}$$

The effect of the equivalent bandwidth approximation is to model the ASE produced by an entire transition by a single bandwidth. We will explore the validity of this approximation in further detail later.

A frequently referenced source for the modeling of ASE is Desuvire and Simpson's work in their 1989 article which laid the foundation for the theoretical model of ASE in fiber amplifiers. [16] The authors use a quantum mechanical argument stemming from photon statistics. The propagation equations derived in this way by the authors are written

$$\frac{dP^{\pm}_s(z,\nu_i)}{dz} = \pm[G_e(z,\nu_i)P^{\pm}_s(z,\nu_i) + P_0 - G_a(z,\nu_i)P^{\pm}_s(z,\nu_i)] \tag{57}$$

The terms $G_e$ and $G_a$ represent the gain coefficients for emission and absorption. The term $P_0$ is the source term used in this derivation. According to the authors $P_0 = h\nu_s\Delta\nu$ being the equivalent input noise power corresponding to one photon per mode in bandwidth $\Delta\nu$. Note that this source term is only applicable in the condition of single mode fibers. The index i is the index of each of the chosen ASE bins. This foundational derivation is the same used by each of the above papers (save the Bjarklev paper). In essence, the ASE is modeled

by taking an arbitrary number of wavelength divisions. In the original article by Desurvire and Simpson, a total of 200 bins with $\Delta\nu = 128$ GHz (equivalently, $\Delta\lambda = 1$ nm) were used in the modeling. [16]

Here we present a final example of ASE modeling in the work of Laliotis, Yeatman, and Al-Bader. [15] They begin with an equation for the power of the coupled spontaneous emission.

$$P_{se} = h\nu g(\nu)\Delta\nu \frac{1}{\tau_2}\frac{\Delta\Omega}{4\pi}N_2 \tag{58}$$

Where the term $g(\nu)$ is the lineshape function defined in words as

$$g(\nu) = \frac{\text{probability of photon emission at } \nu}{\text{frequency interval}} \tag{59}$$

This is, in essence, the source term for ASE. We will show that our own derivation of the ASE source term produces identical results. Most important, however, the authors again use a multiple bin model for ASE propagation. The ASE spectrum was divided in increments of $\Delta\lambda = 5$ nm and the discretization in the direction of propagation was $\Delta z = 0.2$ cm. Finally, the authors provide a schematic diagram of the iterative process used for their modeling. This is shown is Figure 9.

The authors begin by defining the initial values of pump and signal beams. Next, they calculate the emission and absorption rates and solve the rate equation to determine the upper state population. Using these values for population, they calculate the propagation equations and the change in pump, signal, and ASE powers. They then verify the boundary conditions and, if these conditions are not met, repeat the process with the previously calculated values as initial conditions. We will see later that the process implemented in this work is extremely similar to our own model.

In this section we have examined the various methods of modeling signal propagation

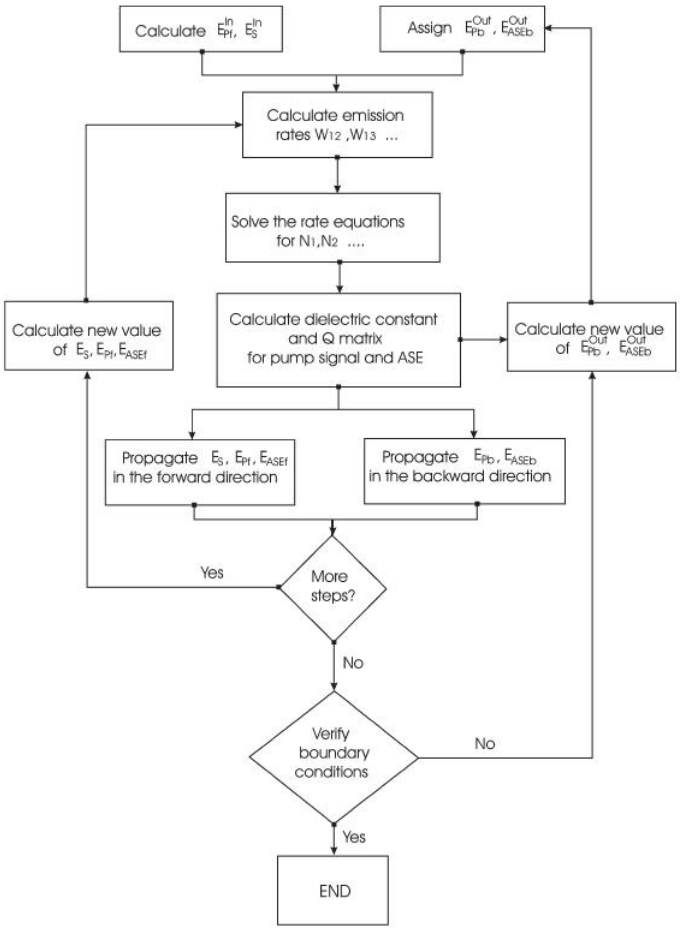


Figure 9: Flowchart from Laliotis Paper

using a rate equation approach for calculating the upper state population. Though many of these results were developed with erbium doped fiber amplifiers in mind, the derivations apply to Yb as well as both transitions of interest are three level transitions. Also, the extension of these three level derivations extend naturally to four level transitions in Nd, as the only substantial difference between these situations is the absence of absorption at the transition wavelengths. Furthermore, we briefly reviewed the approach to ASE modeling taken by other researchers in this field. We have seen that the division of the ASE spectrum into many smaller divisions of frequency interval $\Delta\nu$ (usually on the order of $\Delta\lambda = 1-4\text{nm}$) is the most common approach to ASE. A novel approach called the equivalent bandwidth

approximation was briefly discussed; however, a primary goal of this work is to analyze the validity of this approximation, so we leave a more comprehensive analysis for later. Finally, we mentioned a detailed step by step numerical model that is very similar to the method used in this work, as we will see in the following sections.

# 7 Derivation of the ASE Source Term

Amplified spontaneous emission is a phenomenon associated with the random emission of photons from excited ions. In a fiber, excited ions will emit a photon in a random direction in a characteristic time, $\tau$. A fraction of these photons will be trapped within the fiber and propagate identically in the manner of a signal. In deriving a model for signal gain in a fiber amplifier, it is necessary to include ASE in order to properly account for upper state depletion and the resulting signal gain limitation. In a given length of fiber, $dz$, a portion of the excited ions will spontaneously emit. The ASE source term is the power associated with the emitted photons trapped in the fiber in units of Watts. In the following intermediate steps, we seek to develop expressions first for the probability of spontaneous emission, second, for the probability per unit time per ion of emission, third, for the total number of photons spontaneously emitted in a given volume, and finally for the associated power of the coupled spontaneously emitted photons in a volume element. We begin with the lineshape function, given in this case by

$$g(\nu) = \frac{8\pi n^2 \tau}{\lambda^2} \sigma_e(\lambda) \tag{60}$$

And defined as

$$g(\nu) = \frac{\text{probability of photon emission at } \nu}{\text{frequency interval}} \tag{61}$$

where $\sigma_e(\lambda)$ is the emission cross section at the ASE wavelength, $\lambda$ and $\tau$ is the radiative lifetime. In the case of Yb, the fluorescence lifetime is approximately equal to the total spontaneous emission lifetime; however, in Nd, significant non-radiative transitions also contribute to the spontaneous emission lifetime. The factor $\tau$ appearing in the above equation is only representative of the photon emission lifetime and does not include non-radiative processes. Finally, $n$ is the refractive index of the fiber. In the case of silica glass, this is approximately 1.5. By multiplying by the factor $\Delta\nu$ we achieve a calculation of the probability of photon emission at the ASE frequency per ion. This is given by

$$\text{probability per ion of spontaneous emission} = g(\nu)\Delta\nu \tag{62}$$

Next, the total number of spontaneously emitted photons is given by multiplying the above equation by the total number of ions in a volume element, $dV$ which is given by the product $N_2 dV$. In addition, multiplying by the spontaneous emission rate $\frac{1}{\tau}$ gives the total number of spontaneously emitted photons in a volume per unit time

$$\text{total number of spontaneously emitted photons} = \frac{g(\nu)\Delta\nu N_2 dV}{\tau} \tag{63}$$

Only a fraction of the spontaneously emitted photons will be trapped by total internal reflection, however. The percentage of these photons trapped in the fiber, given by $\frac{\Delta\Omega}{4\pi}$, is the solid angle into which photons can be trapped within the fiber divided by the solid angle of a sphere ($4\pi$) (represented in Figure 10). The solid angle for a cone of half angle $\alpha$ is given by

$$\Omega = 2\pi(1 - \cos(\alpha)) \tag{64}$$

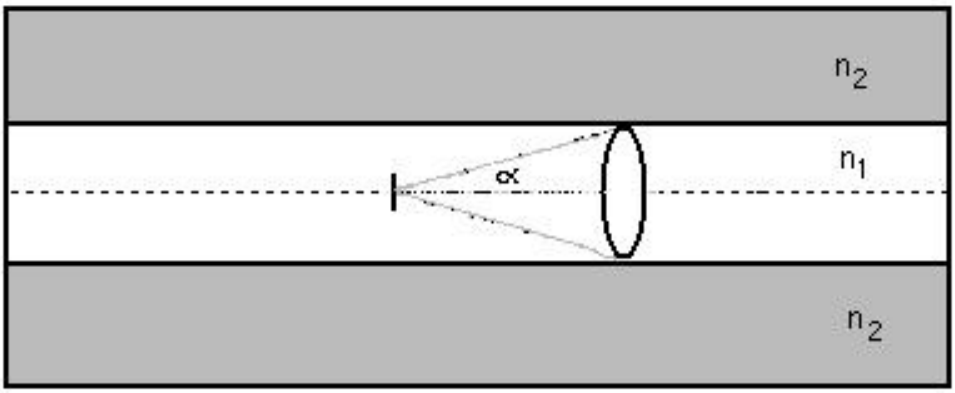


Figure 10: Solid Angle Trapped in Fiber

In this case, the half angle $\alpha << 1$, thus we us the small angle approximation [9]

$$\Omega = \pi\alpha^2 \tag{65}$$

The half-angle $\alpha$ can be determined by considering the critical angle, $\theta_c$. The angle $\theta_c$ is found as the critical angle of the core cladding interface (depicted in Figure 11). Light traveling at any angle greater than the critical angle inside the fiber will be reflected at the interface. This angle is found from Snells law when $\theta_2$ is set to $90^o$.

$$n_1 \sin(\theta_1) = n_2 \sin(90^o) \text{ (Snell's Law)} \tag{66}$$

then solving for $\theta_1$,

$$\theta_1 = \arcsin \frac{n_2}{n_1} \tag{67}$$

Under this condition $\theta_1$ is the critical angle, $\theta_c$. The half angle $\alpha$ is related to $\theta_c$ as shown in Figure 11. A widely used measurement which describes fiber parameters is the numerical aperture; it specifies the maximum acceptance angle with a relation between the indices of the core and cladding.

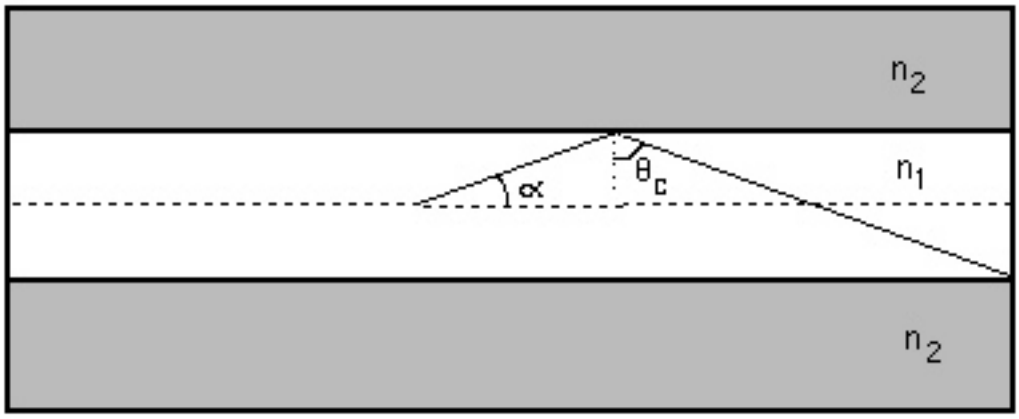


Figure 11: Relation of Critical Angle to Half Angle

$$\text{NA} \equiv \sqrt{n_1^2 - n_2^2} \tag{68}$$

This equation can be rewritten by factoring $n_1$ and using the identity in Equation 67 (in which we simply take the sine of both sides)

$$\text{NA} = n_1 \sqrt{1 - \sin^2(\frac{n_2}{n_1})} \tag{69}$$

Using the basic trigonometric identity and the identity $\cos(90 - \theta_c) = \sin(\alpha)$, we find

$$\text{NA} = n_1 \sin(90 - \theta_c) = n_1 \sin(\alpha) \tag{70}$$

This is related to the solid angle, $\Omega$, by the expression

$$\text{NA} = n_1 \sin \sqrt{\frac{\Omega}{\pi}} \tag{71}$$

Where we have just inserted Equation 65 from above. Finally, in the case of a fiber, the small angle approximation is valid, allowing the above equation to be written as,

$$\mathrm{NA} = n_1\sqrt{\frac{\Omega}{\pi}} \tag{72}$$

From this, we can easily relate the fraction of solid angle trapped by the fiber to the numerical aperture by

$$\frac{\Omega}{4\pi} \approx \frac{1}{4}(\frac{\mathrm{NA}}{n_1})^2 \tag{73}$$

An additional subtlety arises in this configuration due to our choice to employ cladding pumping. Cladding pumping is the configuration in which the core is surrounded by two layers of differing index, referred to as the inner and outer claddings. Cladding pumping is often employed to allow for the efficient coupling of greater pump powers. By using cladding pumping, we allow for the possibility of spontaneous photons to be trapped within the inner cladding. This will result in separate ASE terms that propagate within the cladding as well as the core. A diagram of this process is shown in Figure 12

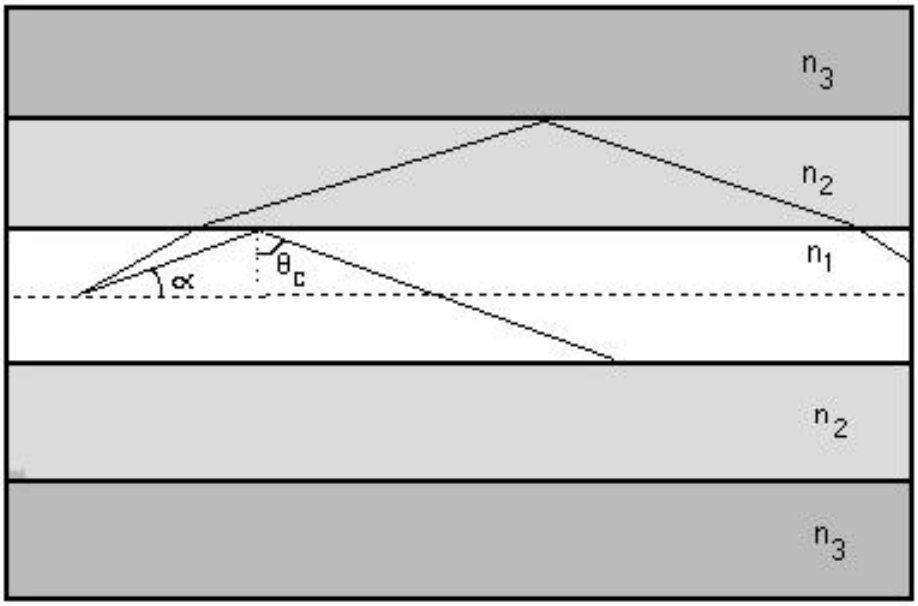


Figure 12: ASE trapped in cladding

These cladding trapped ASE terms only affect the upper state when they are in the core. Therefore, just as we did in deriving the rates of absorption and emission for the pump light, we include the factor $\eta$. We include this factor because only ASE light within the core area will have an effect on the upper state population. In effect, this allows us to consider ASE only within the core of the fiber.

Using typical fiber parameters, we will determine the magnitude of this effect. We will consider a fiber which has a $3.4\mu m$ core radius and a $43\mu m$ cladding radius. In this case, the ratio

$$\frac{A_{core}}{A_{cladding}} = \frac{\pi r_{core}^2}{\pi r_{cladding}^2} = 0.0063 \tag{74}$$

is extremely small. In order to find the trapping fraction for the inner and outer cladding boundary, it is necessary to subtract the fraction of light trapped exclusively in the core.

$$(\frac{\Delta\Omega}{4\pi})_{effective} = (\frac{\Delta\Omega}{4\pi})_{cladding} - (\frac{\Delta\Omega}{4\pi})_{core} \tag{75}$$

With a core-inner cladding NA of .5, an inner cladding index of 1.5, and an outer cladding index of 1.4, the trapping fraction is found as

$$(\frac{\Delta\Omega}{4\pi})_{effective} = 0.0333 - 0.0313 = 0.002 \tag{76}$$

Therefore, of all the spontaneously emitted light that is trapped within the fiber, only 6% is trapped at the inner and outer cladding boundary. Combining these two values (.06 for the fraction of light trapped by the inner and outer cladding boundary and .0063 for the ratio of core to cladding areas) yields $3.75 * 10^{-}4$. This extremely small product represents the effect of cladding trapped ASE as compared to core trapped ASE. Because these fiber parameters are typical, we have chosen to ignore this effect.

With an expression for the fractional solid angle in hand, we multiply this fraction by

the total number of spontaneously emitted photons, given in Equation 63:

$$\text{photons trapped in the fiber} = g(\nu)\Delta\nu\frac{\Delta\Omega}{4\pi}N_2 dV \tag{77}$$

The energy of these photons is $h\nu$. Multiplying the number of photons trapped in the fiber by the energy per photon yields the total energy trapped in the fiber in a unit volume

$$\text{total energy of trapped spontaneously emitted photons} = h\nu g(\nu)\Delta\nu\frac{\Delta\Omega}{4\pi}N_2 dV \tag{78}$$

The rate at which this energy is coupled into the fiber is related to the fluorescence lifetime. The inverse of $\tau$ is the rate at which excited ions emit spontaneously per second. The rate at which energy is coupled into the fiber can also be called the power coupled into the fiber. We thus arrive at our result for the ASE power coupled into the fiber:

$$P_{ASE} = h\nu g(\nu)\Delta\nu\frac{1}{\tau}\frac{\Delta\Omega}{4\pi}N_2 dV = h\nu g(\nu)\Delta\nu\frac{1}{\tau}\arcsin^2(\frac{\text{NA}}{n_1})\frac{N_2 dV}{4} \tag{79}$$

and with the small angle approximation,

$$P_{ASE} = h\nu g(\nu)\Delta\nu\frac{1}{\tau}(\frac{\text{NA}}{n_1})^2\frac{N_2 dV}{4} \tag{80}$$

# 8 The Equivalent Bandwidth Method for ASE

The physical reality of ASE propagation in fiber amplifiers involves an infinite number of independent ASE terms at unique wavelengths. In practice, the accurate computation of a large number of ASE wavelengths can be prohibitive on computing resources. A solution to this problem involves the approximation of a multiple number of ASE wavelengths by a single "equivalent" wavelength. The important parameter in the calculation of ASE propagation

is the stimulated emission cross section; therefore, the equivalent bandwidth method also requires the calculation of an equivalent emission cross section.

In order to calculate an equivalent cross section, the following relation is used

$$\int \sigma_{SE}(\nu) d\nu = \Delta\nu \sigma_{SEmax} \tag{81}$$

In practice, the integral appearing in Equation 81 is actually a summation as data points are discretized. The term $\sigma_{SEmax}$ is the equivalent emission cross section that can be used in the modeling of ASE, and the term $\Delta\nu$ is the equivalent frequency interval. This is in contrast to the ideal case where $\Delta\nu$ is the differential $d\nu$, with infinite, distinct values for the emission cross section along the spectrum. In geometric terms, the area under the cross section versus frequency curve is equal to the rectangle of height $\sigma_{SEmax}$ and width $\Delta\nu$. The absorption cross section for the equivalent ASE band is taken at the frequency for which the stimulated emission cross section is a maximum.

The equivalent bandwidth method is most appropriate for approximating transitions from one multiplet to another. For example, if the data being modeled extends over a range that includes transitions from different multiplets, it is most appropriate to use a single equivalent bandwidth for each transition. In the modeling of a single transition, the equivalent bandwidth method, in its pure form, is used to build a single ASE band to approximate an entire spectrum as shown in Figure 13. However, evidence will be shown that if the number of ASE bands is increased the accuracy of the approximation can be increased. This is to be expected, as a large number of bands more closely models the physical actuality.

It will be shown in this work that the equivalent bandwidth method provides results that are accurate only for a certain subset of conditions. Notably, if the configuration of interest extends beyond the optimum fiber length the accuracy of the equivalent bandwidth method degrades considerably. The reason for this that the absorption cross section for

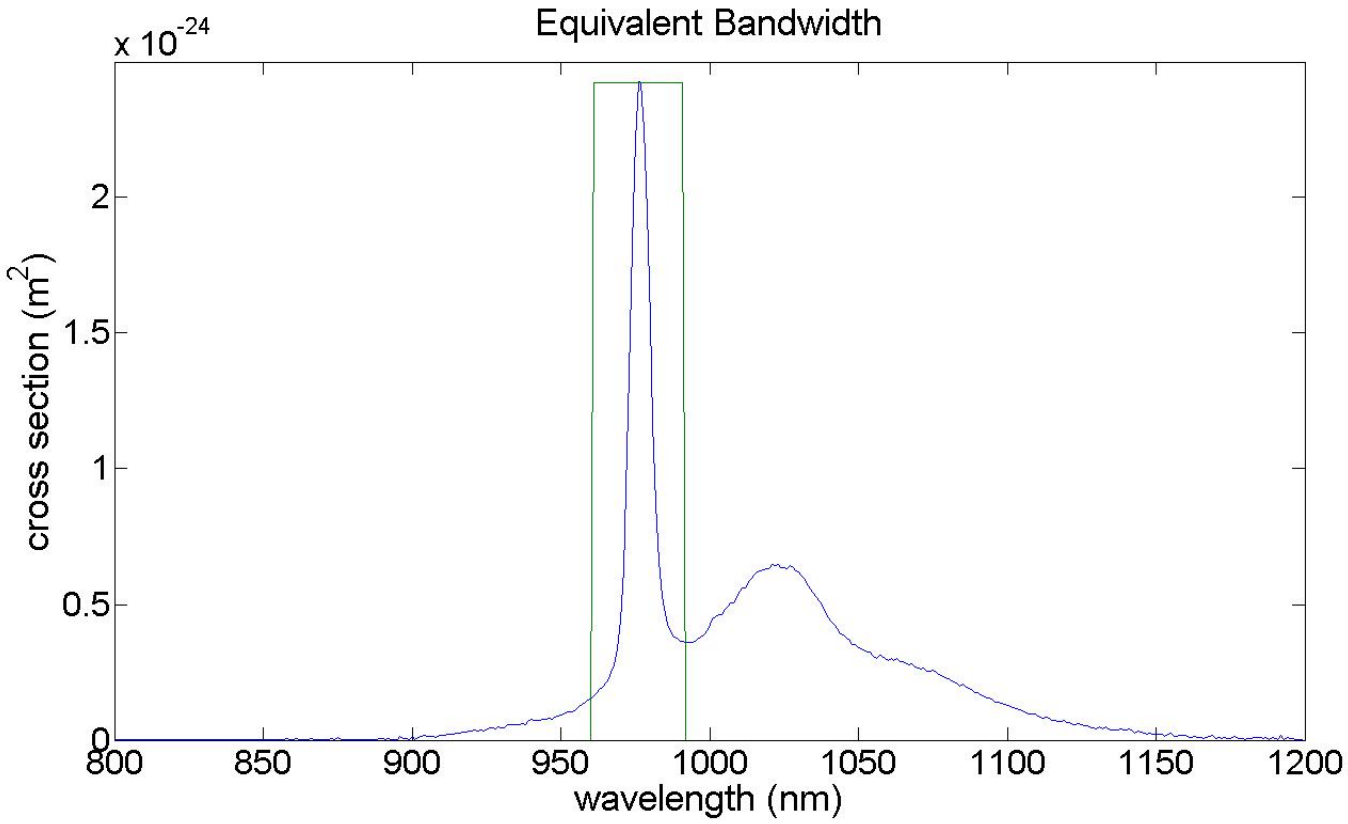


Figure 13: Emission Cross Section Spectrum with Equivalent ASE Band, One Bin

the equivalent ASE band is taken at the same wavelength as the emission cross section. This arbitrary choice tends to ignore much of the absorption cross section which becomes important for many configurations.

# 9 Pseudo Code for Amplifier Modeling

The modeling of fiber amplifiers in this work is done by a method of numerical integration that is meant to replicate physical reality as accurately as possible. However, several sacrifices must be made because of the limits of numerical computation. The length step used in this model, dz, is the infinitesimal length division in an actual fiber. Also, ASE bands are separated by infinitesimal frequency divisions whereas in this model the maximum number

of divisions is limited by the structure of our data: emission and absorption cross sections are available for divisions of one nanometer in Yb and two nanometers in Nd.

The first step in our model is to define the fundamental physical constants to be used later and the parameters of the fiber which may be variable. The fundamental constants necessary in this model are c, the speed of light, and h, Planck's constant. Fiber parameters that are necessary are the core and cladding radii (our model includes cladding pumping), the core index of refraction, the numerical aperture (from which the fractional solid angle used in the ASE source term can be derived with the aid of the core index), the radiative lifetime, the dopant ion concentration, and the appropriate signal and pump wavelengths. Next, the emission and absorption cross section values for the signal and pump wavelengths as well as the spectrum of data for the large number of ASE bands is extracted from the provided data. In the models for which equivalent bandwidth is used to approximate ASE, the equivalent cross sections and frequency intervals are calculated in this step instead. Next, the model is provided with initial conditions of pump power and signal power. The ASE is modeled as being generated within the fiber itself in both forwards and backwards directions; therefore, the initial ASE powers are zero.

The model then begins a series of iterations back and forth through the fiber, repeatedly recalculating signal, pump, and ASE powers. When the model enters the forward direction iteration, it calculates the upper state population through the equation

$$N_2 = N\frac{R_{12} + W_{12} + Q_{12}}{R_{12} + W_{12} + Q_{12} + R_{21} + W_{21} + A_{21} + Q_{21}} \tag{82}$$

where the R, W, Q, and A terms are the rates of transition, in units of inverse seconds, to and from the excited state for the pump, signal, ASE, and spontaneous transition terms respectively. In general the rates are calculated through the equation

$$R_{12} = \frac{\sigma_{pabs} P_p \eta}{A E_p}; \tag{83}$$

$$R_{21} = \frac{\sigma_{se} P_p \eta}{A E_p}; \tag{84}$$

where the $\sigma_{abs}$ and $\sigma_{se}$ terms represent the absorption and emission cross sections respectively. Identical terms appear for the signal powers. In the case of pump rates, the factor of $\eta$, which is the ratio of core to cladding areas, is necessary because only pump light that is present in the core is relevant to upper state population: light in the cladding is transparent to the fiber medium. ASE terms obey identical equations; however, the $Q_{12}$ and $Q_{21}$ terms are total transition rates. The power terms appearing these equations are the sum of both forwards and backwards ASE. Also, the energy for the ASE rate terms is unique to each ASE wavelength. Lastly, the $A_{21}$ term is simply the inverse of the upper state lifetime.

Once the upper state population has been calculated, the fractional change in signal, pump, and ASE powers is calculated. In order to do this, the gain coefficient must be calculated as it is defined previously. The fractional change in powers is calculated by the equation

$$\Delta P = P \gamma(\nu) \Delta z \tag{85}$$

where P represents the pump, signal, or ASE powers in each case. The change in ASE power includes the ASE source term derived earlier in addition to the propagation term that is identical to the signal and pump terms.

At this point the position in the fiber is incremented and a new upper state fraction is calculated identically as above but in this case using the power values calculated from the iteration just completed. Power terms are recalculated using the new upper state fraction. This process is repeated until the desired length is reached. In most cases, the fiber length

is divided into 1000 segments; thus, there are 1000 iterations of this process. This completes one pass forwards through the fiber.

Because the backwards propagating ASE is an important term to be considered, it is also necessary to iterate backwards through the fiber in a manner identical to that mentioned above for the forward pass in order to calculate the backwards ASE propagation correctly. When iterating backwards through the fiber, the signal, pump, and forwards ASE powers that were calculated on the forward pass are used to calculate the upper state population in addition to the backwards ASE powers; however, these terms are not recalculated on the backwards class. The first position that is recalculated in the backwards iteration is actually the last position to be calculated from the forwards iteration. In other words, the calculation moves forwards through the fiber, then reverses direction and moves backwards towards the initial position.

In practice, the reflection at the fiber ends can be made to approach zero or close to unity, depending on the preferences of the designer. A fiber laser would likely contain high reflections at the ends in order to achieve resonance. However, the case of zero reflection is also a physical realizable scenario and is thus justifiably modeled.

The backwards iteration is complete when the proper number of iterations has been completed such that the position along the fiber axis is zero. This is simply the condition that powers have been recalculated for the entirety of the fiber length in both forward and backwards directions. At this point, it is necessary to check that the signal and ASE powers have converged to a static value. To do this, the signal gain is calculated as

$$\text{Gain} = \frac{P_s(L)}{P_s(0)} \tag{86}$$

The gain is calculated at the end of each forwards and backwards pass. The process then repeats; however, the model uses the signal, pump, and ASE powers from the previous

iteration as initial conditions. This method is necessary as a single pass through the fiber will not accurately calculate the powers: the backwards ASE and the signal, pump, and forwards ASE cannot be simultaneously determined. Moreover, the upper state population generally experiences sharp spikes near the initial boundary. This phenomenon can be limited by recalculating the upper state population with beam powers that are more accurate.

This process of repeatedly recalculating signal, pump, and ASE powers using previous values continues until the condition that the fractional difference between the signal gain in a given pass and the gain in the previous pass is less than $10^{-3}$. The model then displays the signal, pump, and ASE powers and any other relevant data in graphical format and terminates. Figure 14 is a flowchart of this process.

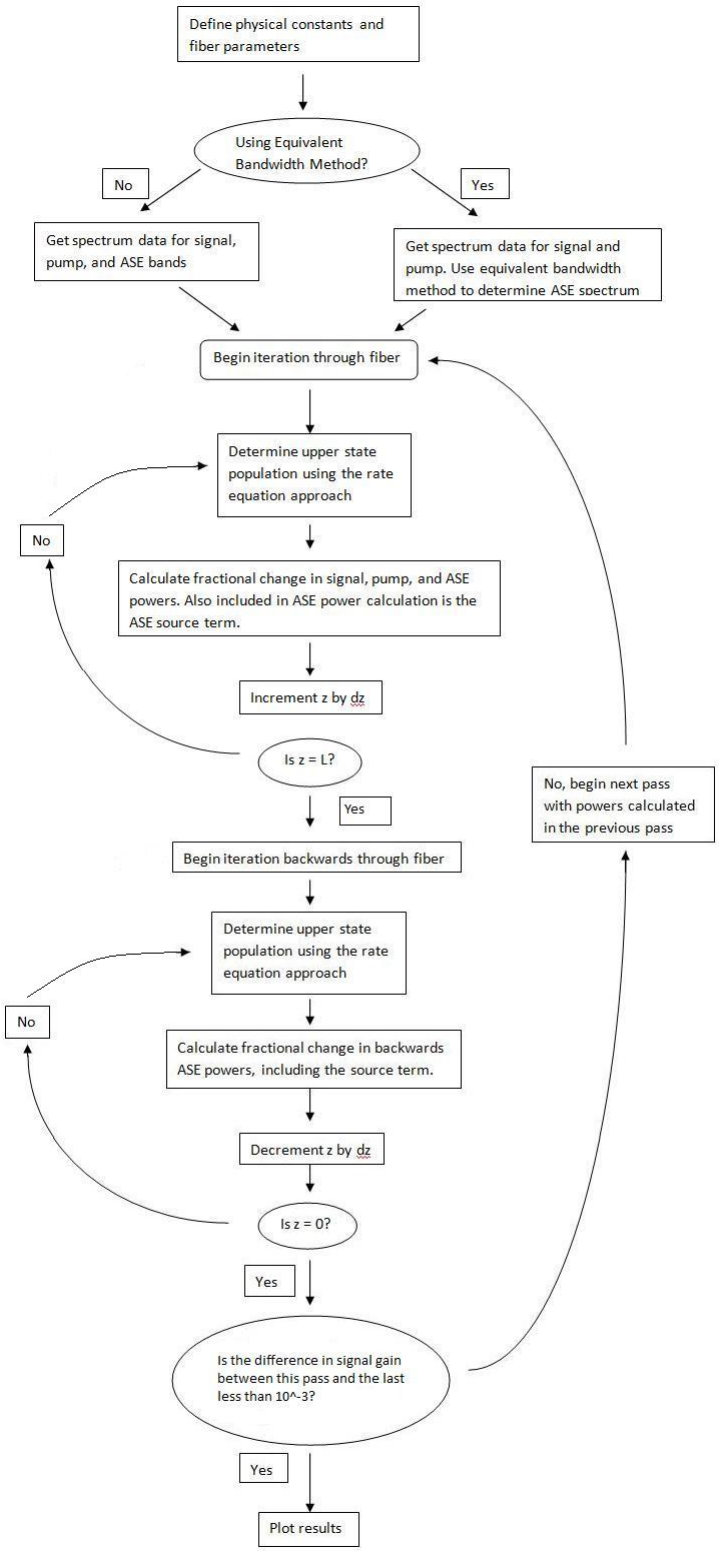


Figure 14: Flow Chart for Model

# 10 Energy Balance

A primary consideration in any physical modeling is the preservation of the fundamental physical principle of energy conservation. Therefore, it was necessary to design our model to neither create nor destroy energy within the system. To do this, the model calculates the absorbed pump power and compares this to the sum of the output powers of the signal and ASE. In addition, for every pump photon added to these beams there is an associated quantum defect that must be accounted for. An excited ion can experience stimulated emission via the pump, signal, or ASE beams, and can also undergo the process of spontaneous emission. Each of these possible emissions has a characteristic quantum defect that is defined as the difference in energy between the energy of a pump photon and the energy of the photons in the associated beam. In physical terms, this energy is lost into the fiber as heat in the form of phonons. For stimulated emission caused by the pump, this difference is zero. The signal is approximated by a narrow band; therefore, the quantum defect is constant and easily defined simply as

$$E_p - E_s = \text{quantum defect from signal} \tag{87}$$

ASE terms, however, are approximated by either the equivalent bandwidth method or the more thorough integrated approach. Because of this, the quantum defect varies for each ASE bin as calculated by the equivalent bandwidth method. Each ASE bin has an associated quantum defect, and these terms are summed to provide a total contribution to the energy balance. Since every bin is approximated at a specific wavelength, their photons have specific energies as well.

Finally, excited ions can undergo spontaneous emission. The energy of these photons is random over the spectrum; therefore, our model calculates an average spontaneous emission

energy. This was done by calculating a weighted average of photon energies according to their associated stimulated emission cross sections in the following way:

$$E_{SEavg} = \frac{\Sigma E(\nu)\sigma_{se}(\nu)}{\Sigma\sigma_{se}(\nu)} \tag{88}$$

where the sum is calculated over the transition spectrum. This average energy is used as a factor in the quantum defect for spontaneous emission. To find the total power associated with these effects it is first necessary to find the total number of ions pumped into the upper state per unit time in a volume element, which is given by

$$\text{total number of ions excited per unit time} = N_1 A dz R_{12} \tag{89}$$

where $A$ is the core area, $dz$ the length element and $R_{12}$ the pump rate. Implicit in this equation is the condition that $R_{12} >> W_{12} + Q_{12}$. This is the condition that pump light is the most dominant term exciting atoms into the upper state. As a typical example in Yb, if the pump power is $10^3$ W with 10 W signal, the value $R_{12}$ is $3.9 * 10^8$ and the term $W_{21}$ is $2.7 * 10^4$. Thus, this is usually a valid approximation. If this is not true, each photon used to excite an atom has its own energy and therefore the term $E_p$ appearing in the first equation and subsequent equations would be replaced by a linear combination of the energies of all possible upwards going transitions with associated probabilities. Next, this above factor is multiplied by the fraction of ions which undergo each specific stimulated emission transition (either through the pump, signal, or ASE). These factors are calculated as the rate for each of these transitions divided by the total rate of downward transitions. In other words,

$$\frac{A_{21}}{A_{21}+R_{21}+W_{21}+Q_{21}} \text{ (spontaneous emission)} \tag{90}$$

$$\frac{W_{21}}{A_{21}+R_{21}+W_{21}+Q_{21}} \text{ (signal stimulated emission)} \tag{91}$$

$$\frac{Q_{21}}{A_{21}+R_{21}+W_{21}+Q_{21}} \text{ (ASE stimulated emission)} \tag{92}$$

We note again that the pump transition is absent as the associated quantum defect is zero. Therefore, the total power associated with the effect of quantum defect is given by

$$\frac{N_1 A dz R_{12}}{W_{21}+R_{21}+A_{21}+Q_{21}}[(E_p - E_{seavg})A_{21} + (E_p - E_s)W_{21} + (E_p - E_{aseavg})Q_{21}] \tag{93}$$

In addition to the quantum defect, any ions which decay spontaneously in a radiative manner and are not trapped by the fiber in the form of ASE must be accounted for and added to the total energy balance. The total number of spontaneous emission photons not coupled into ASE is given by

$$\text{number of spontaneous photons} = N_2 A_{21} A dz (1 - \frac{d\Omega}{4\pi}) \tag{94}$$

where $\frac{d\Omega}{4\pi}$ is the fractional solid angle of spontaneous emission trapped by the fiber. This factor must be multiplied by the average energy of a spontaneous emission photon, which

was calculated earlier, and provides units of power.

$$P_{\text{spontaneous}} = E_{SEavg} N_2 A_{21} A dz (1 - \frac{d\Omega}{4\pi}) \tag{95}$$

The powers associated with the quantum defect, the spontaneous emission photons, the forward and backwards ASE beams, and the signal beam represent the totality of energy concerns. The sum of these powers should be equal to the total absorbed pump power, defined as

$$P_{\text{pump absorbed}} = P_{\text{pump in}} - P_{\text{pump out}} \tag{96}$$

The model was tested using a variety of configurations with both the two bin ASE model and the eighty bin ASE model. The parameters for the tests were 100 W input pump power with input signal powers of $10^{-5}$, $10^{-3}$, $10^{-1}$, 10, $10^3$, and $10^5$ W, with a fiber length of 10 m and signal wavelength of 1023 nm. The fractional difference in power balance is defined as,

$$\frac{P_{\text{pump absorbed}} - \Sigma(P_{\text{quantum defect}} + P_s + P_{\text{ASE forwards}} + P_{\text{ASE backwards}} + P_{\text{spontaneous}})}{P_{\text{pump absorbed}}} \tag{97}$$

The results of these tests are shown in Figure 15.

As can be seen, the fractional difference in pump power decreases markedly from approximately $10^{-7}$ to $10^{-10}$ when the signal power is increased to $10^3$ W. This is because with high signal power, the ASE and spontaneous emission terms are negligible. Therefore, the main component of error in calculating energy balance comes from the quantum defect associated with the signal. This is a much more accurate calculation than the one associated with the

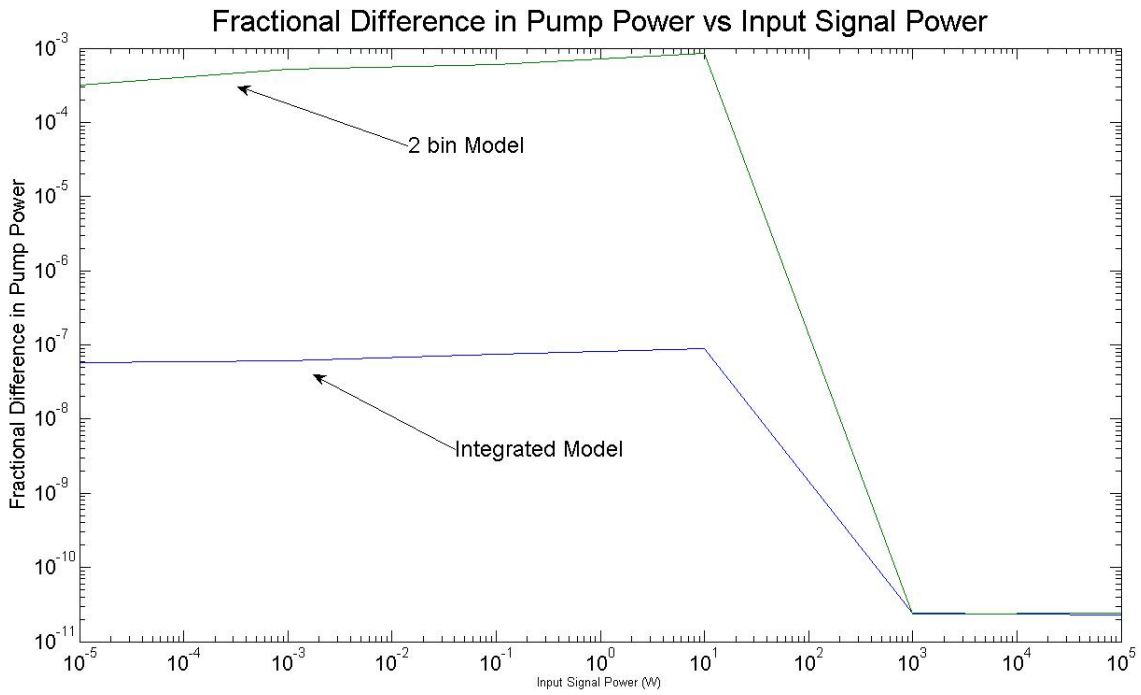


Figure 15: Fractional Pump Power

ASE, as the signal is assumed to be a narrow band with a well defined energy. Also note that the 2 bin ASE model is somewhat less accurate than the integrated ASE model. The reason for this is the same as before: the calculation of the quantum defect associated with ASE is less accurate than for the signal, and the 2 bin model already includes an approximation for the energy of the ASE photons.

Despite these differences between the different ASE models, the general result is the same: the model predicts fractional differences in absorbed pump power that are extremely small. This verifies that the model accurately preserves the physical principle of energy balance.

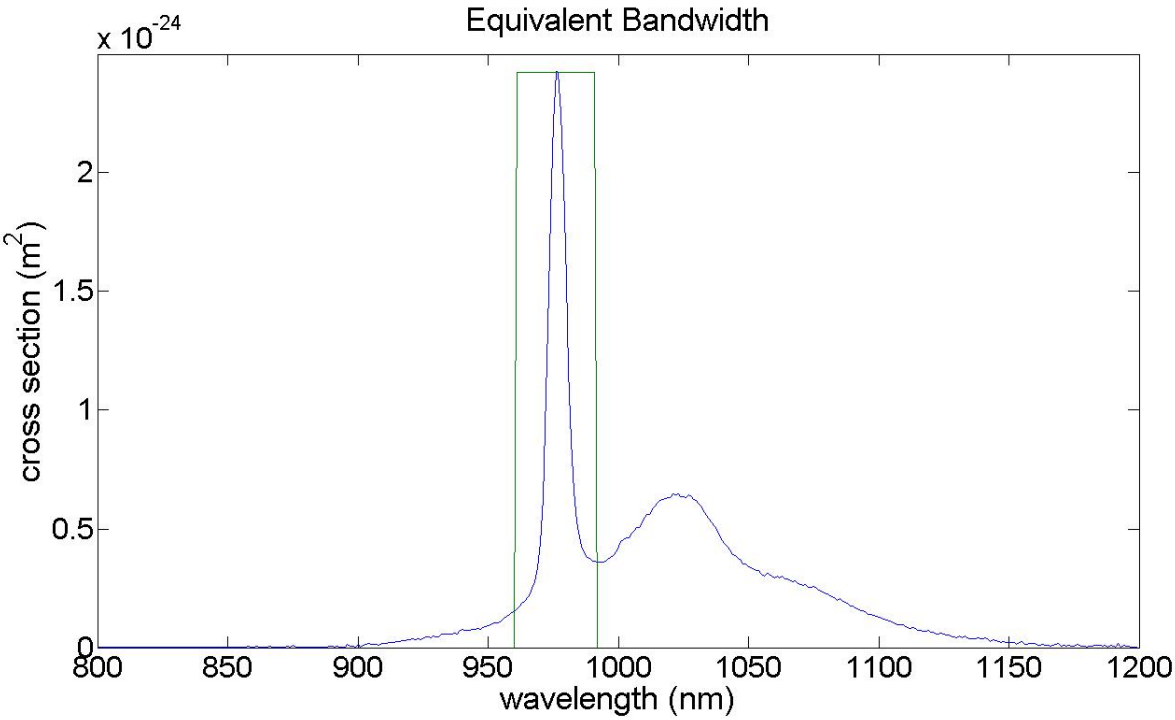


Figure 16: Emission Cross Section Spectrum with Equivalent ASE Band, One Bin

# 11 Validity of Equivalent Bandwidth Method

A major goal of this project was to investigate the equivalent bandwidth method for the approximation of amplified spontaneous emission. The most common application of the equivalent bandwidth method is to build a single ASE bin and approximate the entire transition with a single stimulated emission cross section and frequency interval. We will investigate the validity of this method using a model of Yb doped fiber amplifiers. A demonstration of the one bin equivalent bandwidth approximation is shown in Figure 16.

The one bin model does not accurately predict signal behavior for this transition. Primarily, the reason is because of the exclusion of the 1023 nm ASE from the calculations. This is an important factor that must be considered when modeling fiber lengths longer than approximately 1 meter. This can be seen in Figure 17.

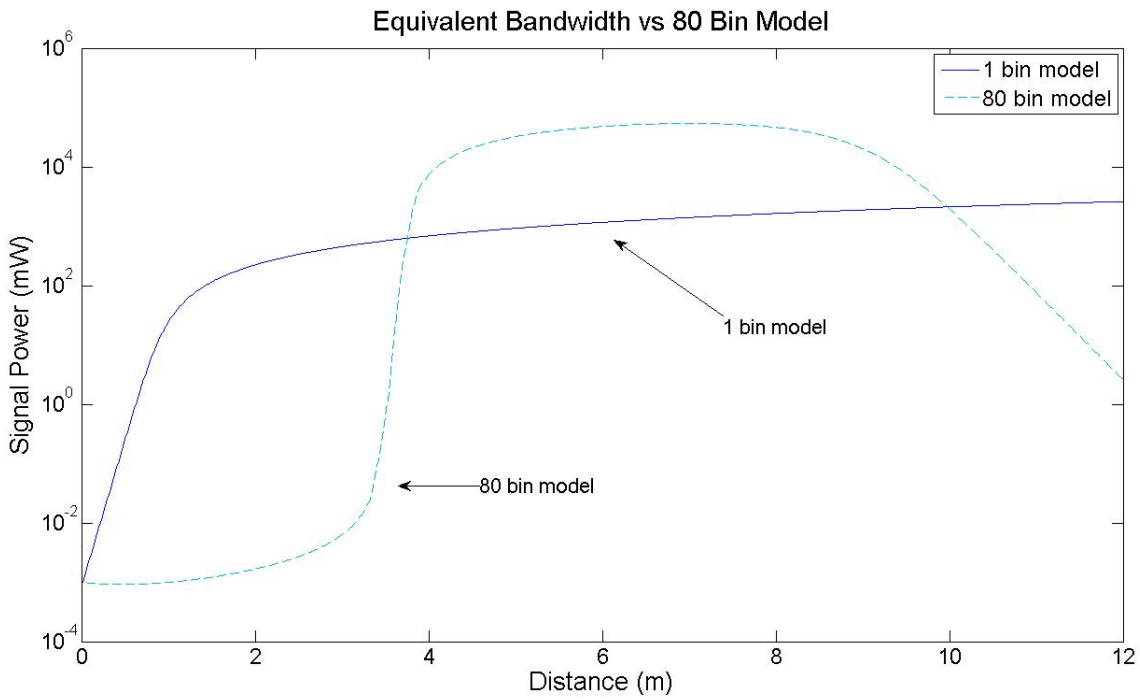


Figure 17: One Bin versus Integrated ASE Model for 12 m, Signal at 1023 nm and $P_s = 10^{-3}$ W

Due to the shape of the emission spectrum for Yb doped silica glass in the region between 800 and 1200 nm, we chose to improve the approximation of ASE by implementing the equivalent bandwidth with two independent wavelengths, as illustrated in Figure 18.

The curve is the actual emission cross section as a function of wavelength. The rectangular lines represents the equivalent bandwidth divisions. The first bin comprises the range 800-990 nm, and the second contains the range 990-1200 nm. The area of the rectangular curve in Figure 16 is equal to the integral of the emission cross section in the associated range:

$$\int \sigma_{SE}(\nu)d\nu = \Delta\nu\sigma_{SEmax} \tag{98}$$

In contrast, the 80 bin ASE model is approximated not by using the equivalent bandwidth

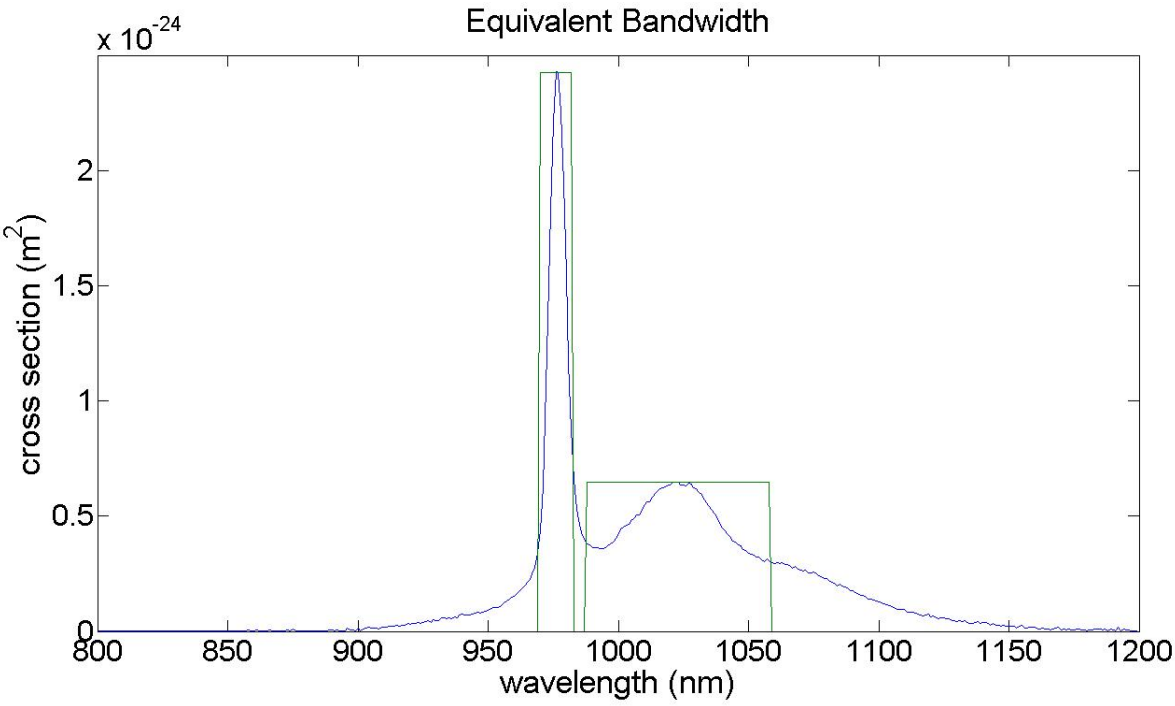


Figure 18: Emission Cross Section Spectrum with Equivalent ASE Band, Two Bin

method, but instead using a numerical integration over the spectrum. This is shown in Figure 19.

In this method, the value of the equivalent cross section is determined simply by taking the value of the cross section at the midpoint of each of the ASE ranges. In this method, $\Delta\nu$ is simply the frequency interval equivalent to 5 nm (the width of the entire spectrum divided by 80). Since the 80 bin model is a closer approximation to the physical reality, we expect the results to be more accurate than the two bin model if there is indeed a discrepancy. In addition, in order to add a second layer of verification to the ASE model, a small number of tests were done with a 400 bin model, which is the maximum number of data points in the original cross section data.

The criterion for measuring the accuracy of the two bin versus the 80 bin ASE models was that the calculation of the signal gain be the same. The signal gain is defined as

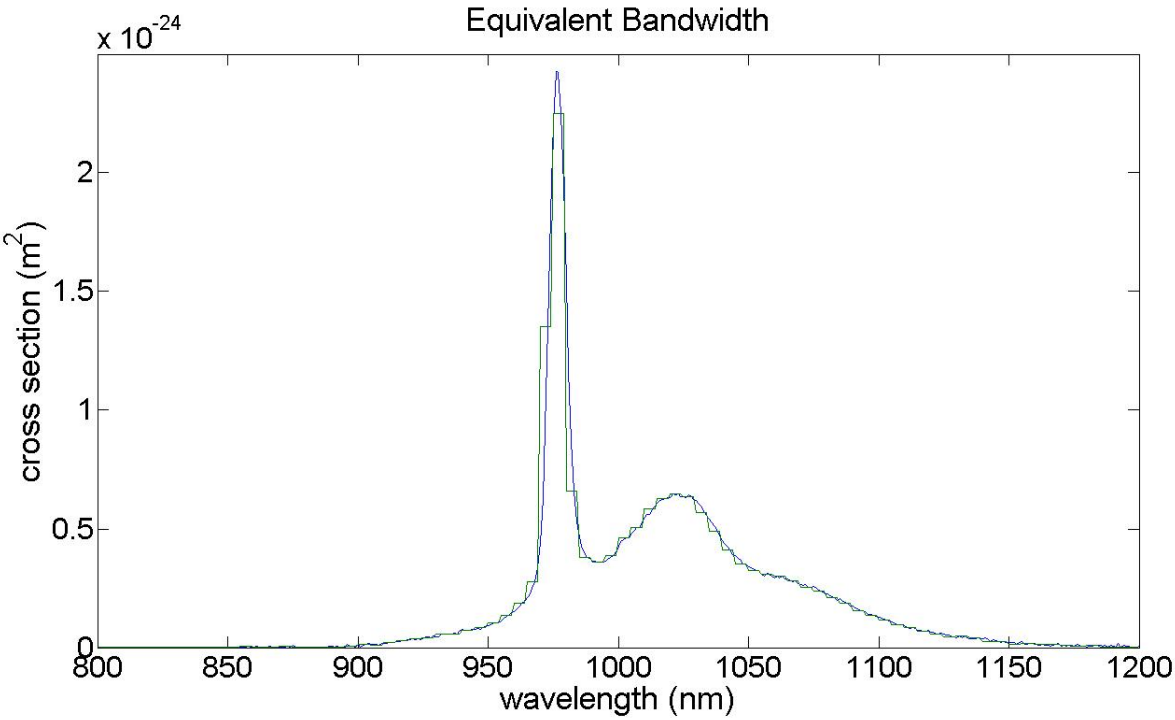


Figure 19: Emission Cross Section Spectrum with Equivalent ASE Band, 80 Bin

$$\text{Gain} = \frac{P_{S_{out}}}{P_{S_{in}}} \tag{99}$$

The model was tested using initial signal powers of $10^{-9}$-$10^{2}$ W, initial pump powers of $10^{-3} - 10^{4}$ W, fiber lengths of 1, 5, and 10 m, all with pumping at 910 nm and signal at 1023 nm. The differences in the two and 80 bin models can be seen most clearly in the results of the 10 m fiber length tests. Though both models agree for shorter fiber lengths, they begin to diverge uniformly across the range of input signal powers as the fiber length is increased. The reason for this change is subtle. In the two bin model, for each bin, the emission and absorption coefficients are defined to be at the same wavelength. This wavelength is chosen as the wavelength of maximum emission cross section in the spectrum. This method yields

a somewhat arbitrary choice of absorption cross section. In the case of ytterbium, ASE at wavelengths longer than 1023 nm cannot be accurately modeled by a two-bin method. This is because the fiber is actually transparent to ASE at the longer wavelengths, but by choosing the absorption coefficient in the manner described, our model does not represent this transparency. By failing to consider this feature, the influence of ASE at these longer wavelength is in turn ignored as well.

Because the long wavelength ASE has low absorption with significant emission, it will reduce the upper state population more than the two bin model represents. As was shown earlier, signal gain is directly dependent on maintaining a certain ratio of upper to lower state population. Therefore the two bin model does not accurately predict signal gain. As can be seen in Figures 20 and 21, the two-bin model does not depict signal depletion for longer fiber lengths. The upper state population remains approximately constant for distances longer than 5 m. This is due to the ASE near the signal wavelength being reabsorbed into the fiber. This results in the signal power being maintained for longer distances.

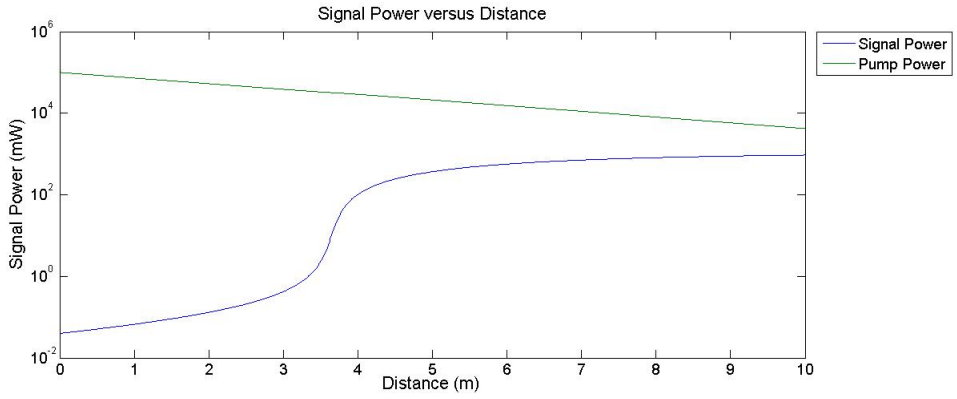


Figure 20: Signal and Pump Powers, Two Bin ASE Model

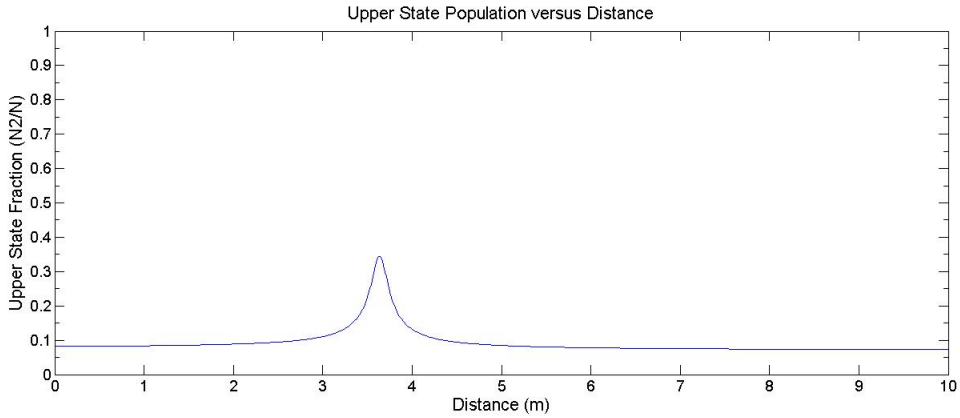


Figure 21: Upper State Population, Two Bin ASE Model

The absorption cross sections at wavelengths longer than 1023 nm are smaller than the cross section used for the 990-1200 nm bin in the two bin ASE model. The 80 bin model includes these longer wavelengths as independent entities, instead of approximating them as a single term. For longer fiber lengths, these ASE terms not included in the two-bin model can grow to significant levels as they are not limited by absorption. This can be seen in Figure 22.

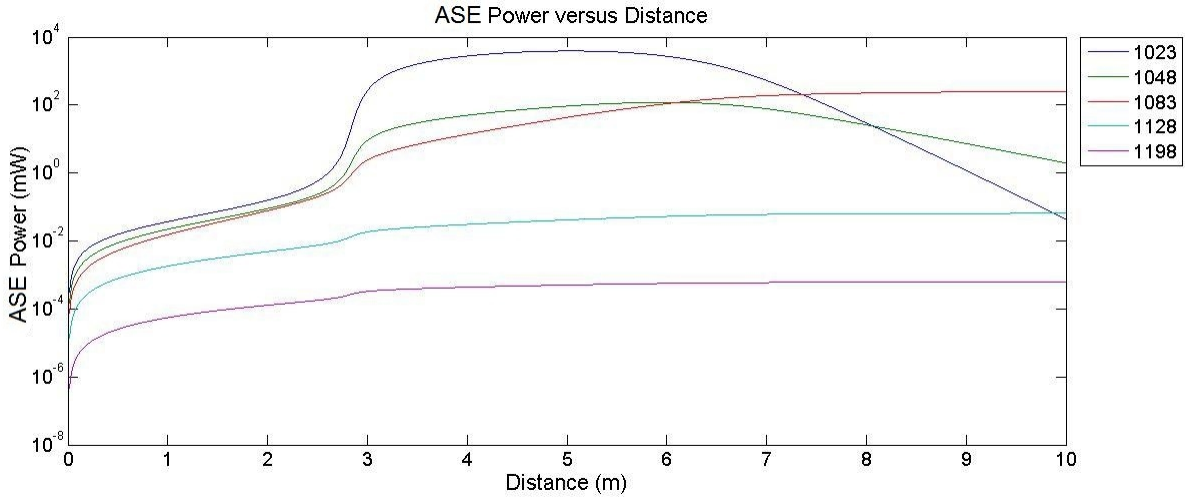


Figure 22: Long Wavelength ASE, 80 Bin Model

However, the emission cross section in this wavelength regime is comparable to the emission cross section at the signal wavelength, and this contributes to the depopulation of the upper state. When the pump power declines to insignificant levels, the upper state population will be quickly depleted by both the signal and long-wavelength ASE bands. This phenomenon is shown is Figure 23 and Figure 24.

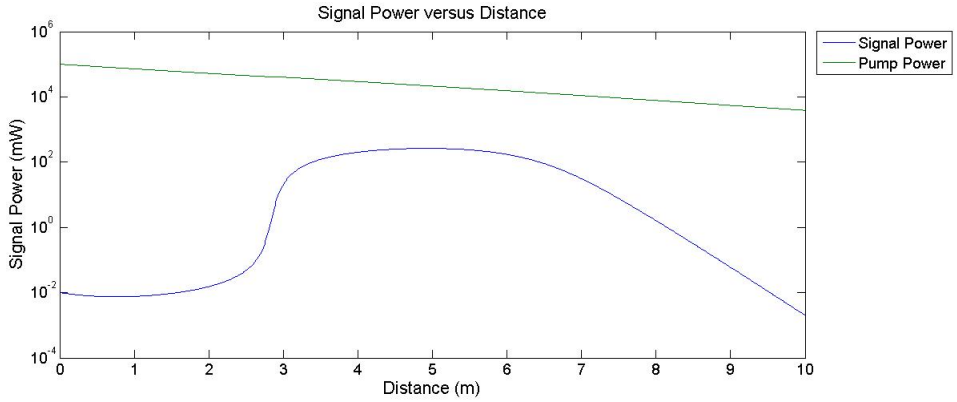


Figure 23: Signal and Pump Powers, 80 Bin ASE Model

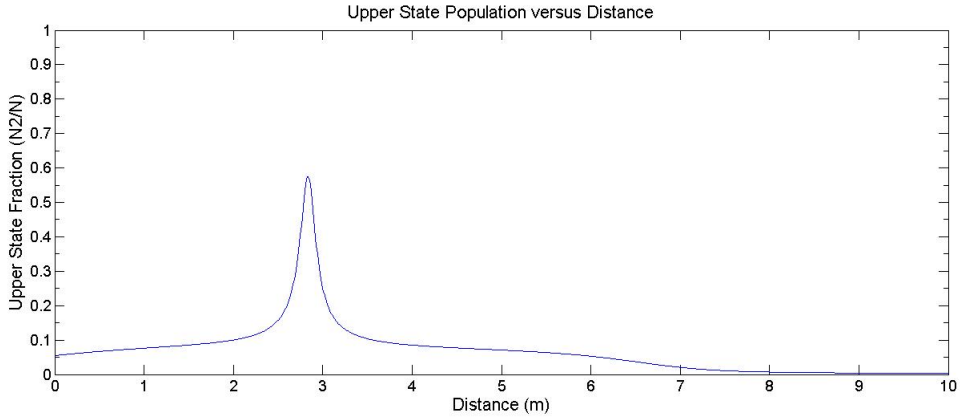


Figure 24: Upper State Population, 80 Bin ASE Model

The net result on signal gain is that the signal will be quickly attenuated by the fiber once the upper state is no longer maintained by the pump. In the two bin model, the ASE near 1023 nm was responsible for maintaining a certain upper state population; however, the 80

bin model includes long wavelength ASE terms which contribute to upper state depopulation. Therefore, the signal experiences less significant upper state population in the 80 bin model than in the two bin model, thus resulting in decreased signal gain.

This discrepancy has significant impact on the validity of the equivalent bandwidth method. The difference between the two bin and 80 bin model becomes more apparent is longer fibers. In fact, significant differences appear at lengths beyond the optimum length. Repeated tests with signal at 1023 nm using a variety of parameters indicate that this length is approximately 5 m. Therefore, the equivalent bandwidth method begins to lose validity around 5 m. For lengths much longer than 5 m, the two bin model fails to provide any valid data. Because of these caveats, we have chosen to use the integrated, 80 bin ASE model in the analysis that follows. The pure, one bin equivalent bandwidth approximation is not appropriate for use when modeling these types of three level transitions.

Despite these shortcomings, the equivalent bandwidth does provide reasonable results for fiber lengths close to or shorter than the optimum length. This is shown in Figure 25. As we can see, the 2 bin model predicts signal evolution that is remarkably similar to the 80 bin model. In fact, only when the ASE at longer wavelengths (which are excluded in the 2 bin model) become important does the 2 bin model begin to lose accuracy.

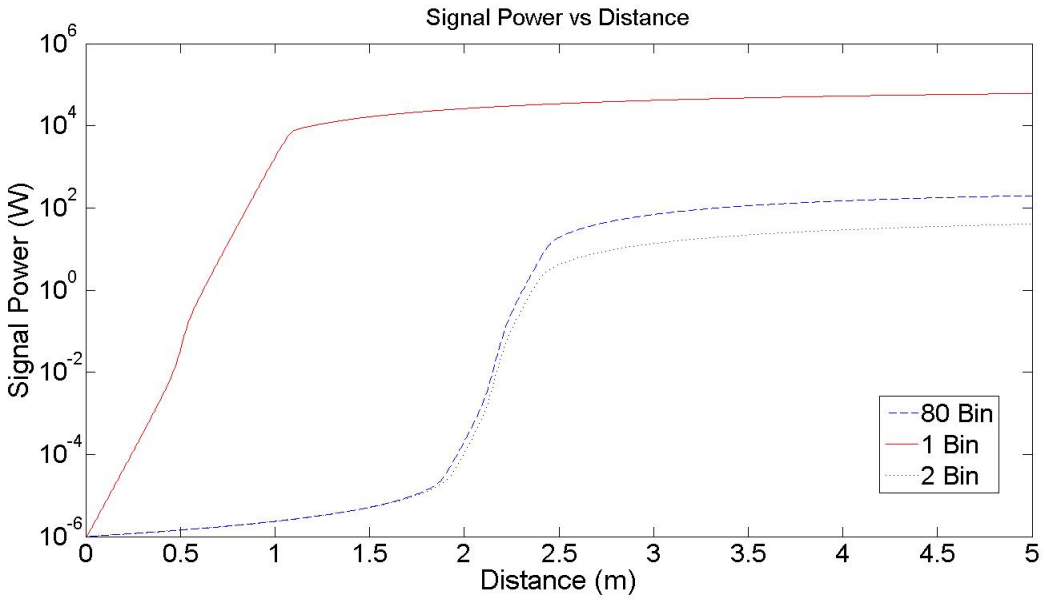


Figure 25: Signal Power vs Distance for 1, 2, and 80 bin ASE Models

# 12 Upper State Population

In this model, the upper state population is the basis for all signal and ASE gain. The evolution of this population are in turn a result of these respective powers. To better understand the properties of this population level, let's consider the solution to the rate equation for $N_2$:

$$\frac{N_2}{N} = \frac{R_{12} + W_{12} + Q_{12}}{R_{12} + W_{12} + Q_{12} + R_{21} + W_{21} + A_{21} + Q_{21}} \tag{100}$$

As one can see, the upper state population is determined by all of the transition terms; absorptions add to the population while emissions deplete it. What happens if we were to consider a system of simply a pump with no emission? We will use ytterbium as an example, with the approximation $R_{12} >> A_{21}$. To validate this assumption, for a pump power of $10^3$ W, $R_{12}$ is $6.4 \times 10^5$ $s^{-1}$, while $A_{21}$ is a constant: $1.4 \times 10^3$ $s^{-1}$.

$$\frac{N_2}{N} = \frac{R_{12}}{R_{12} + R_{21}} \tag{101}$$

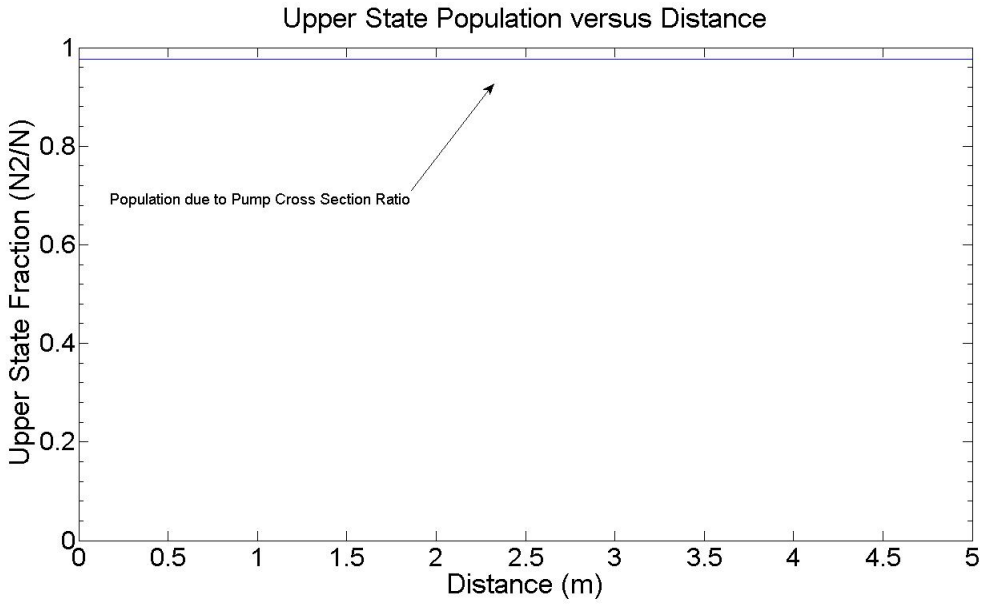


Figure 26: Upper State Population due to Pump Power Alone

which, in term of cross sections, is equivalent to:

$$\frac{N_2}{N} = \frac{1}{1 + \frac{\sigma_{ems}(\nu_p)}{\sigma_{abs}(\nu_p})} \tag{102}$$

From this relation, we can see the the upper state population is dependent purely on the ratio of emission to absorption cross section. If we take our pump wavelength to be 910 nm, we find the above equation to yield 0.9778 from the respective cross section data. We see a perfect agreement between this number and the value given by the graph in Figure 25. This value, 0.9778 as determined by the cross sections, will be called the population inversion. Notice that this value is unique to each wavelength across the spectrum.

We can further investigate the upper state population by now considering a situation in which there is also a signal at 1023 nm which eventually becomes large enough to affect the upper state.

Now we find the rate equation to take the form

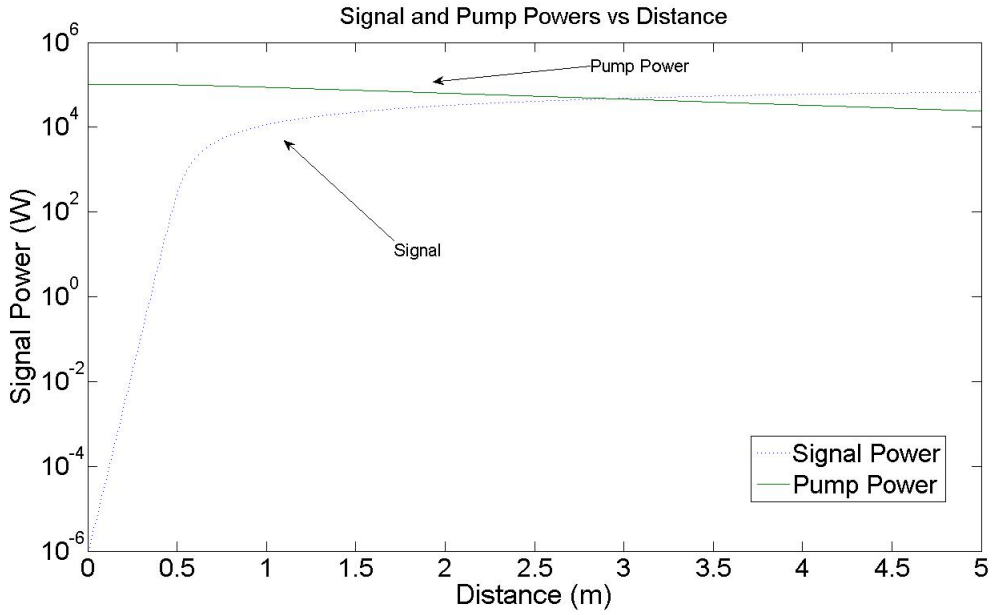


Figure 27: Pump and Signal Power vs. Distance, $P_p = 10^5$ W and $P_s = 10^{-6}$

$$\frac{N_2}{N} = \frac{R_{12} + W_{12}}{R_{12} + W_{12} + R_{21} + W_{21}} \tag{103}$$

or, in terms of the respective cross sections, powers and associated constants,

$$\frac{N_2}{N} = \frac{c_P P_{Pump} \sigma_{abs,p} + c_S P_{Signal} \sigma_{abs,s}}{c_P P_{Pump} \sigma_{abs,p} + c_S P_{Signal} \sigma_{abs,s} + c_P P_{Pump} \sigma_{ems,p} + c_S P_{Signal} \sigma_{ems,s}} \tag{104}$$

where we have, for simplicity, defined $c = \frac{1}{EA}$, A being the area of the core and E being the energy of the respective photon whether it be pump, signal or ASE.

First, if we consider the case where the pump power is significantly greater than the signal power, we see that this expression reduces to the result for pump light only. Alternatively, if the signal power is significantly greater than the pump the above expression reduces to the same cross section dependent expression as before, except with signal cross sections instead

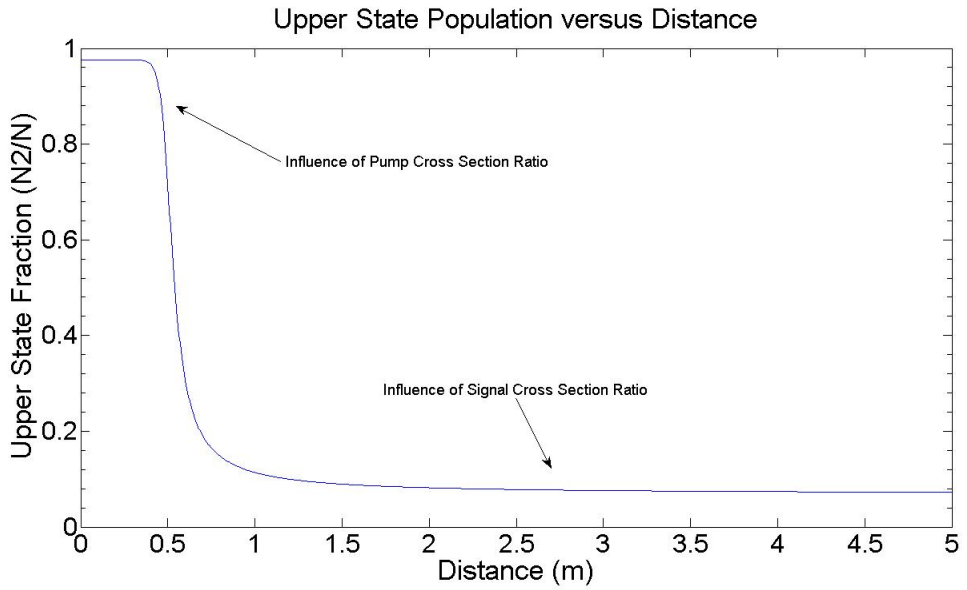


Figure 28: Upper State Population due to Pump and Signal, $P_p = 10^5$ W and $P_s = 10^{-6}$

of pump. For signal at 1023 nm, we find a value of 0.07044N for the population inversion. From Figures 27 and 28, we can see that, during the first few centimeters of the fiber where the pump light has much higher power than the signal, the upper state population is close to the value we saw in the case of only pump light. After this point, the population inversion approaches a much smaller value as the signal grows within the fiber. At the beginning of the fiber, the rate equation will be mostly influenced by the pump term. Later, the signal becomes dominant and this term influences the rate equation. Notice how the graph of upper state population in Figure 27 represents this behavior.

One of the more complex phenomena exhibited by our model has presented itself as a sharp peak in the upper state population in cases where ASE is considered. This upper state can be seen in Figure 29. This spike can be explained somewhat qualitatively by considering terms in the rate equation at this point. First, it is key to understand that our model calculates ASE as two separate terms, one propagating forward through the fiber, the other backward. If we consider Figure 30, we see that the the forward ASE dominates on the left

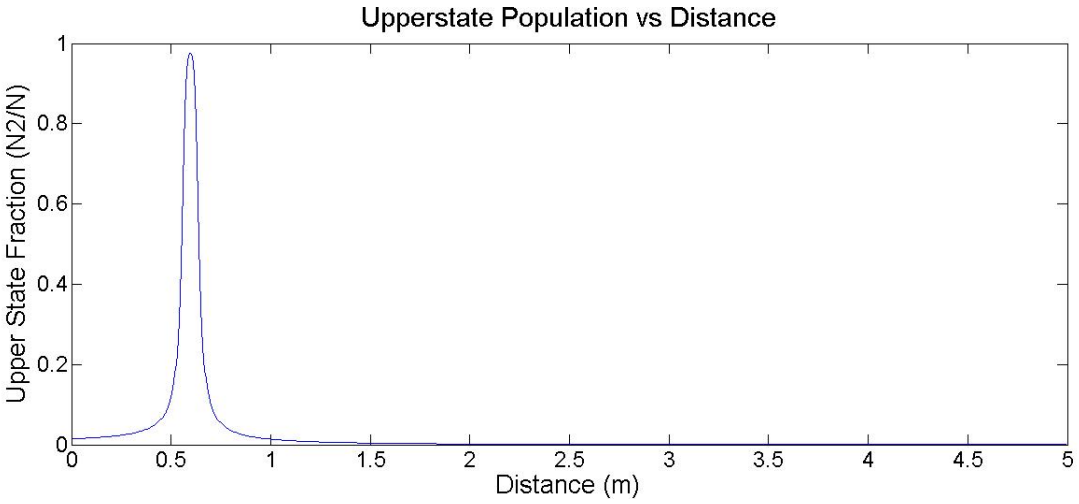


Figure 29: Upper State Population due to backwards and Forwards ASE, $P_p = 10^5$ W and $P_s = 10^{-6}$ W

of the fiber, while the backwards ASE is dominant on the right side. At the point where these powers are equal, we see that both are significantly reduced from where they are at a maximum. If we once again consider the rate equation is this case, one can see that the dominant term where the spike occurs is, in fact, the pump term. Due to this, the upper state population is brought toward the population inversion for the pump wavelength.

Considering the phenomena we just investigated, we can now make predictions on the behavior of a system of more terms based purely on the ratio of the individual term's cross sections. As we saw, the upper state population was most limited by the term of highest power, when the powers were significantly different in magnitude. In the case where two or more terms of comparable magnitude are present in the fiber, the upper state population tends towards the term with the lowest population inversion. This is intuitive, as terms that can achieve gain in this situation will tend to grow and eventually themselves become significant in the rate equation calculation. Finally, notice that this population inversion is the same expression we found earlier for the minimum value of upper state population required to achieve gain. This is the value that the upper state will approach if only one

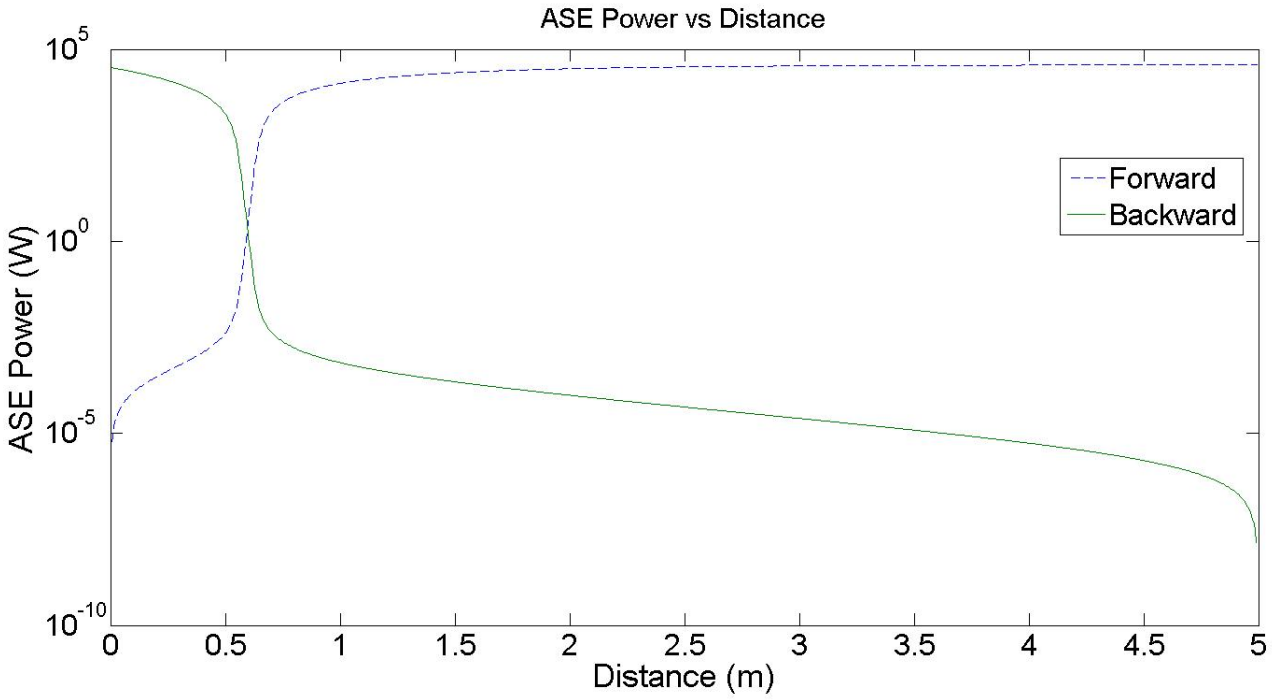


Figure 30: Backwards and Forwards ASE Terms for Ytterbium, $P_p = 10^5$ W and $P_s = 10^{-6}$

term of a specific wavelength is present in the fiber. It is an important figure that, as we will see, will appear in much of the analysis that follows.

# 13 The Ytterbium-Doped Fiber Amplifier

The ytterbium doped fiber amplifier has many advantages. First, the absorption cross section for Yb (Figure 31) ranges from 800 up to 1000 nm. The emission cross section also has a broad range, from 980 up to 1150 nm. Second, the energy level diagram (shown in Figure 32) for Yb is extremely simple, as it is entirely encompassed by the ${}^2F_{5/2}$ to ${}^2F_{7/2}$ transition.

Third, while the transition itself is a three level transition, at longer wavelengths the spectrum behaves more like a quasi-four level system, as there is low absorption (character-

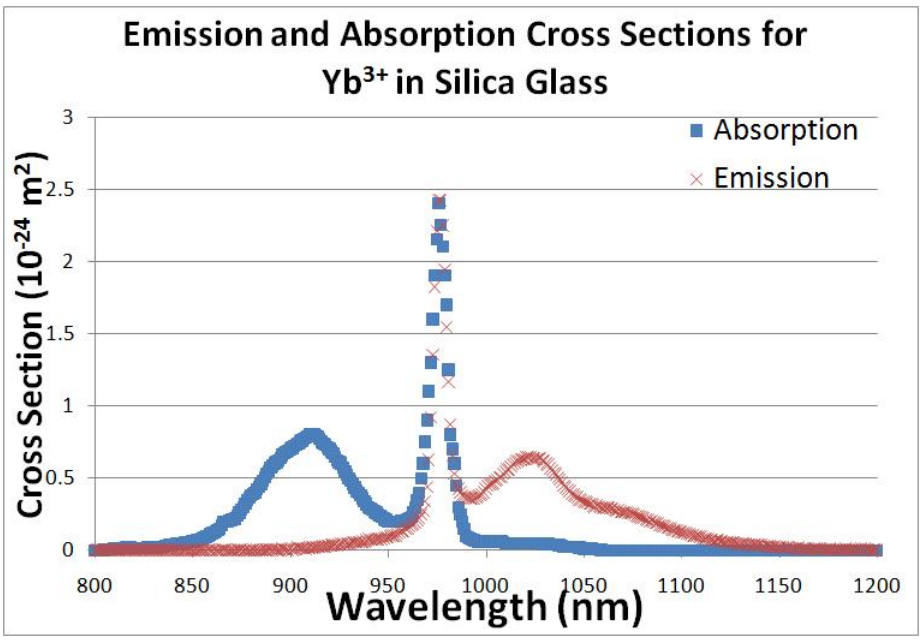


Figure 31: emission and absorption cross section for Yb

istic of four level systems). This has the advantage of low absorption with high emission, ideal for signal gain. Fourth, there is no excited state absorption as there is in Nd, which is a serious limitation on choice of signal wavelength for that dopant. Finally, the longer relaxation time indicates that Yb doped fibers may have lower threshold pump powers for signal gain. All of these factors make Yb an interesting choice for signal amplification.

In this case, we will be examining the case of Yb doped silica glass with pumping at 910 nm. The signal wavelengths will be chosen at three different values: 978 nm, 1023 nm, and 1060 nm. The 978 nm signal choice has the advantage that fibers can be made much shorter and can extract pump power more efficiently than the other choices. However, the range of effective fiber lengths must be carefully chosen, as this wavelength also has considerable absorption. The 1023 band has significantly reduced absorption compared to 978 and therefore allows the designer to be less precise with their choice of fiber length; moreover, the high emission to absorption cross section ratio allows gain with lower population

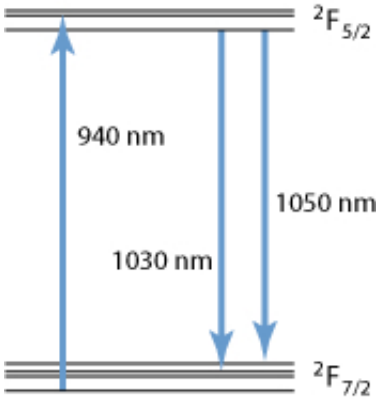


Figure 32: Energy Level Diagram for Yb

inversions. Finally, the 1060 nm band is transparent to the fiber, implying that the choice of fiber length can be extremely imprecise. However, the lower absolute emission cross section compared with the other bands also make it a less efficient choice than 1023 or 978 nm, as the spontaneous decay rate becomes more significant in the rate equation.

The effect of ASE in Yb amplifiers is extremely subtle. There are three major ASE bands in Yb, each overlapping with the potential signal wavelengths. As the signal, pump, and ASE light propagates through the fiber, the different ASE bands become more dominant. For distances up to about 1 m, the 978 nm band is most important, as it grows rapidly due to its high emission cross section. However, this band also has high absorption, and therefore is reabsorbed quickly as the pump power decreases. At this point, the 1023 nm ASE begins to take over, as it generally experiences sufficient upper state population to grow in this range. From about 1 to 5 m, this band is most dominant. For lengths longer than this (after the pump is almost completely absorbed by the fiber), the 1060 ASE becomes the only remaining light in the fiber. This is because the fiber is transparent to this light. The 1060 ASE assures that the upper state population will decrease quickly to zero after sufficient length. Because these bands are each important at different points in the fiber, it is necessary to include at least this many ASE bins in the analysis. We saw earlier that

the one bin equivalent bandwidth approximation was inadequate to model this behavior; moreover, we saw that the two bin approximation, while much more accurate, did not model the correct behavior for longer fiber lengths. The difference in computational time between the two-bin equivalent bandwidth and the eighty bin model, while not insubstantial, was not sufficient to justify the use of the less accurate methods. Therefore, for all analysis in this section the eighty bin approximation will be used.

## 13.1 YDFA at 1023 Signal Wavelength: Varied Signal Power

We will begin by examining the effect of changing the input signal power while maintaining a constant pump and fiber length. In this situation, the range of input signal powers will be $[10^{-9}, 10^{-7}, ..., 10^{3}, 10^{5}]$ W with pump power of $10^5$ W. In practice, a pump power of $10^5$ W is much higher than can feasibly be created; therefore, we include this value as a demonstration of a case of extremely high pump power. The fiber length will be 5 m. It will later be shown that 5 m is close to the optimum fiber length; moreover, the optimum fiber length is dependent on a variety of parameters but is very closely tied to the ratio of core to cladding area.

In the Figures 33-35 the signal power and ASE powers for the two major ASE bands (978 and 1023 nm) are plotted as a function of distance for a variety of signal powers. For large signal powers, the ASE terms are markedly smaller than in other configurations. This is due to the signal power dominating the rate equation and forcing the upper state population towards 0.07N (the population inversion for 1023 nm in Yb) early in the fiber, as can be seen in Figure 36. On the other hand, smaller signal powers tend to have little effect on ASE powers or the upper state population until later in the fiber. This is the reason for the shifting of the spike in upper state population back towards the beginning of the fiber, as the signal becomes a dominant factor in the steady state equation earlier for larger signal powers. During the first few meters of the fiber, smaller input signals experience moderate

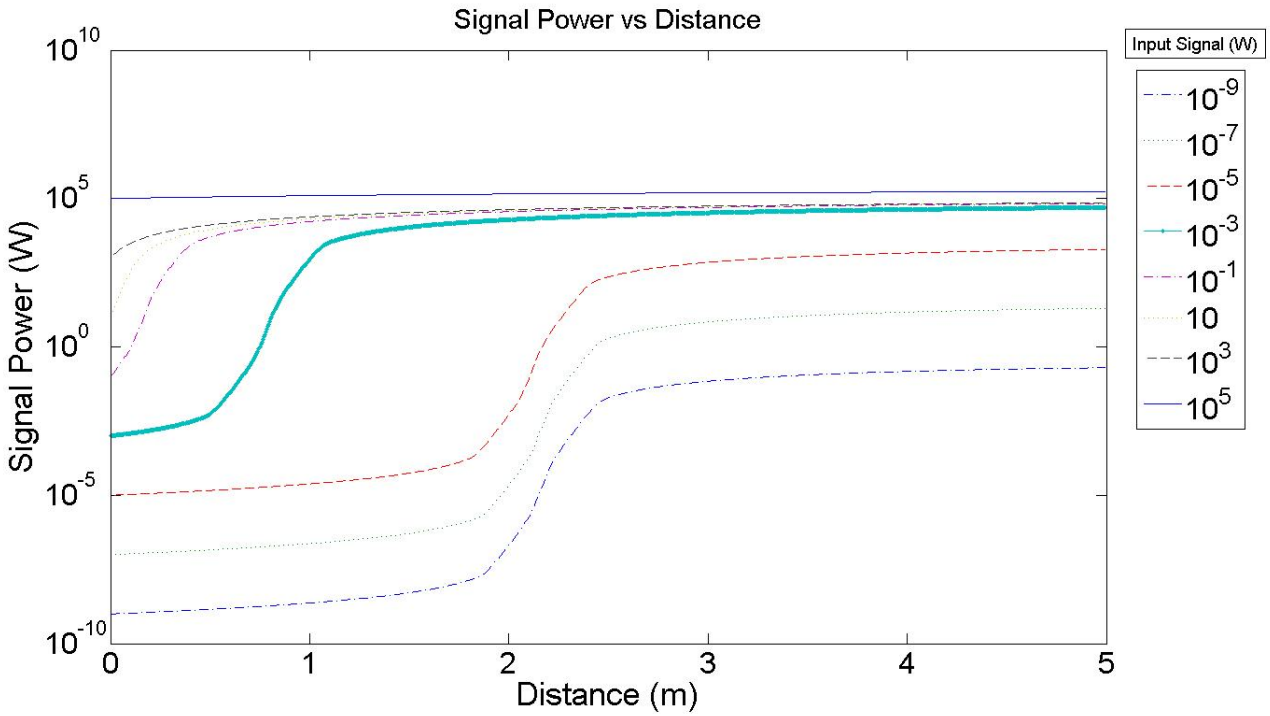


Figure 33: Signal Power vs Distance, $P_p$ $10^5$ W

growth, as they benefit from sufficient upper state population while still having little effect on the upper state. Later, these same low input signal powers grow explosively during the upper state peak and then slow to remain roughly constant for the remainder of the fiber.

In Figure 37, the signal experiences moderate growth for several meters. The reason for this is clear from Figure 38, the graph of upper state population. While the upper state is not as high as it would be with only the pump light present (0.97N), it is still higher than the condition for signal gain ($\frac{N_2}{N} > 0.07N$). This is because the dominant light for much of the early length of the fiber is the 978 nm ASE transition and the pump light. In the 978 nm ASE transition, the absorption and emission are equal, implying that the upper state should be half of its maximum value. It can be seen in Figure 37 that the 978 nm ASE is in fact a significant factor at this point in the fiber. Meanwhile, the signal grows slowly, until about 50 cm, where it grows to a significant level. At this distance, the signal power is now

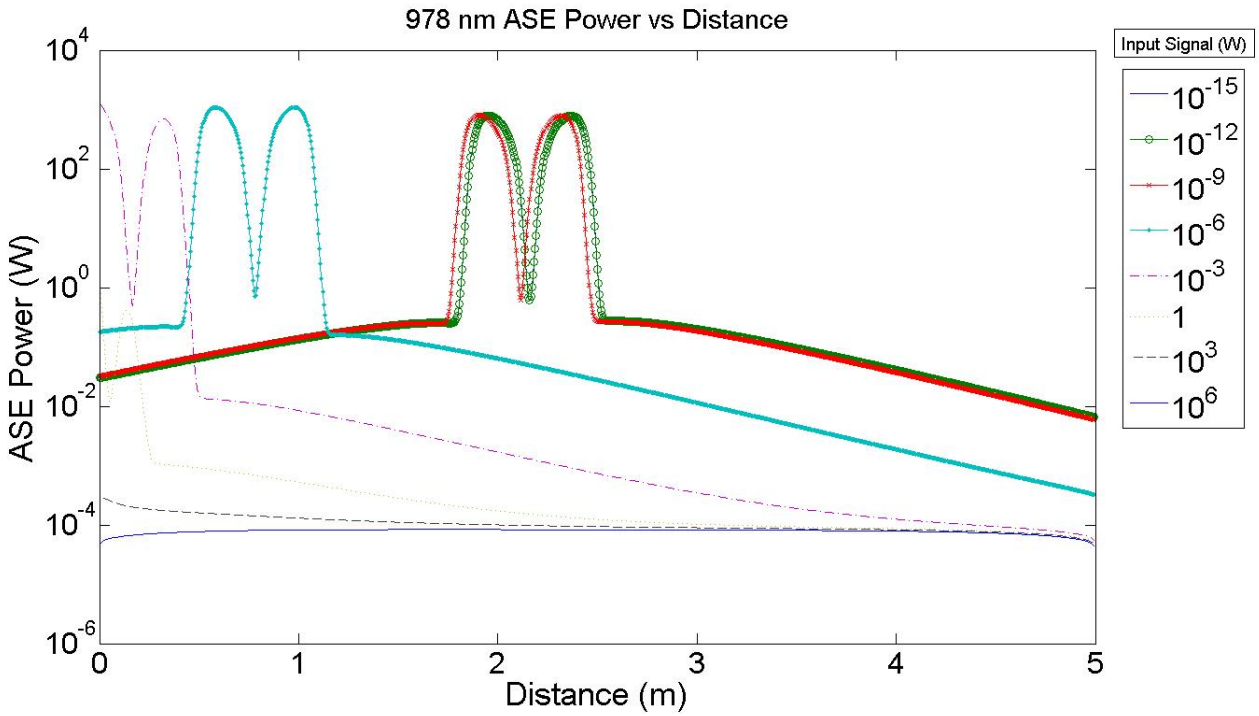


Figure 34: 978 nm ASE vs Distance, $P_p$ $10^5$ W

comparable to the 978 nm ASE power. As mentioned earlier, the upper state population tends to the lowest population inversion if there are more than one dominant terms present in the fiber. At this point, the 978 nm ASE and the signal power are both of comparable magnitude and therefore the upper state will tend towards the level dictated by the signal. This can be seen in the upper state population, as well. At the same point that the signal power ends its period of exponential growth the upper state population plummets to much lower levels as well. The signal then remains roughly constant for the remainder of the fiber. As could be expected, the ASE at 1023 nm in many ways mirrors the behavior of the signal light, as they are both at the same wavelength.

In the following case, the initial signal power is extremely small ($10^{-15}$ W), but all other parameters are the same as the previous configuration. These results are shown in Figures 39-40. Here, a different situation arises. The signal does not have a significant effect on the

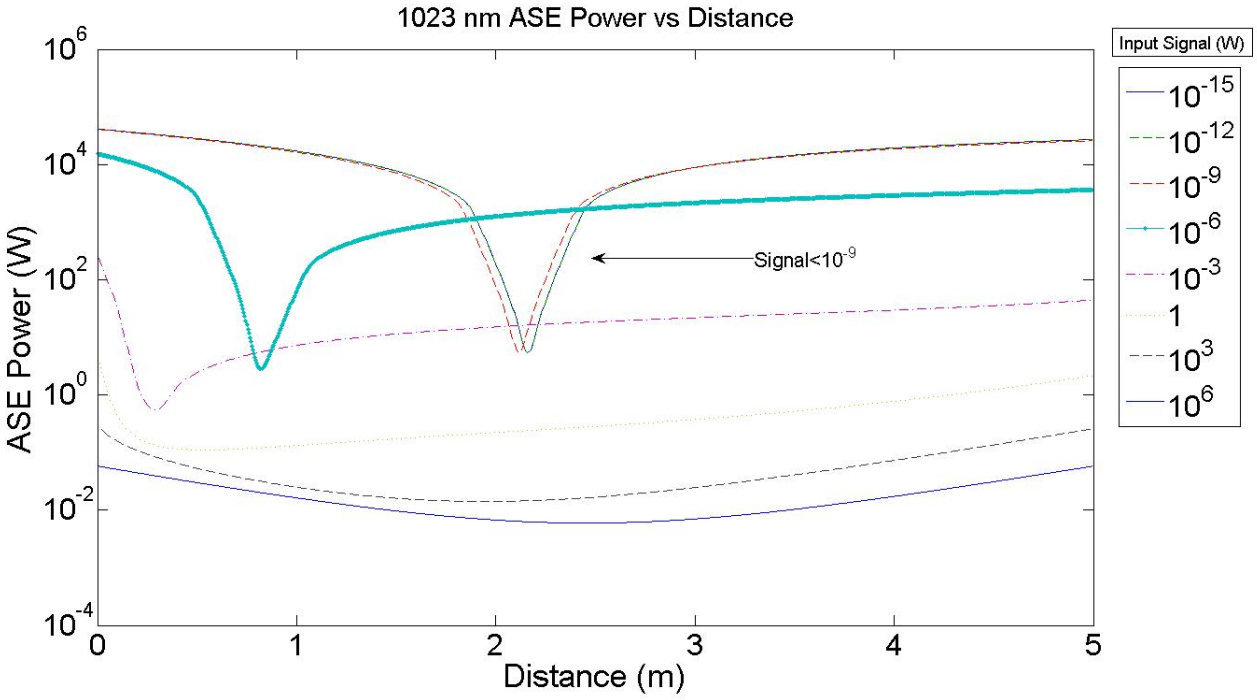


Figure 35: 1023 nm ASE vs Distance, $P_p$ $10^5$ W

upper state during its evolution down the fiber. It experiences explosive growth near the middle of the fiber, where the upper state spike exists. Because the signal has a negligible effect on upper state population, the 1023 nm ASE is not limited by a strong input signal. The population inversion tends to approach 0.07N as the 1023 nm ASE grows. This is the same value as if the signal was the most dominant factor, as both terms are at the same wavelength. The upper state approaches this value while the ASE receives most of the absorbed pump power. Therefore, the 1023 nm ASE presents a serious impediment to signal gain in this case.

As a final scenario, the initial signal power is chosen to be very high, $10^4$ W, again with other parameters the same as the previous examples. These results are shown in Figures 41 - 42. With extremely high signal powers, the upper state population remains much lower than in other cases. The effect is to reduce the growth of ASE and generally provides a more

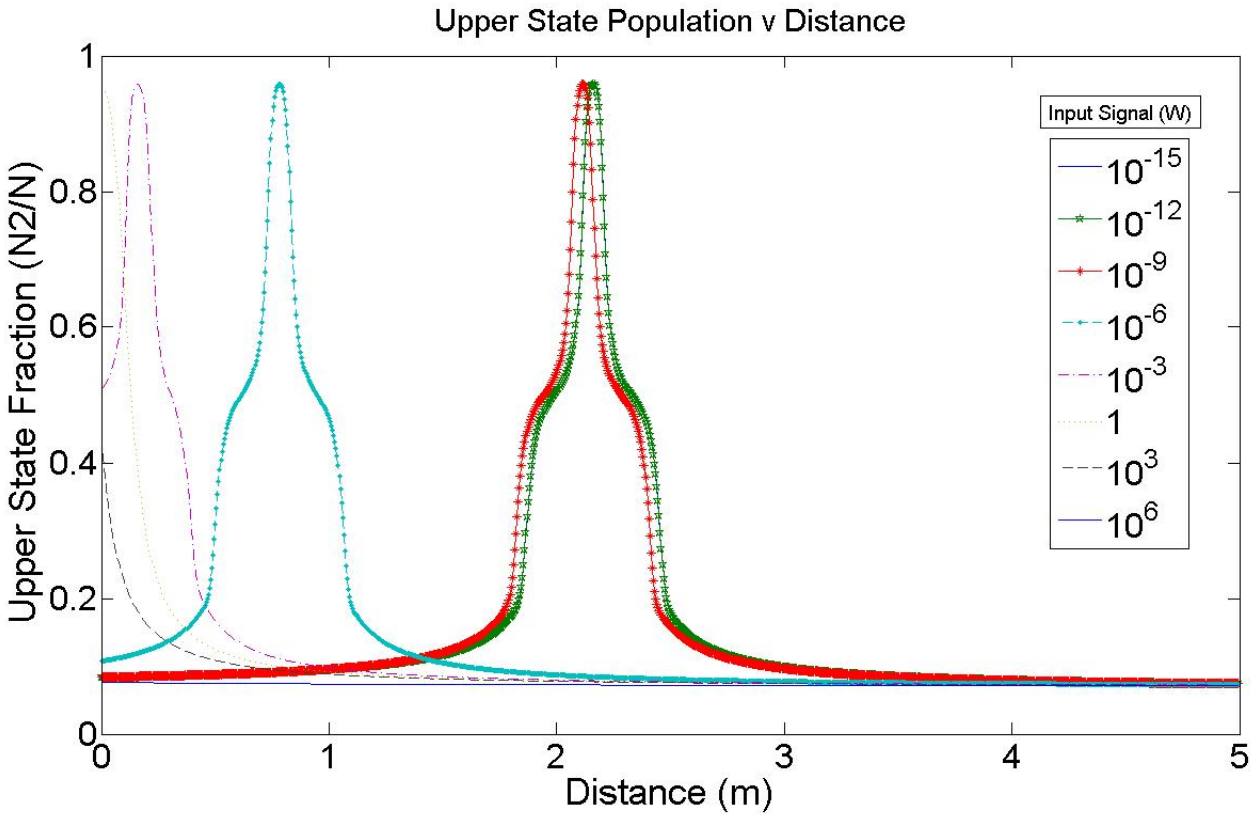


Figure 36: Upper State Population vs Distance, $P_p = 10^5$ W

efficient conversion of pump to signal light.

The most significant point of this analysis is that the effect of changing the input signal power has acute effects on the upper state population level of the fiber. For large input signal powers, the ASE does not grow to nearly the same levels as in other configurations. This is intuitive, as the signal tends to reduce the upper state population to lower values, while the creation and propagation of ASE requires a large upper state population. It is also the case that lower initial signal powers, once amplified, can slow the propagation of ASE terms. When the signal becomes large enough, the situation reduces to the case of high input signal power, once again lowering the upper state population. This is relevant for a smaller range of input signal powers: high enough so that they are able to grow to significant levels but

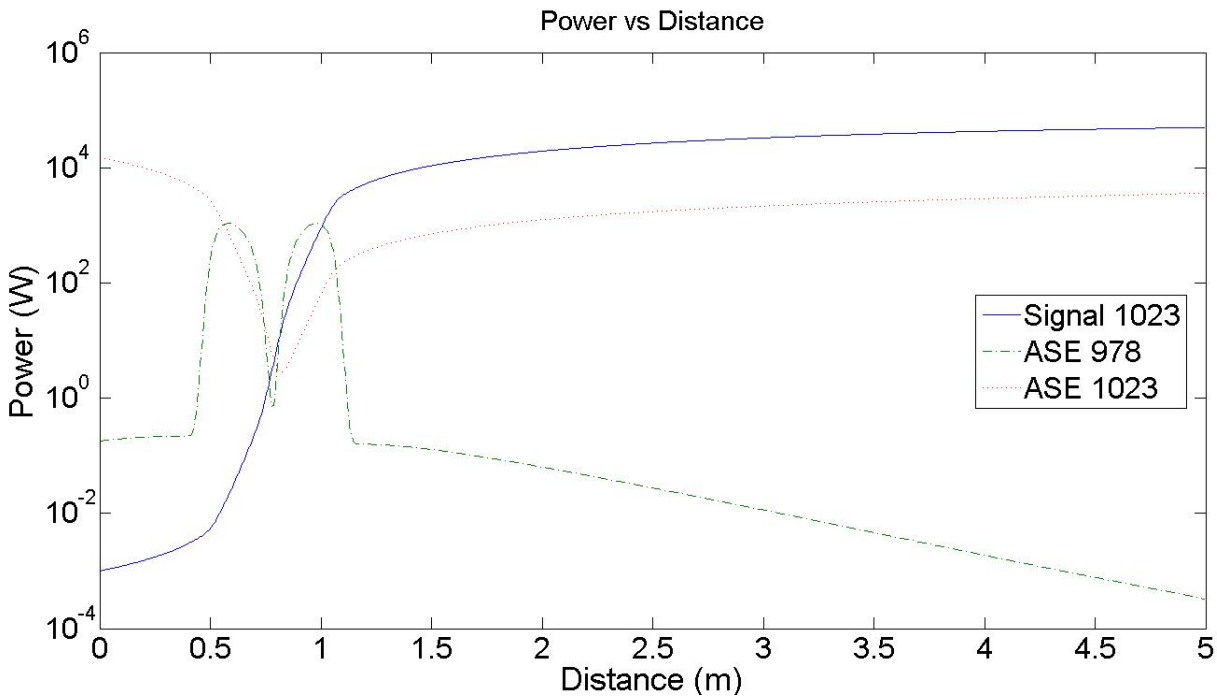


Figure 37: Signal, 978 and 1023 nm ASE Powers vs Distance, $P_s = 10^{-3}$ W, $P_p = 10^5$ W

low enough that population levels in the early part of the fiber remain relativity uninhibited. However, if the initial signal power is extremely small, it will have little effect on upper state population for the entire length of the fiber.

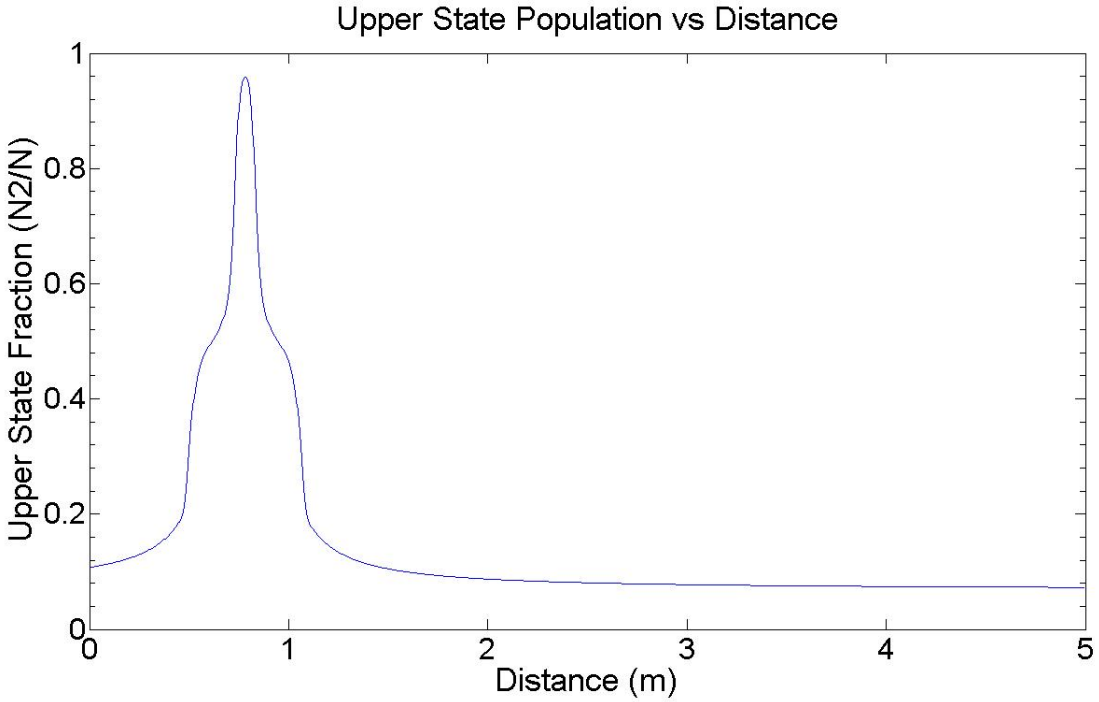


Figure 38: Upper State Population, $P_s = 10^{-3}$ W, $P_p = 10^5$ W

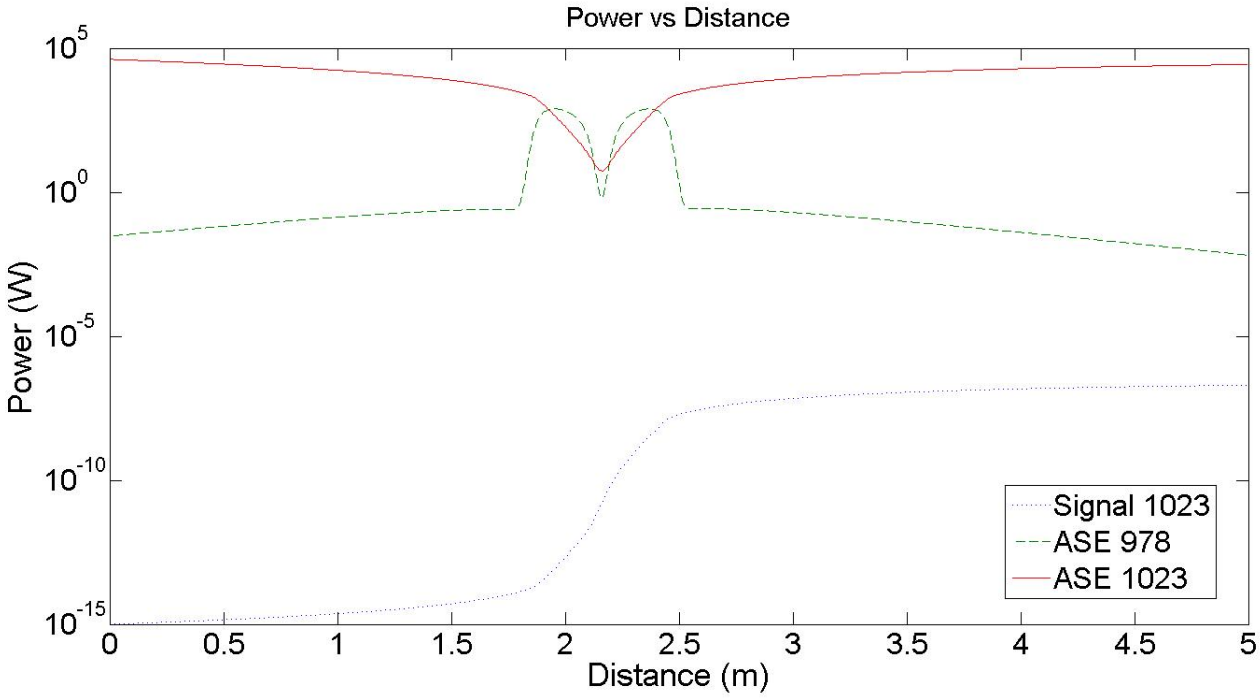


Figure 39: Signal, 978 and 1023 nm ASE Power vs Distance, $P_s = 10^{-15}$ W, $P_p = 10^5$ W

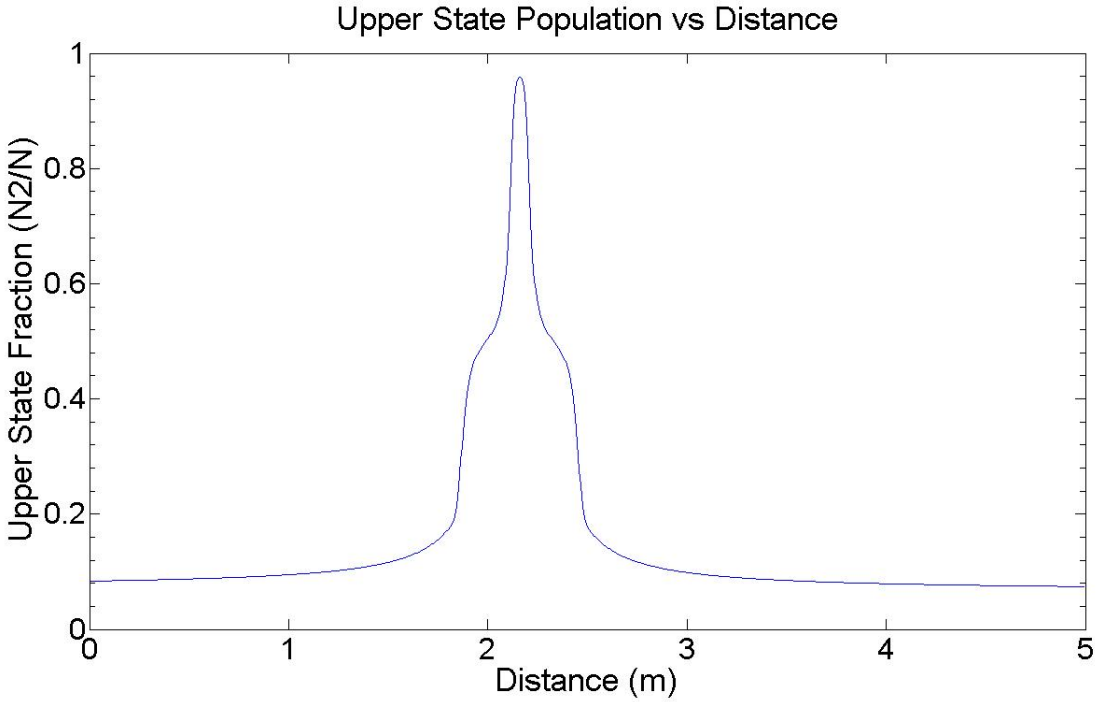


Figure 40: Upper State Population, $P_s = 10^{-15}$ W, $P_p = 10^5$ W

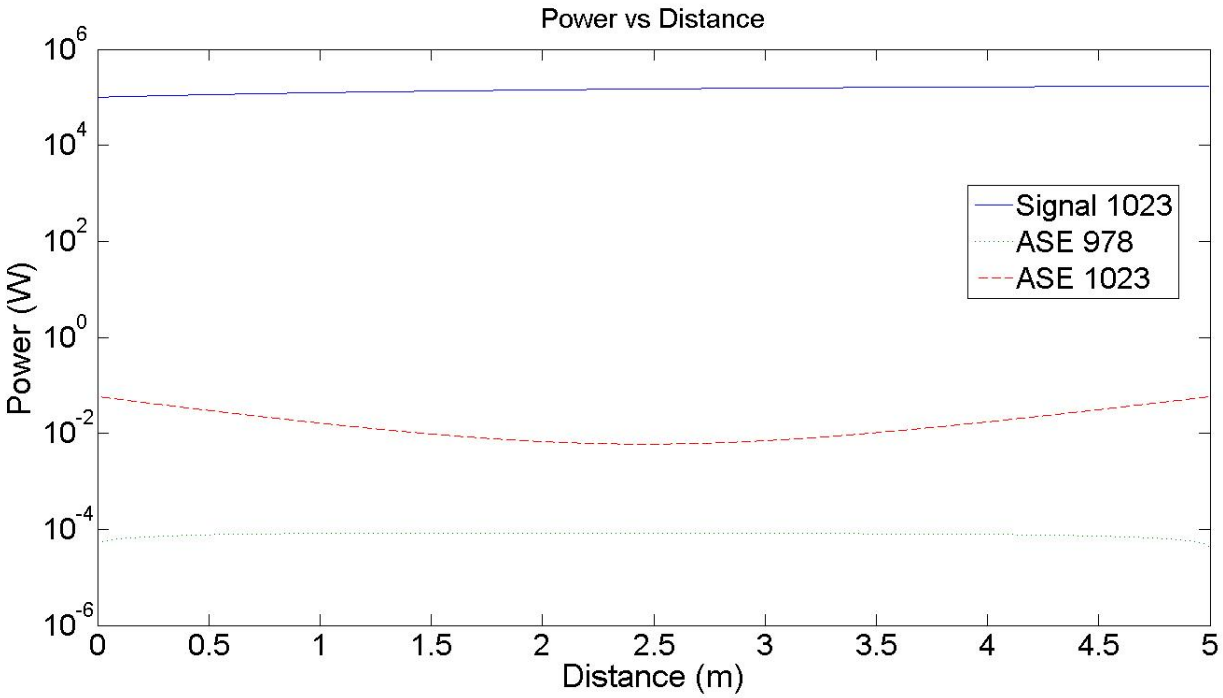


Figure 41: Signal, 978 and 1023 nm ASE Power vs Distance, $P_s = 10^4$ W, $P_p = 10^5$ W

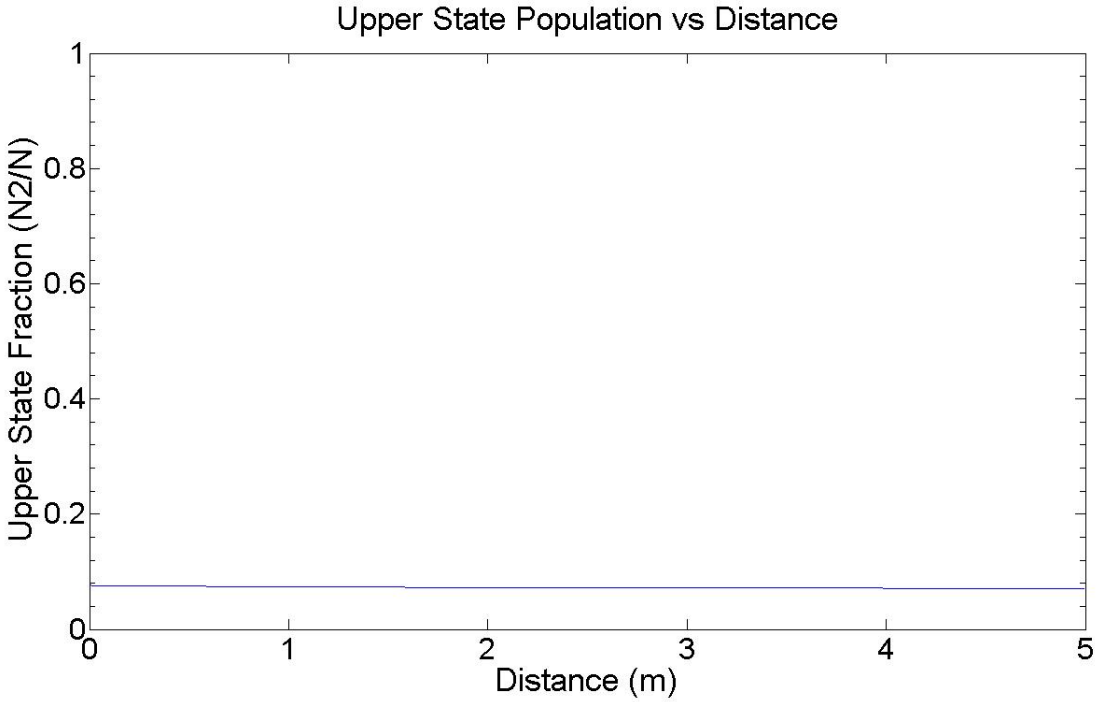


Figure 42: Upper State Population, $P_s = 10^4$ W, $P_p = 10^5$ W

## 13.2 YDFA at 1023 Signal Wavelength: Varied Pump Power

Next we will examine the effect of increasing the pump power while fixing the input signal power. The signal power in this case will be $10^{-5}$ W, which, as we saw in the earlier analysis, is sufficiently large to grow to a significant level within the chosen fiber length (5 m).

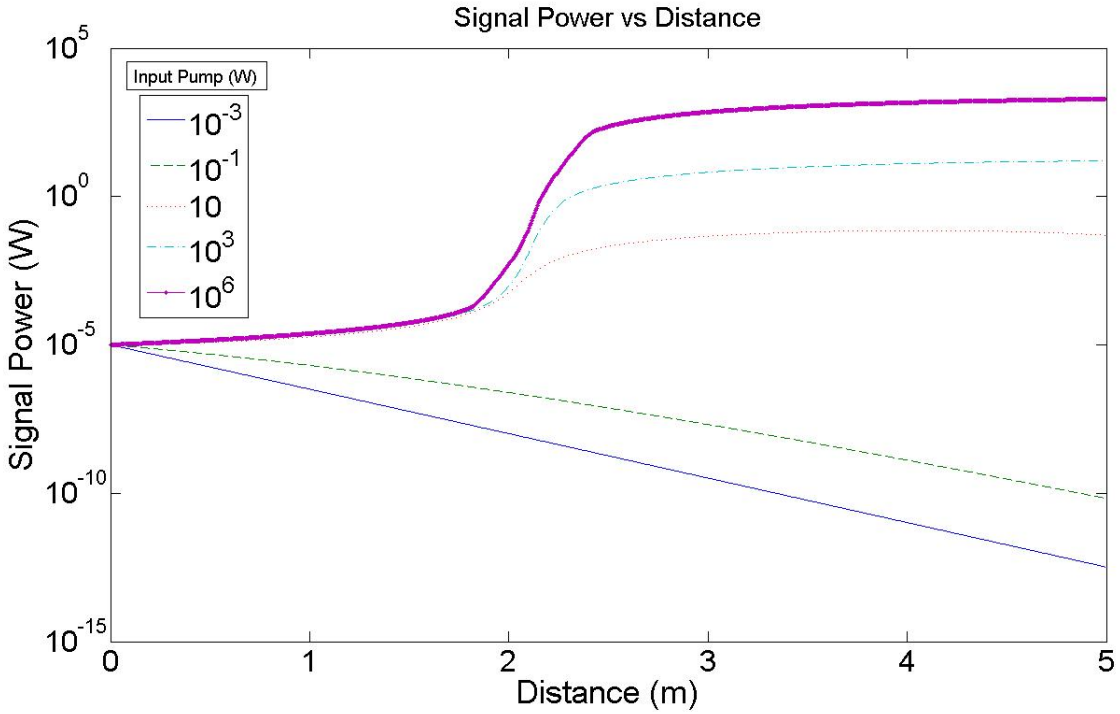


Figure 43: Signal Power vs Distance, $P_s = 10^{-5}$ W, Varied Pump

For small input pump powers, the pump power is not sufficient to provide gain, as shown in Figure 43. For pump power above the threshold pump particular to the input signal wavelength, the signal can experience significant gain. As is expected, higher pump power yield higher output signal powers. As can be seen in Figure 44, the nature of pump power absorption is unaffected by its initial value.

ASE, as expected, is increased by higher initial pump powers, as shown in Figures 45 - 46 . However, the output signal power is not linearly related to input pump power. This is due to the fact that with higher pump powers, the upper state population yields larger

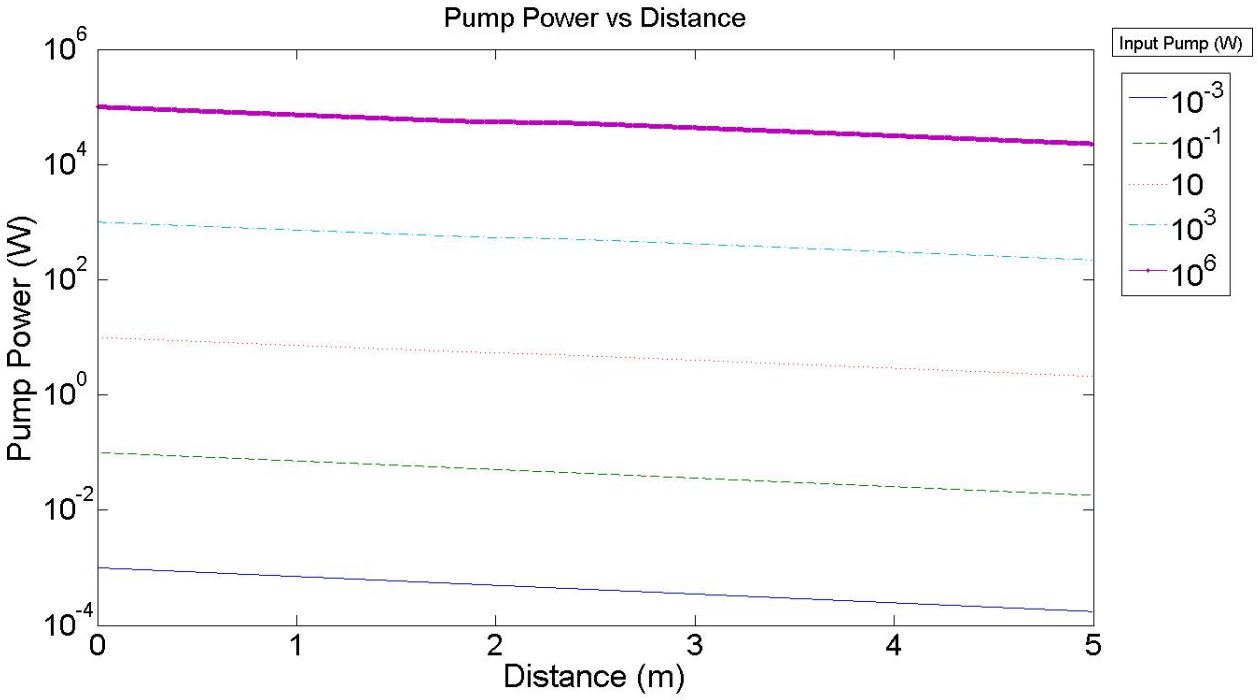


Figure 44: Pump Power vs Distance, $P_s = 10^{-5}$ W, Varied Pump

ASE source terms. Moreover, the signal power cannot take full advantage of this upper state population as compared to the ASE. Since the ASE propagates in both backwards and forwards directions, whereas the signal only propagates forwards, the signal earlier in the fiber is limited by large backwards ASE. The upper state population is illustrated in Figure 47.

As we know, the 1023 nm ASE is composed of two components, one backwards the other forwards. When there is sufficient pump for gain at this wavelength, both terms will grow and at some point intersect. This coincident point is the location of the population spike as neither ASE has grown to prominence. This explains the shape of the ASE power versus distance graph shown above. Finally, the influence of the 1023 nm ASE on the population level is responsible for the rapid depletion of the 978 nm ASE outside the region between 1.7-2.5 m.

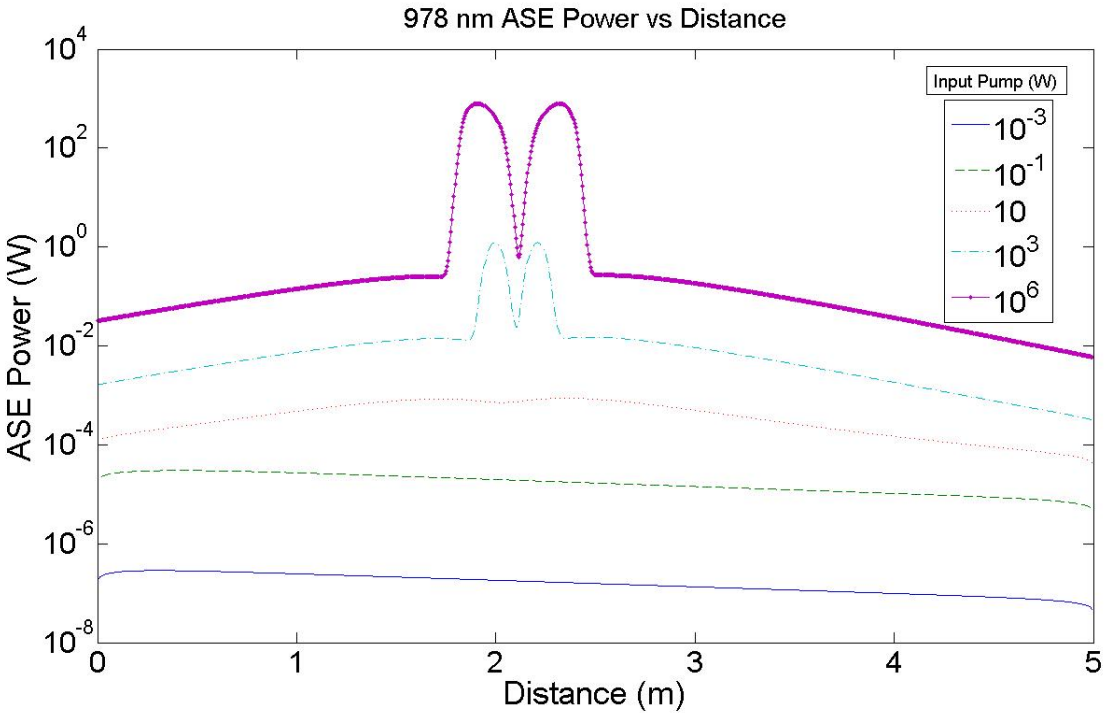


Figure 45: 978 nm ASE Power vs Distance, $P_s = 10^{-5}$ W, Varied Pump

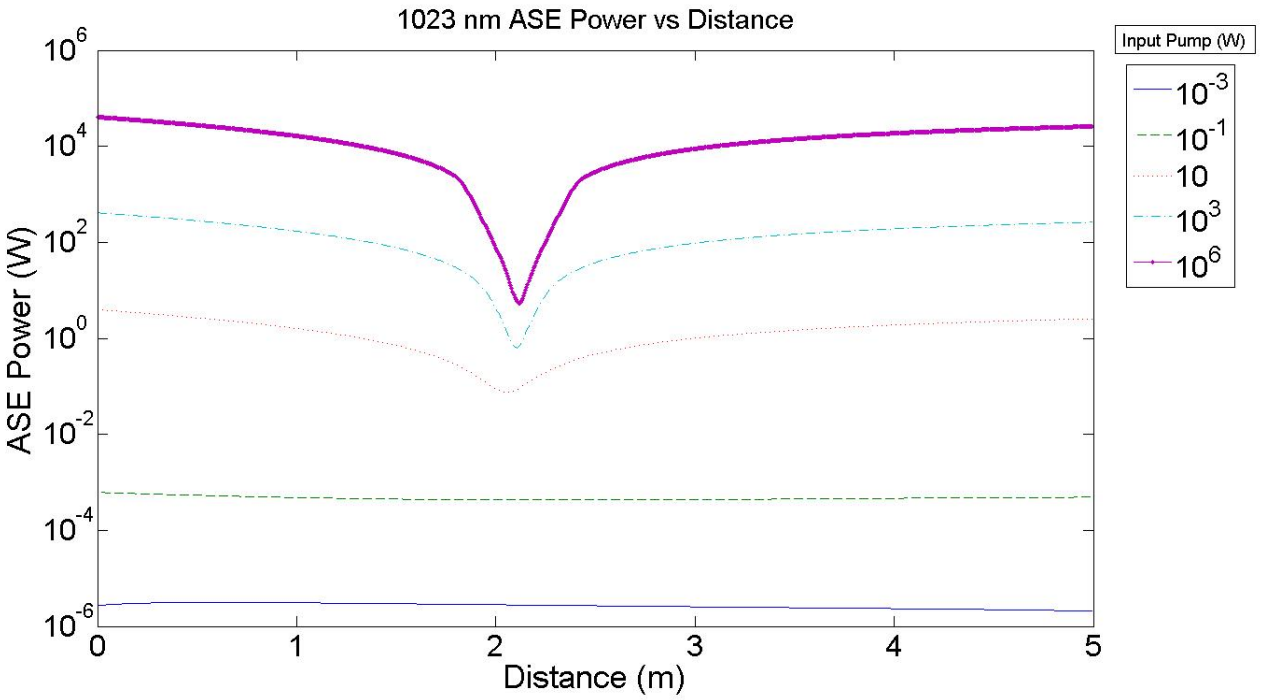


Figure 46: 1023 nm Power vs Distance, $P_s = 10^{-5}$ W, Varied Pump

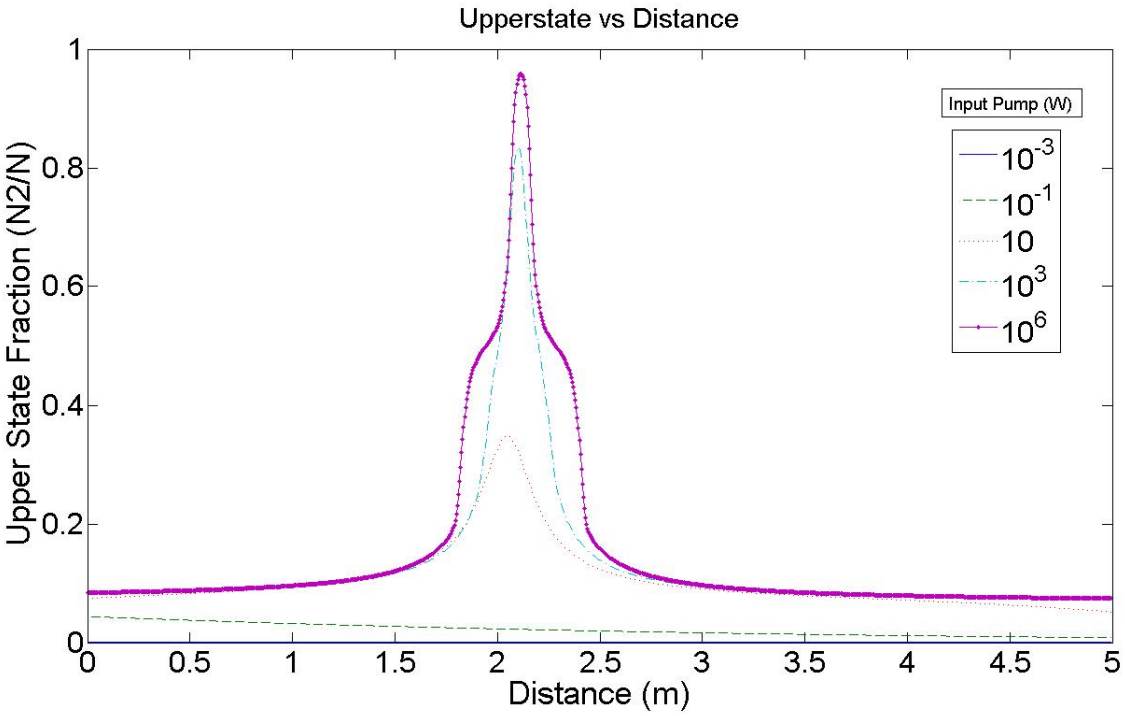


Figure 47: Upper State Population, $P_s = 10^{-5}$ W, Varied Pump

## 13.3 The YDFA at 978 nm

If the signal wavelength is chosen instead to be at 978 nm (near the peak emission cross section), an entirely different behavior is observed. Because the YDFA relies on a three level transition, the emission and absorption cross sections overlap exactly at 978 nm. We have already seen that ASE at this wavelength can both be created and reabsorbed very quickly. This is due to the high cross sections (both the emission and absorption cross sections are at their maximum at this wavelength). Therefore, one would also expect that in order to achieve signal gain at this wavelength, much shorter amplifiers must be built instead of the 5m fibers required for signal at 1023 nm. In fact, we will show that the optimum length for this wavelength is in fact much shorter, close to 50 cm. In addition, because of the large absolute emission cross section at this wavelength, one could expect much higher signal gain to be achieved in situations which might otherwise be inefficient.

We will begin by showing that only shorter fibers can be used to amplify light at 978 nm. In the following figures, a pump power of $10^5$ W and $10^{-3}$ W initial signal power were used, with the fiber length as a variable.

In Figure 48 we can see that for a fiber length that was appropriate for 1023 nm signal (5 m), the 978 nm signal is attenuated to unusable levels. This is due to the extremely high absorption at 978 nm coupled with the 1023 nm ASE restricting the upper state population to low values.

For a shorter fiber length of 1 m, we begin to see the potential for signal gain, as seen in Figure 49. At around 50 cm, the signal does increase dramatically, but is then absorbed. This implies that between 50 and 100 cm is closer to the optimum length for this signal wavelength. Again, the main limitation on signal gain is initiated by the 1023 nm ASE. This fiber length is just long enough for ASE at this wavelength to become a significant factor. The attenuation of the signal near the beginning of the fiber is the result of backwards propagating 1023 nm ASE limiting the upper state population to low levels as before. In

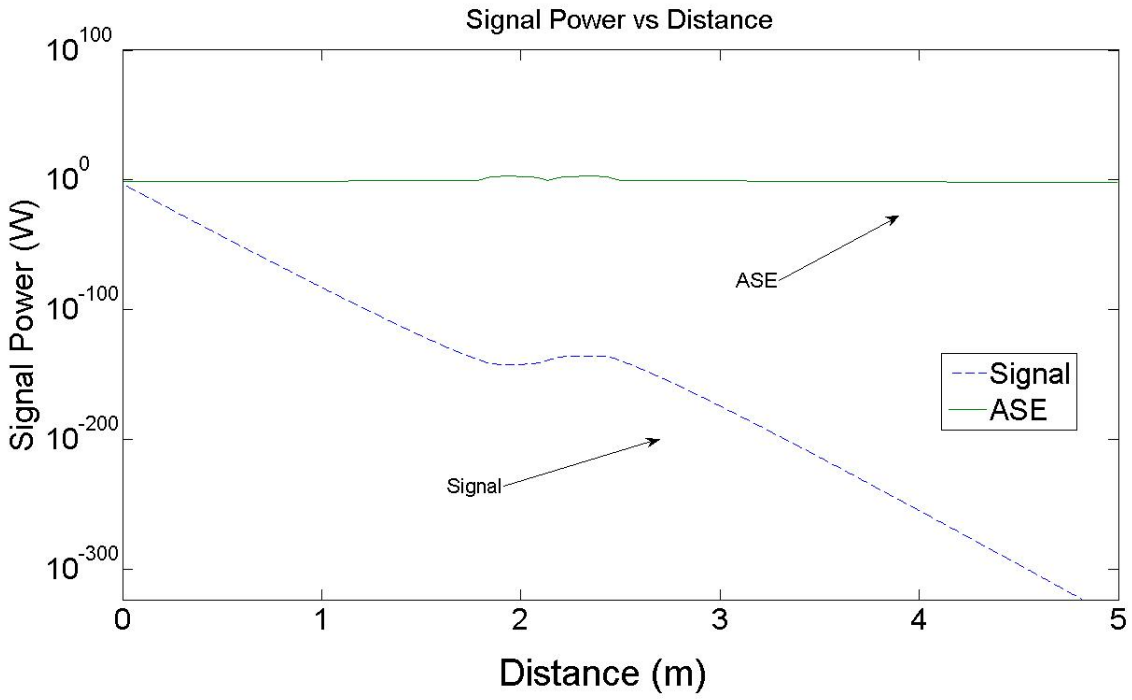


Figure 48: Signal and 978 nm ASE Powers vs Distance for 5 m

this case, however, the large emission cross section of the 978 nm wavelength is exploited near 45 cm, taking advantage of the upper state spike.

Finally, for a fiber of 50 cm, we see significant signal gain, as illustrated in Figure 50. Here, the large absolute emission cross section allows the signal to grow quickly, before the 1023 nm ASE can itself grow to significant levels. The result is rapid growth in short fiber lengths. Notice that near the end of the fiber, the signal power is approaching a plateau. This implies that we are close to the optimum length. Repeatedly running the model with differing fiber lengths until the maximum gain was achieved yielded a value of 53 cm for the optimum length in Yb doped silica glass for signal at 978 nm.

Next we analyze the effect of changing the pump power on signal gain, shown in Figure 51. Because this is a three level transition, a certain population inversion is required to achieve gain. For 978 nm, the required upper state poopulation is approximately 0.5N. Therefore,

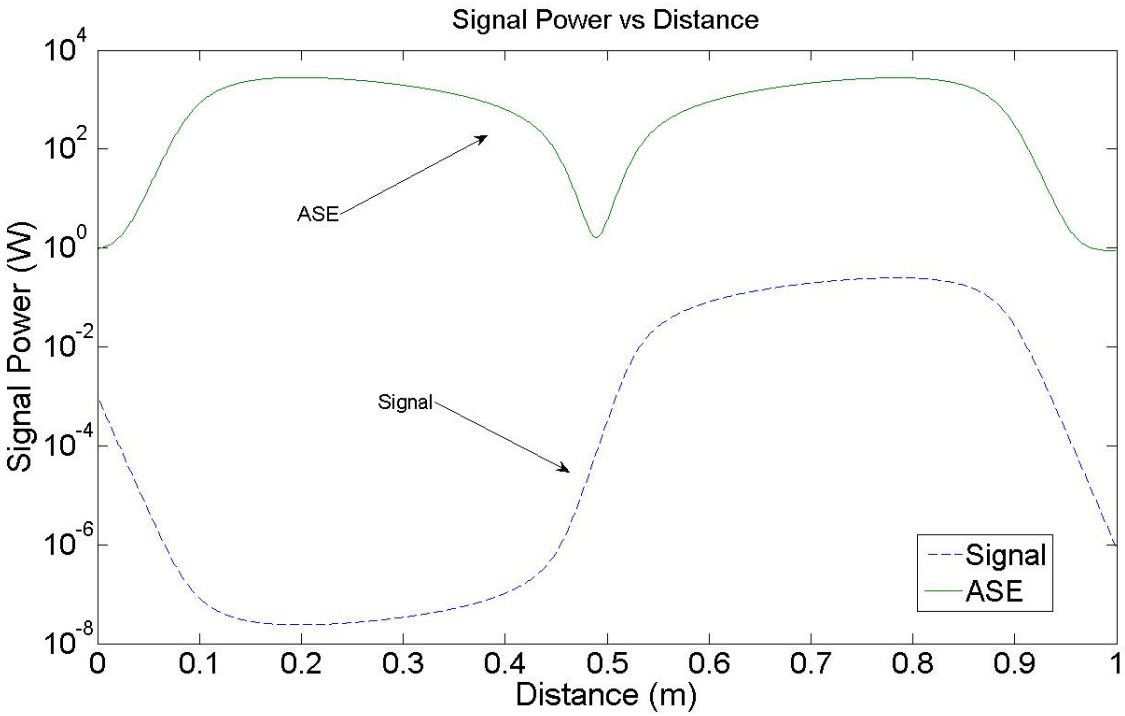


Figure 49: Signal and 978 nm ASE Powers vs Distance for 1 m

the threshold pump power for this wavelength is much higher than for other configurations. We can see that signal gain is approximately proportional to input pump power; however, a certain threshold pump power is required to achieve any signal gain whatsoever.

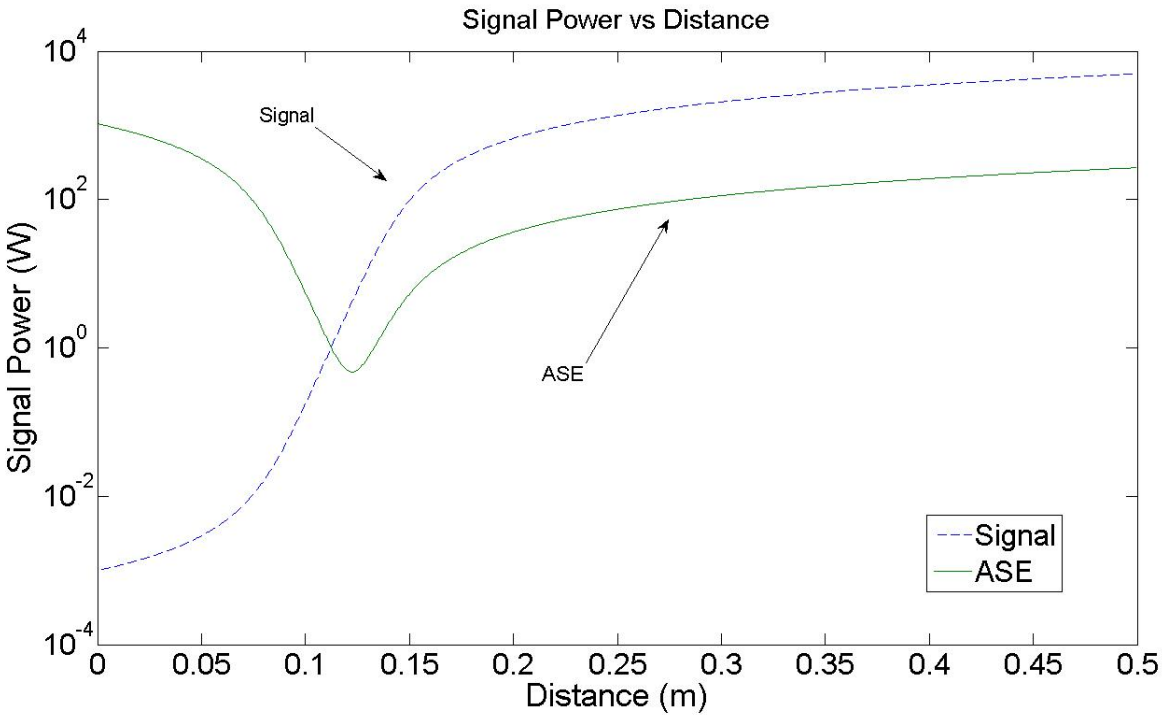


Figure 50: Signal and 978 nm ASE Powers vs Distance for 50 cm

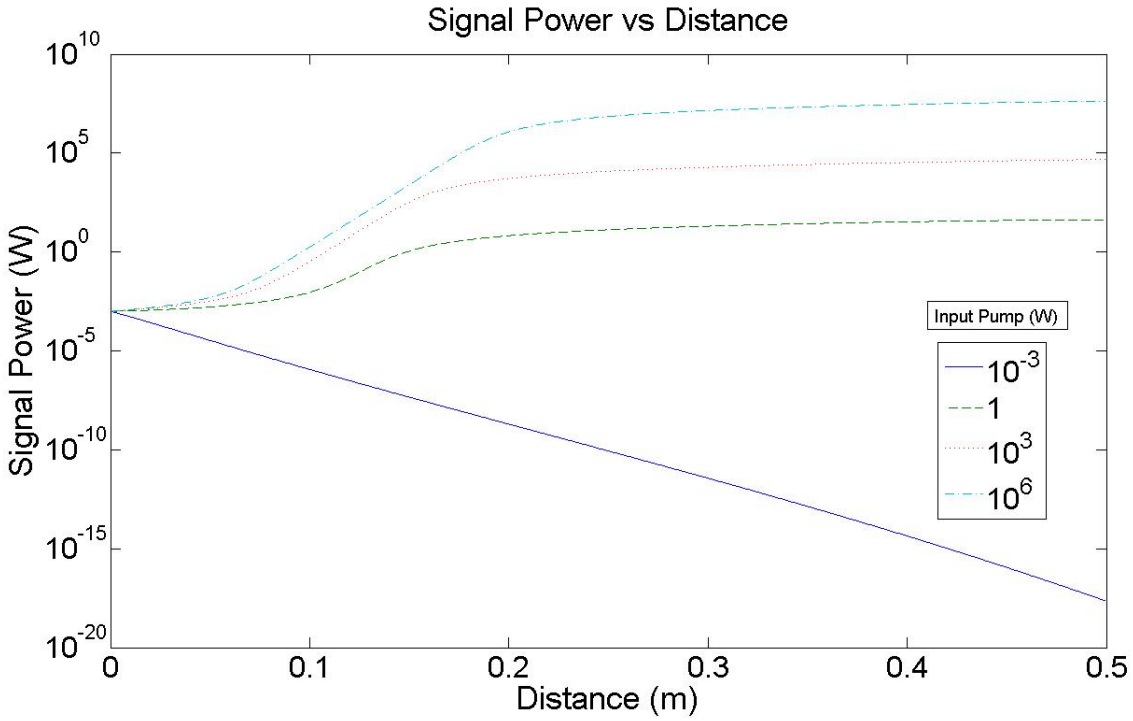


Figure 51: Signal Power vs Distance, $P_s = 10^{-5}$ W, Varied Pump

## 13.4 The YDFA at 1060 nm

We will conclude our analysis of the three potential signal wavelengths in Yd doped silica with 1060 nm signal. The lower absolute emission cross section in this wavelength may imply a lower efficiency than the other choices. There are many definitions of efficiency, but here we mean that, because the signal emission rate is determined by the emission cross section in the rate equation, we expect the term $A_2 1$ to be a more significant factor. This implies that more ions will spontaneously decay back down to the lower level. These ions cannot be used for signal amplification, and therefore the 1060 nm choice may result in lower signal gain at the optimum length than at other wavelengths. On the other hand, because there is no absorption at 1060 nm, longer fibers can be produced without fear of signal reabsorption. The optimum length for this amplifier configuration is much longer than other designs.

In this simulation we have chosen initial pump power to be $10^5$ W and initial signal power to be $10^{-3}$ W. We can see that the 1023 nm choice generally outperforms the 1060 signal at the optimum length of 5 m in Figure 52. However, the 1060 nm signal can continue to grow at longer distances as the 1023 and 978 nm ASE is reabsorbed by the fiber. Since the 1060 nm signal does not require a population inversion to achieve gain, this reabsorption allows the 1060 nm band to grow even further. Therefore, for the identical configuration, it is possible to achieve more gain with the 1060 nm choice than the 1023 nm choice.

We can see in Figure 53, however, that the 1023 nm amplifier can vastly outperform the 1060 nm signal in shorter distances. This gain spectrum was created using the identical configuration as the previous figure, but with a fiber length of 5 m. Extremely large gain can be achieved with the 1023 nm amplifier while the 1060 nm amplifier suffers from its lower absolute emission cross section. The 1060 nm signal choice can be appropriate if longer fibers can be implemented; however, for shorter fibers the 1023 nm signal is generally more efficient. Better still, though, would be the Nd doped fiber amplifier at 1060 if that option is available. We will see later that this configuration can yield much more gain than either

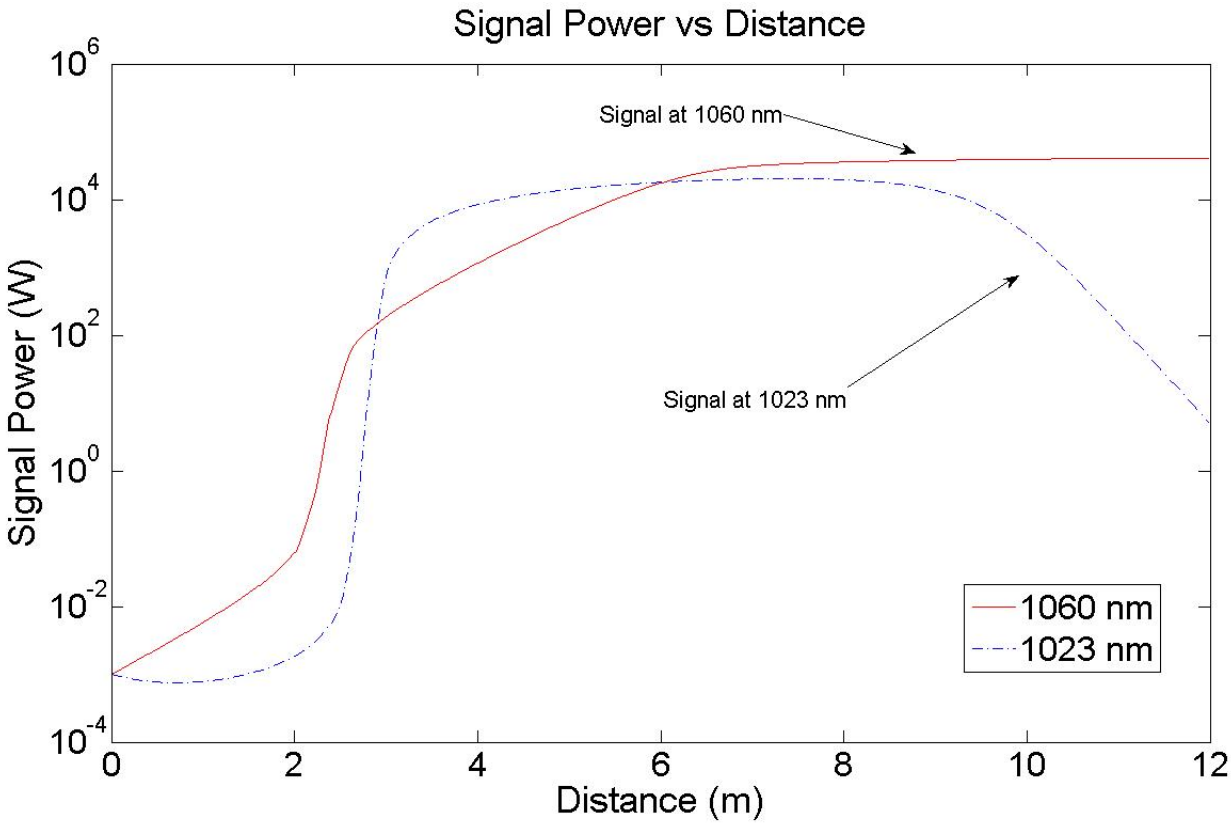


Figure 52: Signal at 1060 nm vs 1023 nm

the 1023 or 1060 nm YbFA.

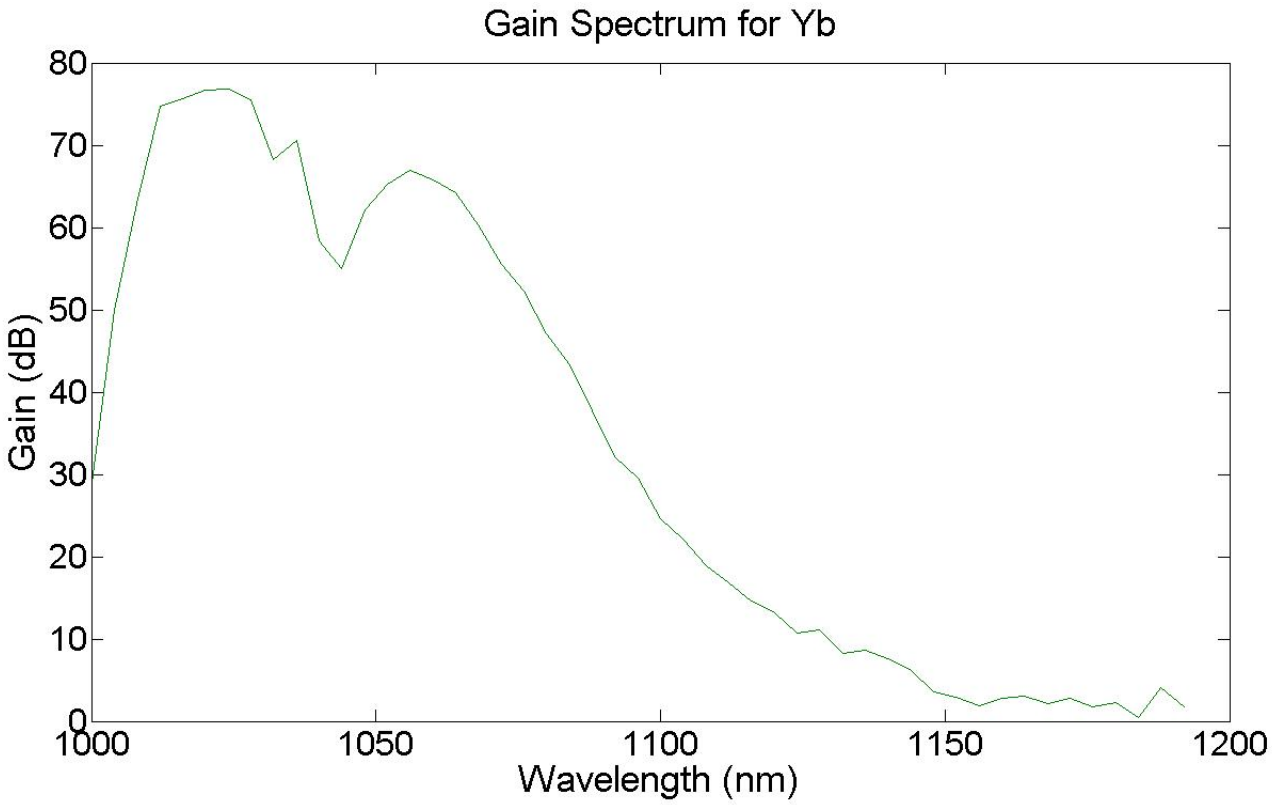


Figure 53: Gain Spectrum in Ytterbium, 5 m

## 13.5 Conclusions for the YDFA

There are three major signal wavelengths that can be chosen for the ytterbium doped fiber amplifier. The first, at 978 nm, requires much shorter fiber lengths than either of the other two, but can provide much more gain for the same pump power. Second, the 1023 nm signal wavelength provides strong gain characteristics with a forgiving fiber length. The low absorption allows the signal to exist in the fiber with generally low attenuation even if the optimum length is unrealizable. Finally, the 1060 nm signal is transparent to the fiber, implying that longer fiber amplifiers can be used. However, the lower emission cross section does not allow the same efficiency in converting pump to signal light. Moreover, the 1060 nm amplifier can be better implemented in Nd doped hosts instead of Yb, as we will see

later.

# 14 The Neodymium-Doped Fiber Amplifier

The wavelength range of interest in neodymium fiber amplifiers spans approximately 700 to 1440 nm. Figure 54 shows the emission, absorption, and excited state absorption cross sections for Nd doped in silica glass. [2] Because of the high absorption cross section in the $700 - 850$ nm range, this is a common choice for pumping. In our model, we will choose to pump at 808 nm, the largest peak in the absorption cross section in this range. This is the transition from the ${}^4I_{9/2}$ to the ${}^4F_{5/2}$ level. The ${}^4F_{5/2}$ level quickly decays to the ${}^4F_{3/2}$ non-radiatively. For Nd, this ${}^4F_{3/2}$ level is the upper laser level for all signal and ASE transitions. We will explore the possibility of a signal at each of the remaining transitions: the three level transition near 900 nm, the four level transition near 1060 nm and the four level transition near 1400 nm. The 1060 nm transition is the famous Nd laser transition, commonly used in the Nd:YAG laser. In our studies, we will focus most of our attention on the 1400 nm transition.

The 1400 nm transition from the ${}^4F_{3/2}$ to the ${}^4I_{13/2}$ is particularly interesting for telecommunications as recent developments have shown the advantages of signals at this wavelength. In silica fiber, however, two major problems limit the signal gain at this wavelength. The first is the effect of ASE from the 1060 nm laser transition. The second problem is the considerable excited state absorption (ESA) near 1330 nm. The ESA may eliminate the possibility of achieving signal gain at long wavelengths. In the phenomenon of ESA, incident photons are absorbed by an ion already prepared in an excited state and promoted to an even higher energy level. These levels decay non-radiatively quickly back to the original excited state; however, the incident photon is essentially lost. Therefore, if the probability that an incident photon will be absorbed by ESA is greater than the probability that it will elicit

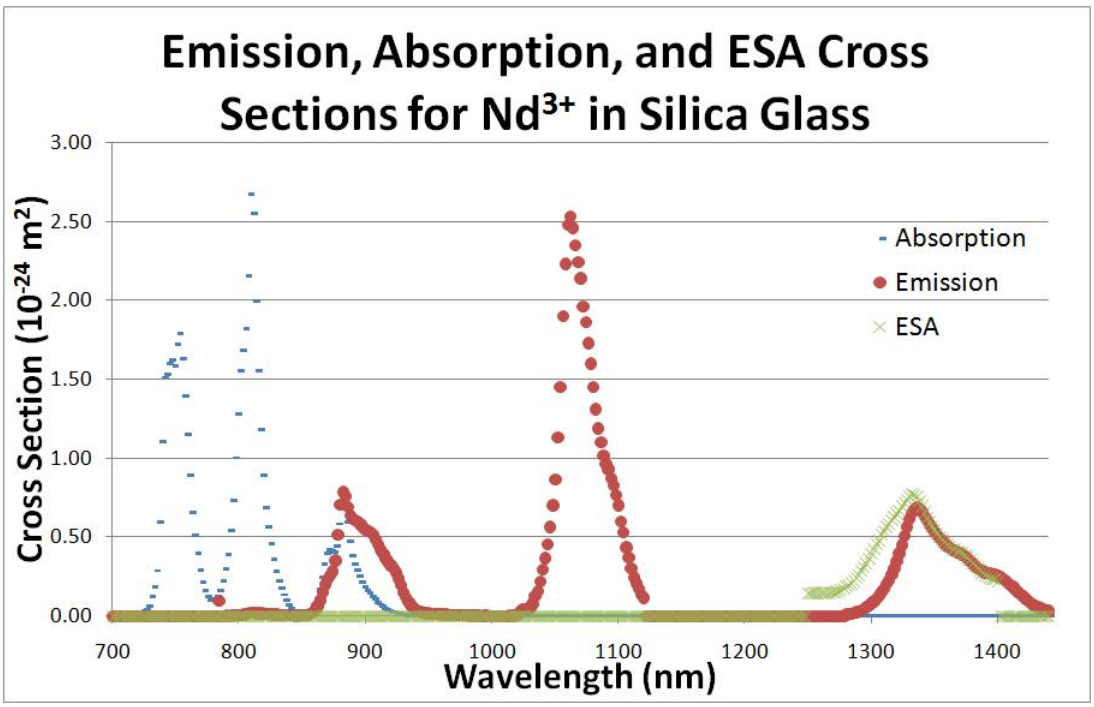


Figure 54: Cross Sections for Nd [2]

a stimulated emission, more signal photons will be lost to ESA than can be multiplied by stimulated emission. An ESA cross section can be defined in the same way as the emission and absorption cross sections can be. By taking the difference of the emission and ESA cross sections at these wavelengths we define the effective cross section.

$$\sigma_{eff} = \sigma_{se} - \sigma_{esa} \text{ (effective emission cross section)} \tag{105}$$

If the effective cross section is negative, it will not be possible to achieve gain. In this situation, a signal photon is more likely to be absorbed than to emit. Figure 55 is a graph of the effective cross section near 1330 nm. At every point where the effective cross section is negative, signal gain cannot be achieved.

It has been shown that the ESA is dependent on the host material. ZBLAN fibers demonstrate a shifting of the ESA cross section to lower wavelengths; thus, it may be possible

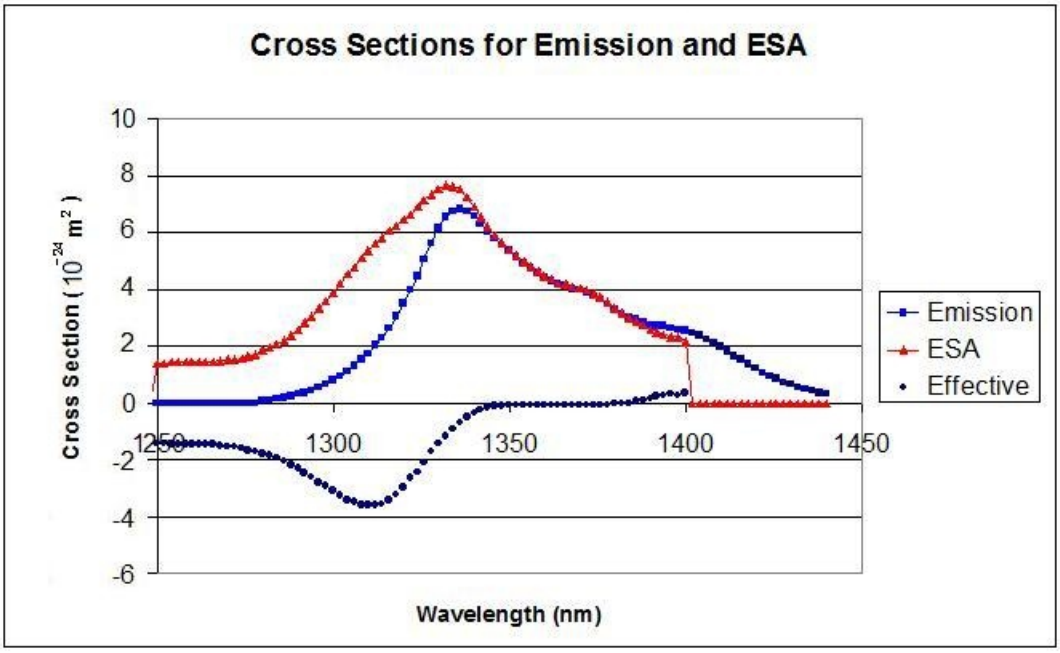


Figure 55: ESA and Effective Cross Section for Nd Near 1330 nm

to achieve signal gain in this material. Because of this, we are examining the possibility of signal gain in the absence of ESA in silica. With this in mind, it stands to be shown what the effect of ASE on signal gain will be.

Signals at 1400 nm will not experience attenuation, since the absorption cross section is zero for this four level transition; however, the absolute value of emission cross section is significantly smaller than the cross section at 1060 nm (the major ASE transition). Therefore, while the ASE will not cause the signal to shrink in power, as it can in three level systems such as Yb, it will provide a significant limitation on maximum signal gain.

The ${}^4F_{3/2}$ to ${}^4I_{9/2}$ transition near 910 nm is a three level transition that is also of interest. The issue of the 1060 nm ASE is still present in this configuration. Moreover, the absorption at this wavelength is non-zero as well. Because of this, significant ASE may be expected to result in signal loss, which may be a serious impediment to the effectiveness of 910 nm as a signal wavelength. This is in contrast to the case of signal at 1400 nm, which is immune to

signal loss.

Perhaps the most well known feature of Nd is the 1060 nm four level transition. This is the transition that is responsible for the Nd:YAG laser and has been very well studied. We will briefly explore this topic and demonstrate quantitatively how the spectrum of this transition gives rise to extremely high signal gain.

## 14.1 Quantum Defect in Nd

In Yb, the pump wavelength was chosen as 910 nm, with the signal usually chosen at 1023 nm. For this common wavelength, the quantum defect was given as

$$E_{pump} - E_{signal} = h(\nu_{pump} - \nu_{signal}) \text{ (Quantum Defect)} \tag{106}$$

$$\text{Quantum Defect} = h(2.1844 * 10^{-19} - 1.9431 * 10^{-19})J \tag{107}$$

As a fraction of pump power, this is given by

$$\text{Fractional Difference in Energy between Pump and Signal} = \frac{E_{pump} - E_{signal}}{E_{pump}} \tag{108}$$

For this case, this value is 0.12. In other words, 12% of the input pump power is necessarily lost through nonradiative processes. Whether this is a severe problem in practice depends on the design requirements of the system.

In Nd, however, the quantum defect is much larger. Since pumping occurs at 808 nm, the difference in energy between the signal and pump light is much larger. For a signal at 1400 nm, the fractional difference in energy between pump and signal light is 0.42. In this case, 42% of the pump light is lost to nonradiative effects before it can be converted to signal light.

Again, while it is up to the designer whether this is a significant issue, it is much more of a consideration when dealing with Nd doped amplifiers with signal near 1400 nm as compared to Yb.

Of course, if the signal wavelength is chosen to be closer in energy than the pump, the quantum defect is smaller. In the case of signal wavelength chosen at 910 in Nd, the quantum defect is only 11%, a significant improvement over the case of signal at 1400 nm.

## 14.2 ASE Approximation in Nd

Because the 1060 nm ASE is a four level transition, it lends itself to approximation using the equivalent bandwidth method discussed earlier. Moreover, the application of the equivalent bandwidth method to Yb required extreme subtlety. This was because much of the ASE across the spectrum was on comparable orders of magnitude. Therefore, the effects of smaller power ASE bands were important in sufficiently analyzing Yb. By contrast, in Nd, the ASE at 1060 nm is a dominating and significant effect. In many situations, the power of the ASE band near 1060 nm is many orders of magnitude greater than any other band or signal. The net result is to reduce the importance of the other bands in calculating upper state population.

As an example, Figure 57 is a graph of the relative ASE powers in a typical situation. In this case, the signal has been excluded so that only the ASE and pump light is present in the fiber.

It is clear that the ASE band near 1060 is a much more significant factor than either of the other two ASE bands. In fact, the difference of over 7 orders of magnitude implies that ASE near 910 or 1400 nm could be ignored. Also note that the 910 nm band tends to increase for about 10 cm and then decrease to smaller levels. This is typical of three level transitions in general, and as discussed earlier is related to the delicate relationship between gain and upper state population. The 1060 nm ASE tends to limit the upper state to near

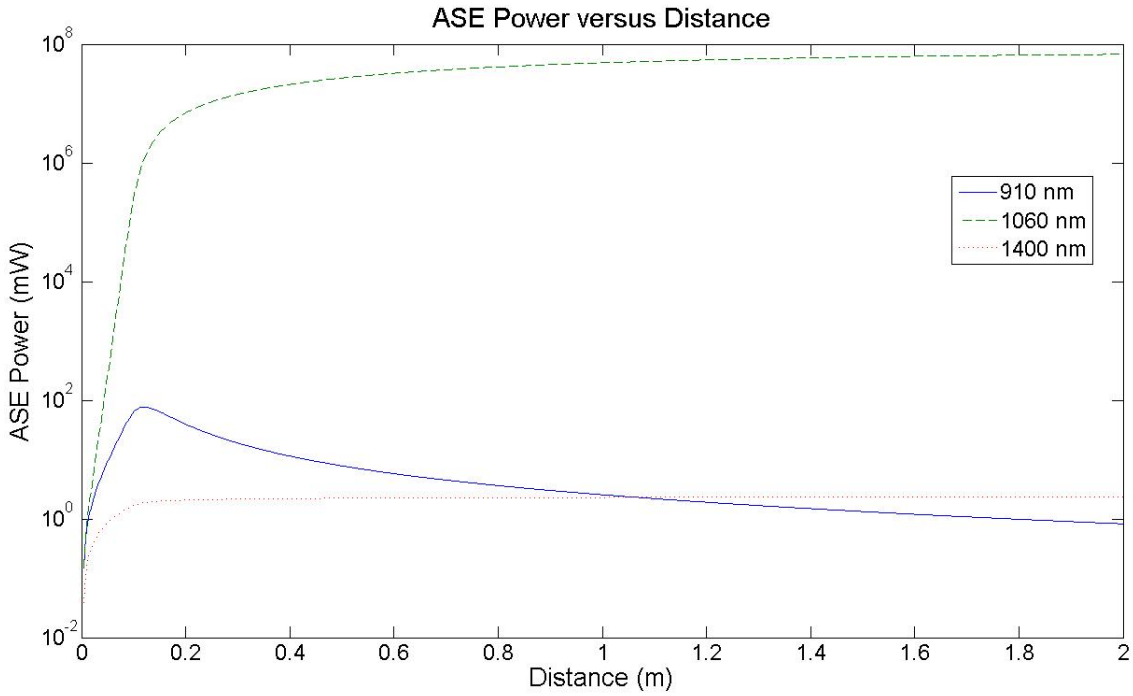


Figure 56: 910, 1060, and 1400 nm ASE, No Input Signal, $P_p = 10^5$ W

zero, while the 910 nm ASE band requires a population of around .8N to achieve gain. If the upper state is less than this value, the 910 nm ASE light will tend to be absorbed and the power will decrease.

Despite the many reasons that justify the use of the equivalent bandwidth method for this configuration, the significant caveats that have been raised by the use of this method in Yb have suggested that the most accurate data will be produced by using a model with more ASE bins. For Nd, a total of 145 bins, separated into three different ranges, each spanning a range of 2 nm were used. These 145 bins covered the wavelengths $884 - 936$ nm, $1006 - 1068$ nm, and $1268 - 1438$ nm.

## 14.3 The NDFA at 1400 nm

In analyzing the Nd doped fiber amplifier with signal at 1400 nm, we will examine the effect of ASE at 1060 nm in limiting gain. To do this, experiments will be performed with the model with ASE included. Then, the identical configuration will be analyzed with the exclusion of ASE at 1060. In order to remove the ASE at 1060, the source terms for these wavelengths are simply defined to be zero. Later, we will examine potential methods to actually limit the ASE, such as long period gratings.

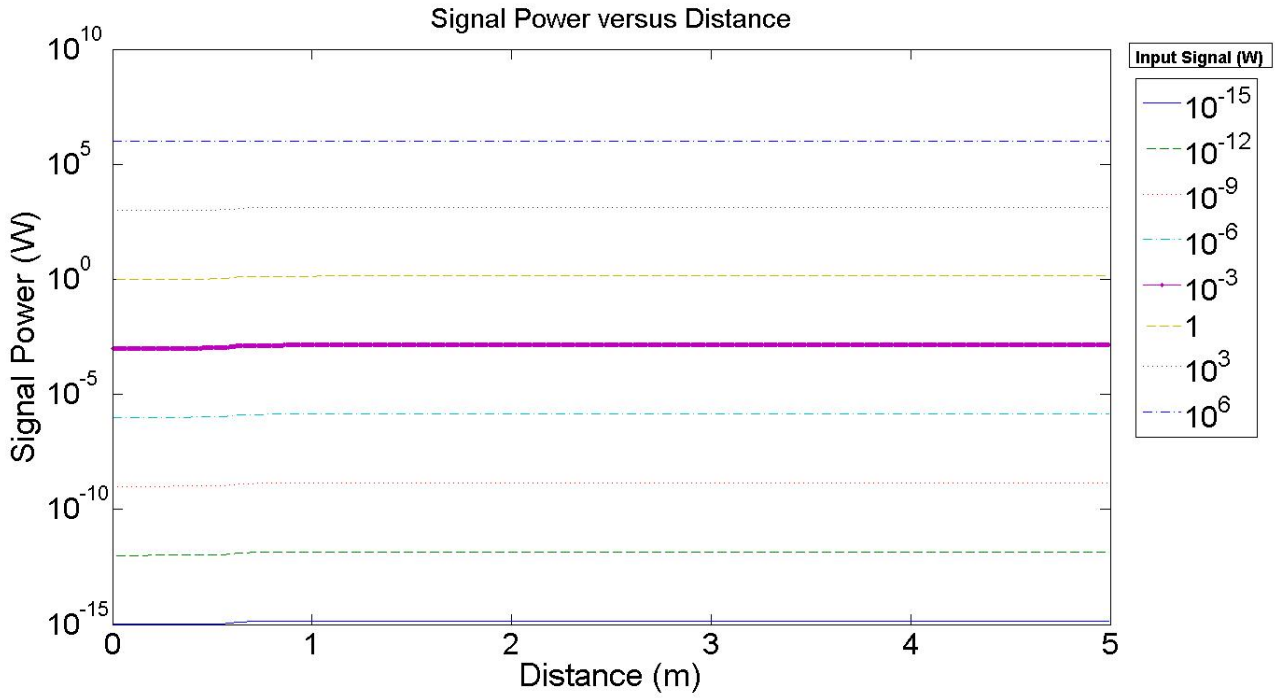


Figure 57: Signal Power vs distance, $P_p = 10^5$ W, Variable Signal

First, we will explore the effect of changing the input signal power while keeping the pump power constant. The range of signal powers used in this example is $[10^{-15}, 10^{-12}, ..., 10^3, 10^6]$ W.

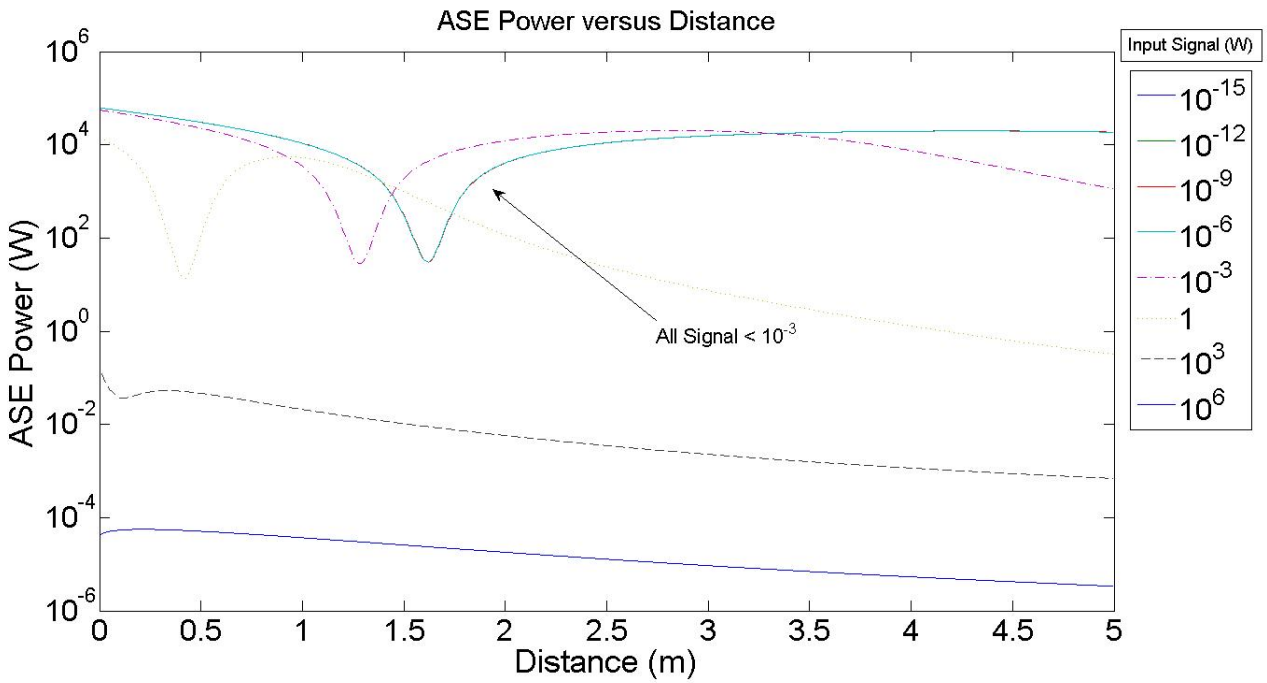


Figure 58: Total ASE Power vs Distance, Varied Signal Power in Nd, $P_p = 10^5$

As can be seen in Figure 57, the signal power remains roughly constant in each case. This is due to the significant depletion of the upper state population by ASE at 1060. Since the ASE tends to limit the upper state to a low value, the gain achieved by the signal remains low as well. To demonstrate this effect, the next two graphs show the ASE power as a function of distance for one of these experiments, as well as the upper state population as a function of distance along the fiber (see Figures 58 - 59). Note that regardless of the input signal power, these results remain essentially unchanged, as the signal power has very little effect on the upper state population in these configurations.

The 1060 nm ASE power rises dramatically during the first few centimeters of the fiber. Moreover, the upper state population quickly depletes from its initial values near 90%. After the initial growth of the ASE power, it rises slowly for the remainder of the fiber length. The steady increase in ASE power is due to the pump constantly providing a nonzero upper state

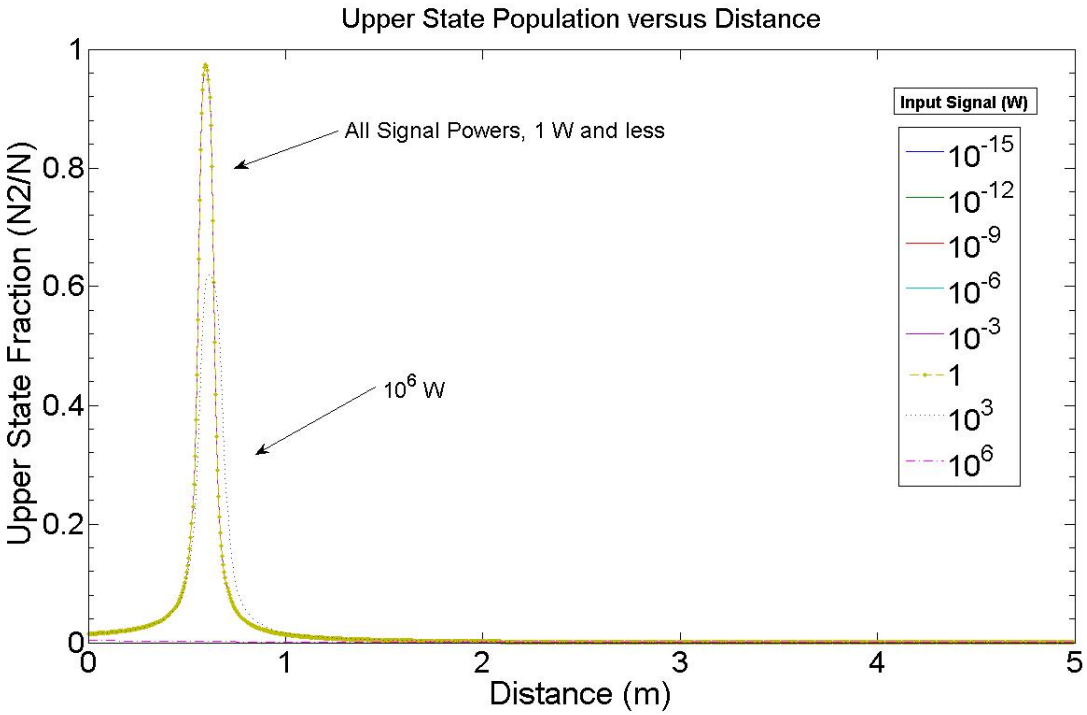


Figure 59: Upper State Population, Varied Signal Power in Nd, $P_p = 10^5$

population. Because of the large emission cross section for the 1060 ASE, it is possible to achieve gain with extremely small upper state population. The signal has a smaller absolute cross section and is overwhelmed by the ASE power. Therefore, for each pump photon that excites an ion to the upper state, the ASE is much more likely to elicit a stimulated emission than the signal is. A quantitative analysis can be examined as follows. The gain coefficient, $\gamma$, is given as

$$\gamma = N_2\sigma_{ems} - N_1\sigma_{abs} \tag{109}$$

Since the absorption cross section for both the signal and 1060 nm ASE band is zero, the second term vanishes (this is also the reason why the signal power cannot decrease within the fiber, as the quantity $\gamma$ is strictly positive). The emission cross section for ASE near 1060

nm is $2.48 \times 10^{-20}$ cm$^2$. For the signal at 1400 nm, the emission cross section is $2.53 \times 10^{-21}$ cm$^2$. Therefore the cross section for ASE is almost ten times that for the signal. This implies that the gain coefficient for the ASE is also ten times larger than that of the signal. The propagation equation is given by

$$\frac{dP}{dz} = \gamma P(z) \tag{110}$$

Thus we expect the 1060 ASE to grow ten times faster than the signal if they begin with comparable initial values. This is a severe impediment to signal gain as we see below. If the 1060 ASE were removed with identical conditions as before, the signal power would grow to much higher levels.

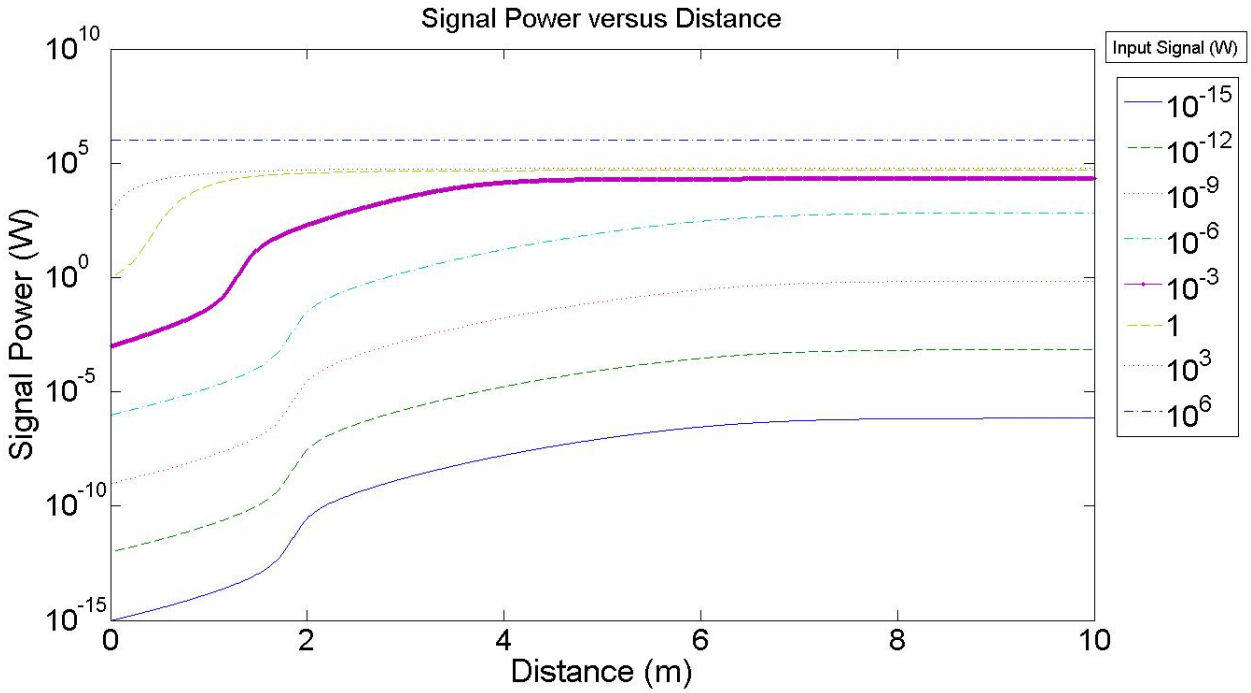


Figure 60: Signal Power vs Distance, 1060 ASE Excluded, $P_p = 10^5$ W

With the 1060 ASE included, the signal power grew slightly and then remained constant. In contrast, Figure 60 shows that with 1060 ASE excluded, the signal power now rises to

much higher levels. This is because, with the 1060 nm ASE excluded, only the 910 nm ASE is a significant effect. However, because the 910 nm ASE band is a three level transition, the upper state population does not deplete to zero, as seen in Figure 61. In fact, after the pump power decreases to lower levels, the 910 ASE becomes reabsorbed by the fiber, creating an upper state population that is above zero. The 910 nm ASE power can be seen in Figure 62.

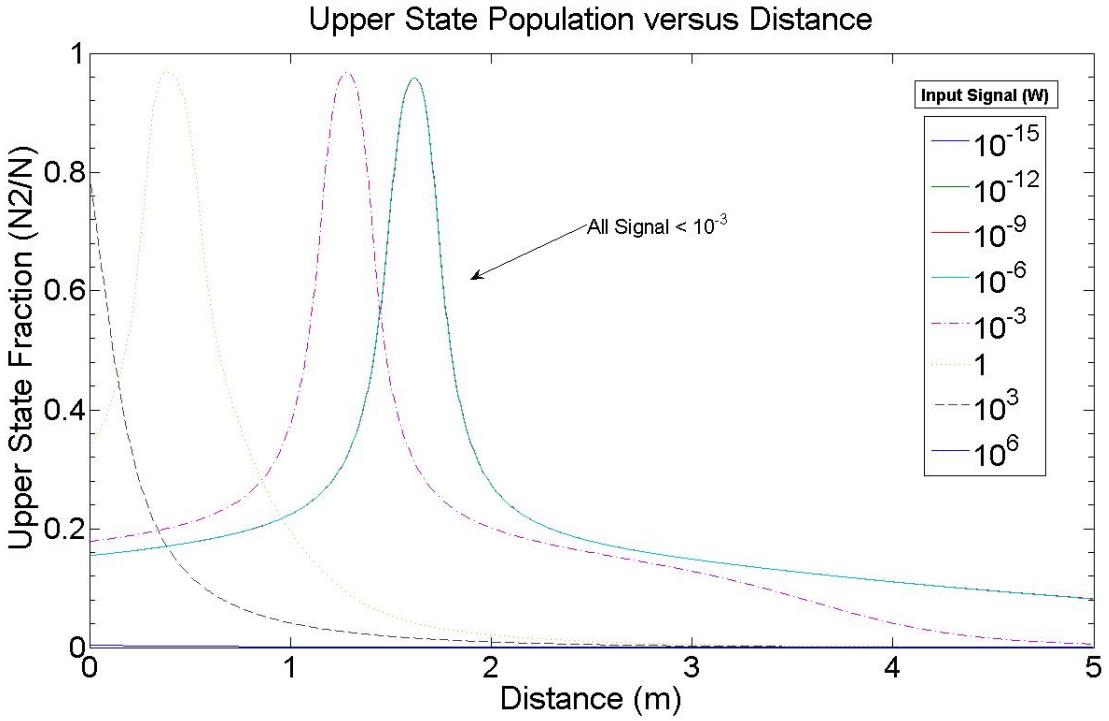


Figure 61: just N2 vs distance, no 1060 ASE

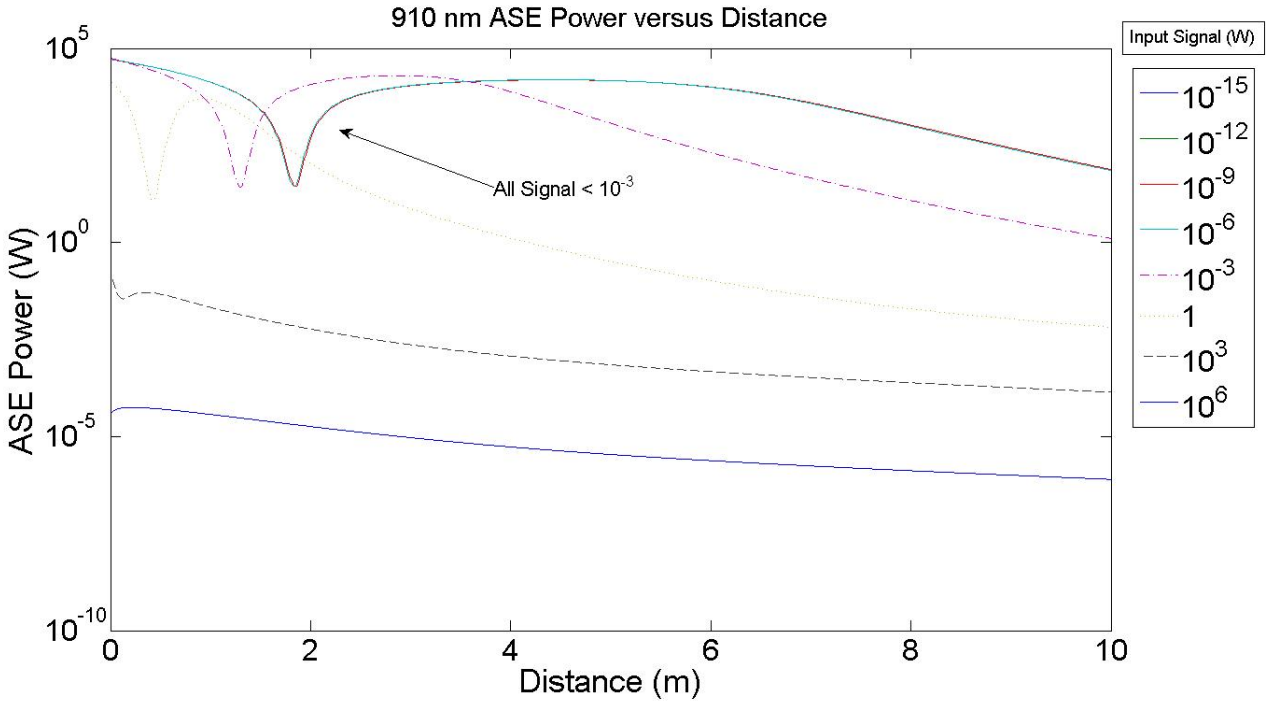


Figure 62: 910 ASE Power vs Distance, no 1060 ASE

As can be seen, the 910 nm ASE band contains high power in the first few meters of the fiber but then is reabsorbed at longer distances. As the 910 ASE is reabsorbed, it creates an upper state population that is above zero. This upper state population allows the 1400 nm signal to experience gain. A similar effect was seen in Yb with the 978 nm ASE band. The result was that the 978 ASE band grew quickly at the beginning of the fiber, but was then reabsorbed, creating an upper state population that was sufficient for the signal to experience gain. A reproduction of these results is below in Figure 63.

The 910 nm ASE in Nd has an equivalent effect. In other words, the pump power is simply being converted into ASE power, which can then be reabsorbed and provide more potential signal growth; however, the overall signal gain does tend to be reduced by this effect. This implies, though, that a careful choice of fiber length is essential to achieve optimum signal gain. The fiber must be long enough that any three level transition ASE is reabsorbed by

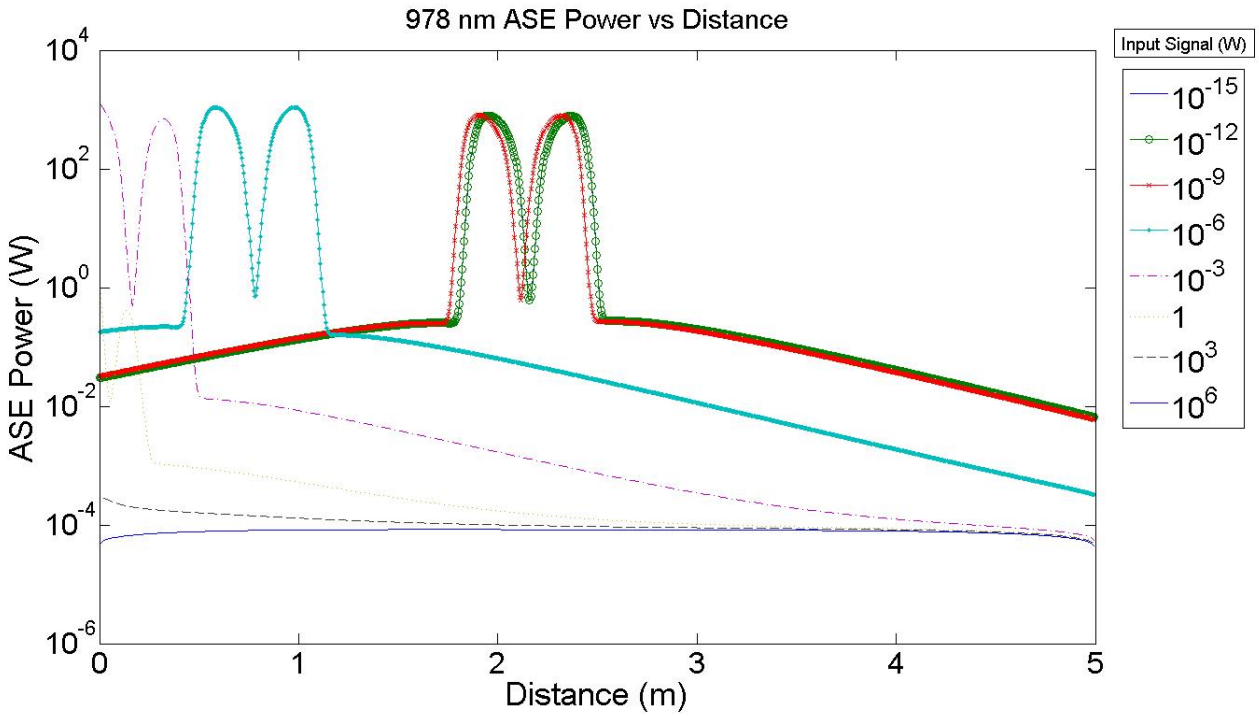


Figure 63: 978 nm ASE Power vs Distance in Yb, Signal at 1023 nm, Varied Signal Power, $P_p = 10^5$

the fiber, but short enough that the signal itself is not reabsorbed. In Yb with signal at 1023 nm, it was possible to build a fiber that was too long and the signal could be reabsorbed by the fiber, resulting in loss. However, with signal at 1400 in Nd, this is not a concern, as the absorption cross section is zero for this four level transition.

Now, we examine the effect of changing the input pump power. The behavior of the signal light is different with a variable input signal, but the general form of the propagation is the same. For low input powers, the signal grows in an almost identical manner. Behavior related to gain saturation is observed at higher signal powers. The absolute change in signal power therefore is also related to the input signal power. This implies that for larger input signal powers, a larger percentage of pump light is being converted into signal light.

Because the 910 nm transition has a larger absolute emission cross section than the 1400

nm signal transitions, it tends to absorb more of the pump light than the signal. We saw above that larger input signal powers tends to lower the total ASE power in the 910 nm transition. For longer fiber lengths, one would expect this 910 nm ASE to be reabsorbed into the fiber because of the nonzero absorption cross section in this three level transition. However, even though the signal may benefit from this additional source of upper state population, the lower power of the signal light does not extract the same benefit from this population. The signal will have to compete with the natural radiative relaxation of this upper state, which tends to decrease the upper state before the signal can take advantage.

To reiterate the results of this analysis, the effect of changing the input signal power is negligible if the 1060 nm ASE is included. This 1060 ASE band quickly takes over and limits the upper state to nearly zero percent, except in the case of extremely high signal powers. The large emission cross section for this ASE is responsible for the dramatically high powers. With this ASE band excluded, however, an entirely different situation is realized. Here, the 910 nm ASE band is the only significant competitor to the signal for pump power; however, after a sufficient fiber length, this three level ASE transition is reabsorbed by the fiber, where it can be reconverted into signal light. The net result is that the output signal power depends heavily on the input signal power in the case where the latter value is small. This sort of three level ASE transition behavior was seen in Yb as well, when analyzing the ASE at 978 nm. Changing the input signal with the 1060 ASE band excluded did have an effect on the population levels of the fiber, but the form of the propagation was similar. The percentage of pump light that is converted to signal light depends on the input signal. Therefore, the Nd doped fiber amplifier with signal at 1400 nm can be an efficient method of boosting the signal power of a wide range of inputs if the 1060 nm ASE is somehow suppressed.

Next, we will examine the effect of changing the pump power while maintaining a constant input signal. The input signal in this case will be $10^{-3}W$, and the fiber length will be 5 meters. We will again examine the comparison between including and ignoring the 1060

nm ASE band. To begin, initial pump powers of $[10^{-3}, 10^{-1}, ..., 10^{5}, 10^{7}]$ W were selected and modeled. Figure 64 shows the signal power as a function of distance for each of these configurations. Figure 65 shows the upper state population for these configurations.

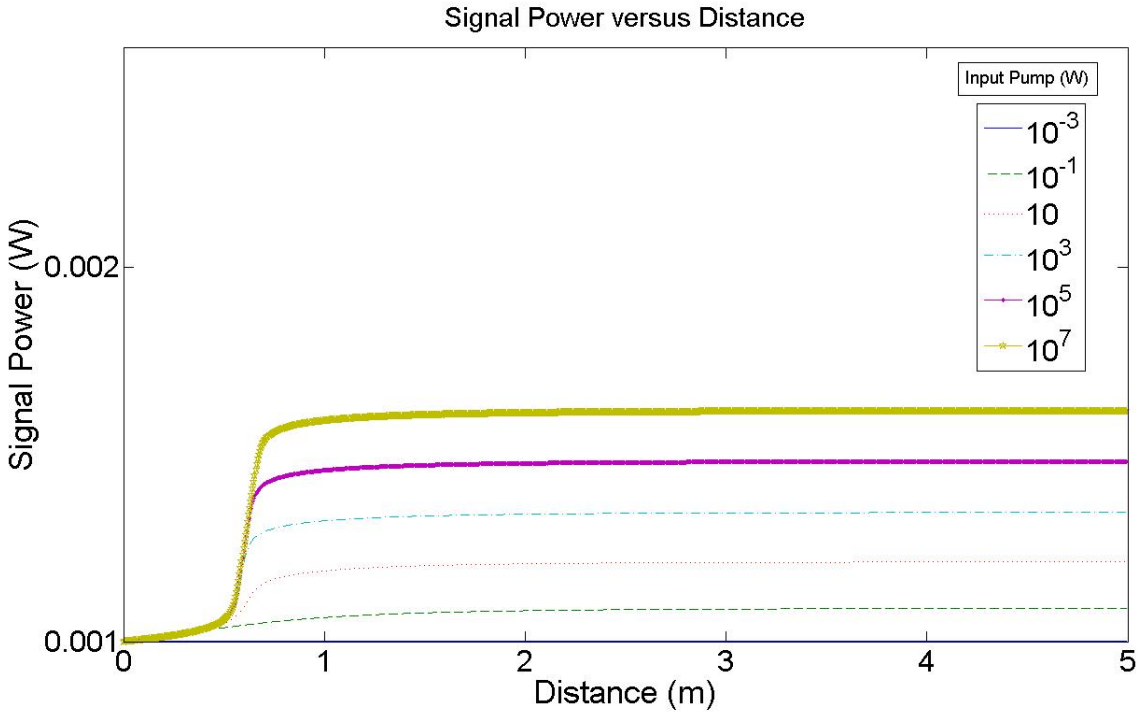


Figure 64: Signal Power vs Distance, $P_s = 10^{-3}$ W, Varied Pump, 1060 ASE included

As we can see, with the 1060 nm ASE included, changing the input pump power increases the output power of the signal. This is because, while the 1060 nm ASE still depletes the upper state quickly, the larger pump power increases the portion of the fiber which does experience nonzero upper state population. This implies that the signal can grow for a longer distance before becoming constant. Also, the ASE power grows to much higher levels as the pump power is increased. This is expected as the 1060 ASE tends to extract most of the pump power.

The ASE power also reaches a higher maximum with higher pump power, as seen in Figure 66. Once again, however, the situation is markedly different without the 1060 ASE.

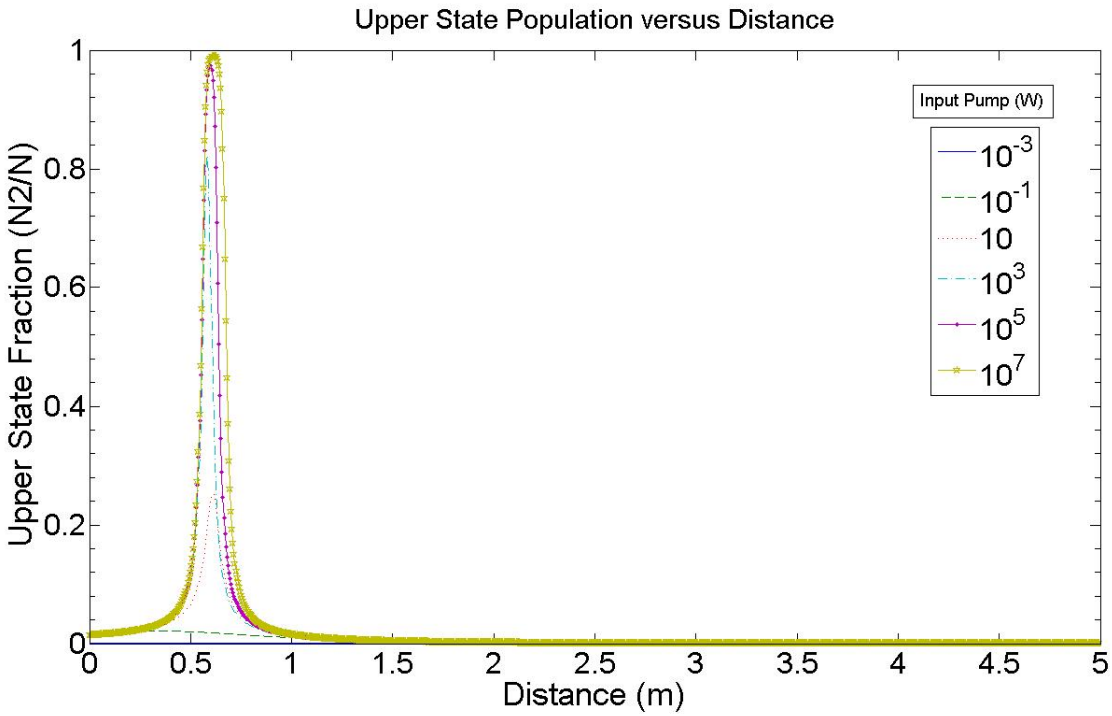


Figure 65: Upper State Population, $P_s = 10^{-3}$ W, Varied Pump

In Figure 67, in the same manner that the 1060 ASE grows to higher levels with pump power, the signal now reaches a higher maximum with greater pump power. At longer fiber distances (around 3-4 m depending on initial pump power), the signal power tends to remain roughly constant. This can be explained by the upper state population, which is shown in Figure 68. In all configurations, the upper state population decreases for longer fiber distances as the signal grows to significant levels.

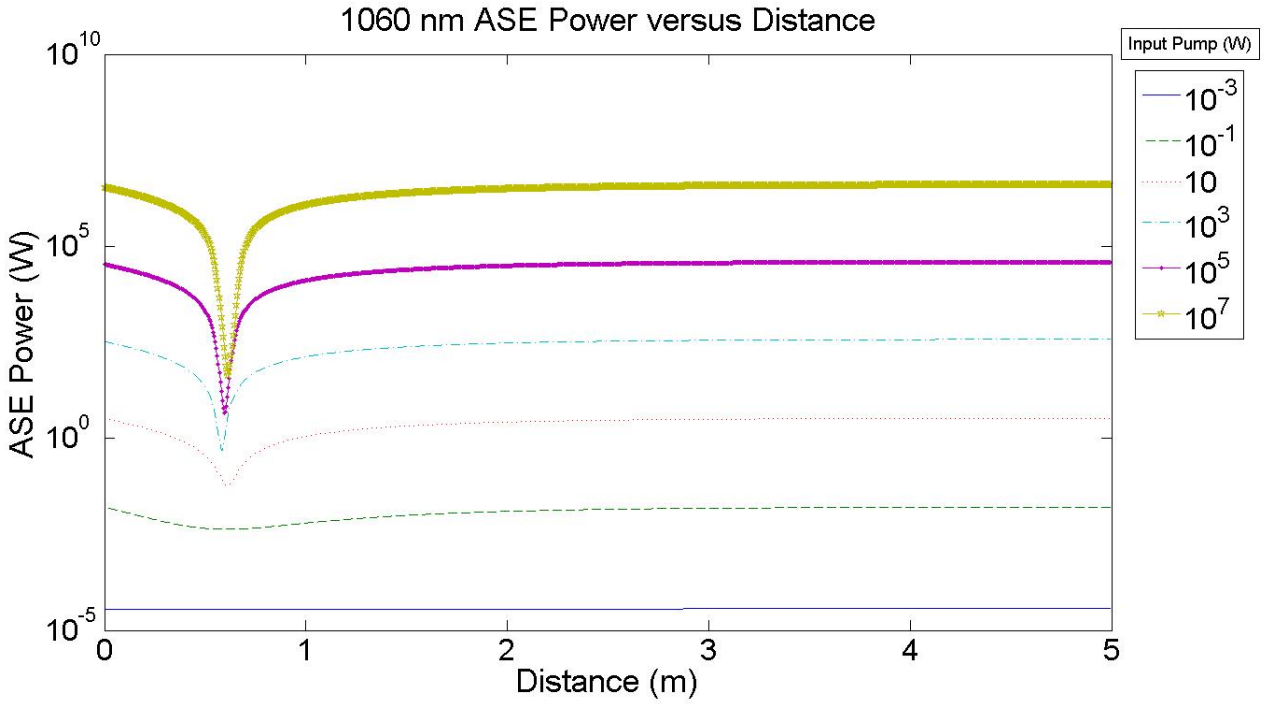


Figure 66: 1060 nm ASE Power, $P_s = 10^{-3}$ W, Varied Pump

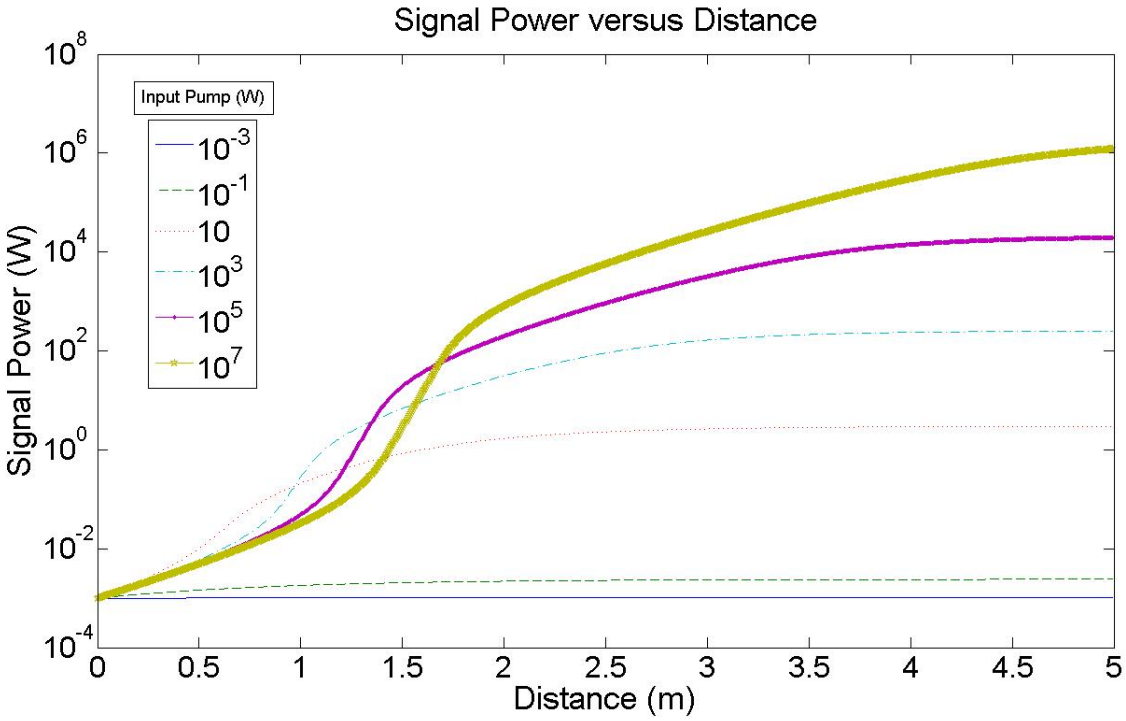


Figure 67: Signal Power vs Distance, 1060 ASE Excluded, $P_s = 10^{-3}$ W, Varied Pump

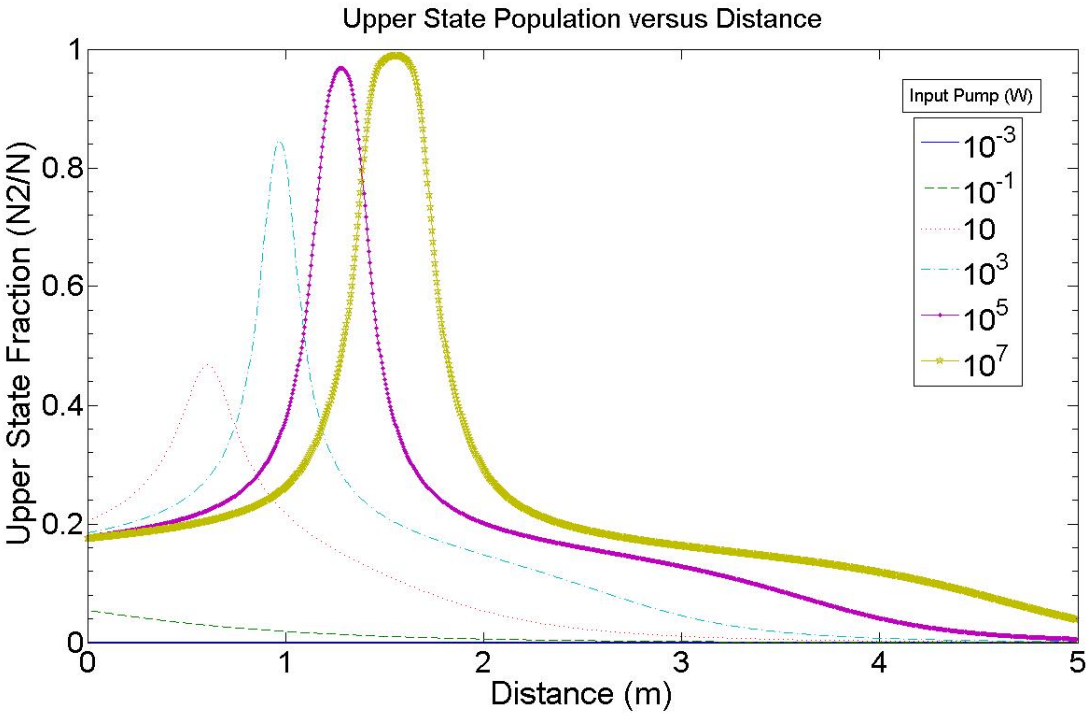


Figure 68: Upper State Population, without 1060 ASE

## 14.4 The NDFA at 1060 nm

The ${}^4F_{3/2}$ to ${}^4I_{11/2}$ four level transition in Nd is the strongest transition in this wavelength. It has an extremely high emission cross section and no absorption. It also ranges between approximately 1020 and 1120 nm, providing gain across a large number of wavelengths. This transition has been studied thoroughly and is used in many applications, including the well known Nd:YAG laser. Because of this, we will restrict our discussion to the most general features of this transition. Because the transition is four level, it does not require a population inversion to achieve gain. It is also extremely efficient at extracting pump power from the fiber as well.

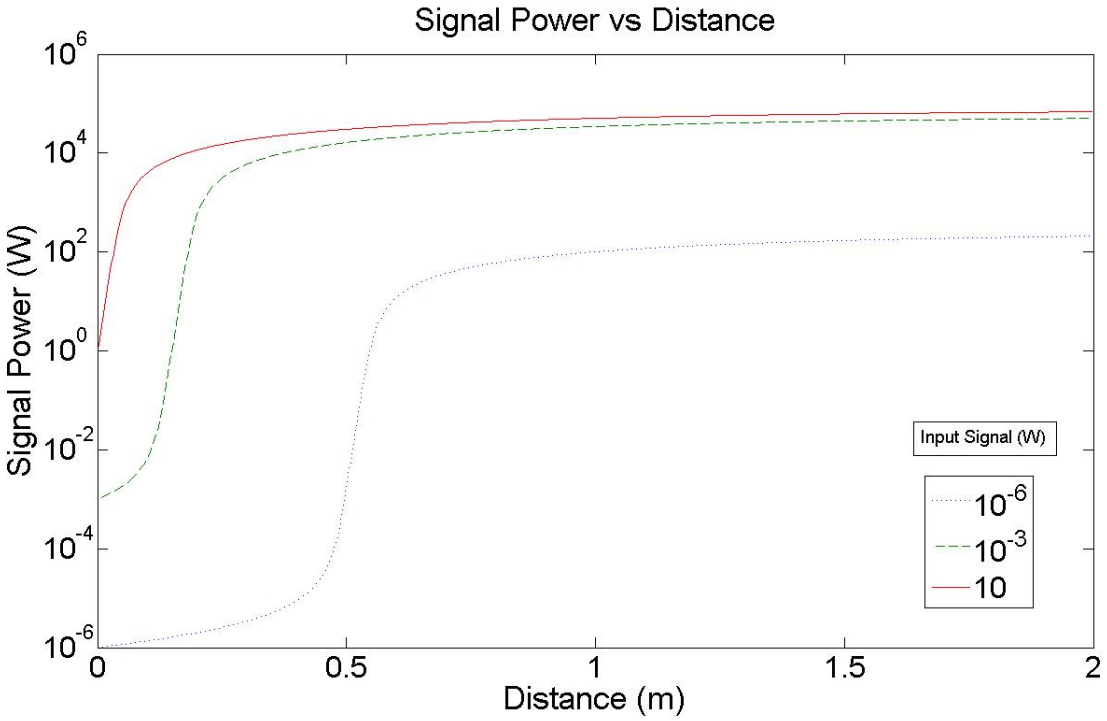


Figure 69: Signal vs Distance, 1060 nm Signal, $P_p = 10^5$ W

We will examine three different input signal powers, while maintaining a constant pump power and fiber length. The signal powers used in this example are $10^{-6}$, $10^{-3}$, and 10 W initially. The pump power was held constant at $10^5$ W with a fiber length of 2 m. The

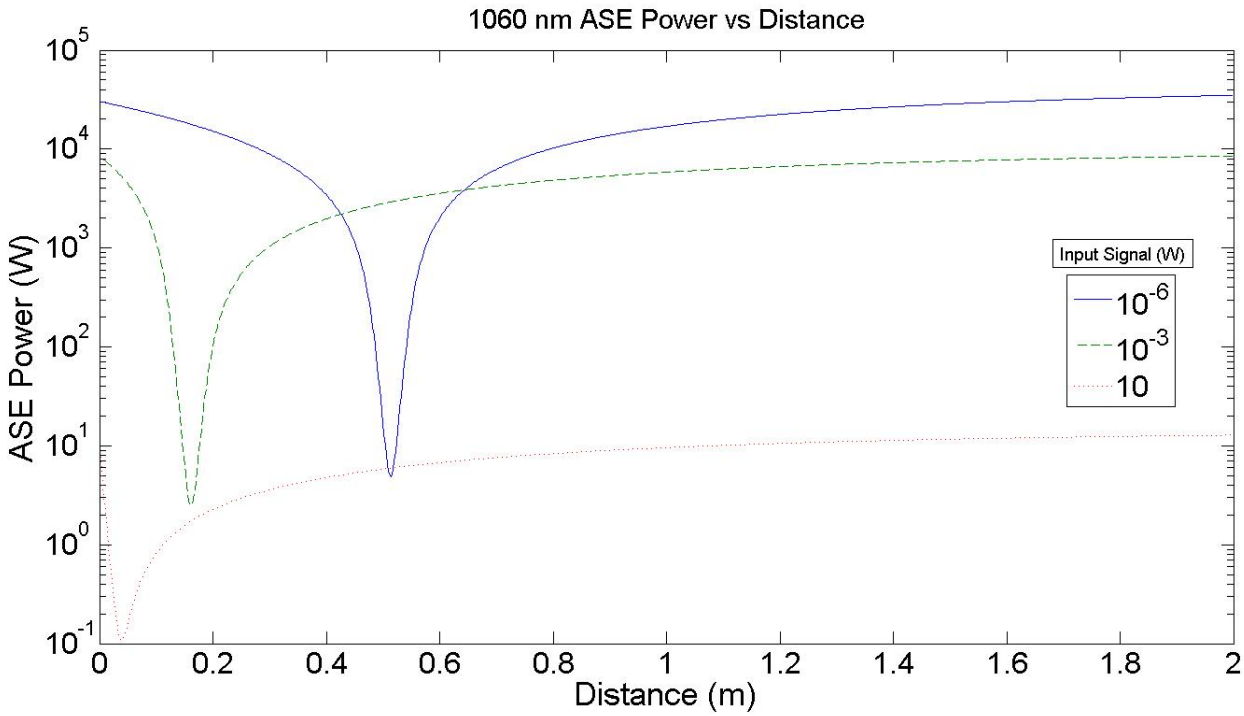


Figure 70: 1060 nm ASE vs Distance, Signal at 1060 nm, $P_p = 10^5$ W

length of 2 m was chosen because it was clear that it was not necessary to increase the fiber length beyond this to extract the maximum pump power. This is another advantage of this transition: only a short fiber length is required to obtain maximum efficiency. Figure 69 is a graph of signal power versus distance for these parameters.

As we can see, regardless of the input signal power, the signal light itself is significantly amplified. Moreover, most of the amplification occurs during the first few centimeters of the fiber. In fact, fiber lengths beyond 50 cm do not provide additional amplification. Also, for larger signal powers, the signal experiences gain saturation. Note however, that in other cases where gain saturation was observed, the input signal powers were much lower. Since the 1060 nm transition is so efficient, more pump power can be extracted from the same initial signal power in this configuration. Next, we will see how the ASE evolves in this configuration as well.

It is evident from Figure 70 that the maximum ASE power is inversely related to the input signal power. This is intuitive since the signal tends to deplete the upper state population, limiting maximum ASE growth. For smaller signal powers, the ASE at 1060 nm tends to limit the maximum signal gain. We have seen that the 1060 nm signal wavelength is extremely efficient at extracting pump power even for smaller input signals. Only short fiber lengths are required for such large gain. Finally, gain saturation is experienced for larger signal powers, but the minimum signal power for which this is observed is much smaller than in other configurations.

## 14.5 The NDFA at 910 nm

The final transition we will be examining is the ${}^4F_{3/2}$ to ${}^4I_{11/2}$ three level transition in Nd near 910 nm. This transition suffers from the same problem of ASE limitation that the 1400 nm signal wavelength does; however, the larger absolute emission cross section makes it more efficient than the 1400 nm transition. Because it is a three level transition, the 910 nm signal wavelength can experience attenuation for longer fiber lengths. This makes a careful choice of fiber length imperative for finding optimum gain. The 1060 nm ASE limits the upper state population to low values in such a short fiber length that achieving gain in this configuration is generally impossible. Therefore, we will examine this transition with no 1060 nm ASE included. To simplify the analysis of this transition, we will be comparing this transition to the 1023 nm signal wavelength in Yb. We have chosen to do this because both the 1023 nm signal in Yb and the 910 nm transition in Nd are three level transitions. Both include absorption at longer fiber lengths but relatively high emission to absorption cross section ratios.

In Figure 71, we are using $10^5$ W initial pump power and $10^{-3}$ W initial signal power. We have used the same parameters for both the 910 nm Nd amplifier and the 1023 nm Yb model. When shown together, we can see the remarkable similarities between the behavior

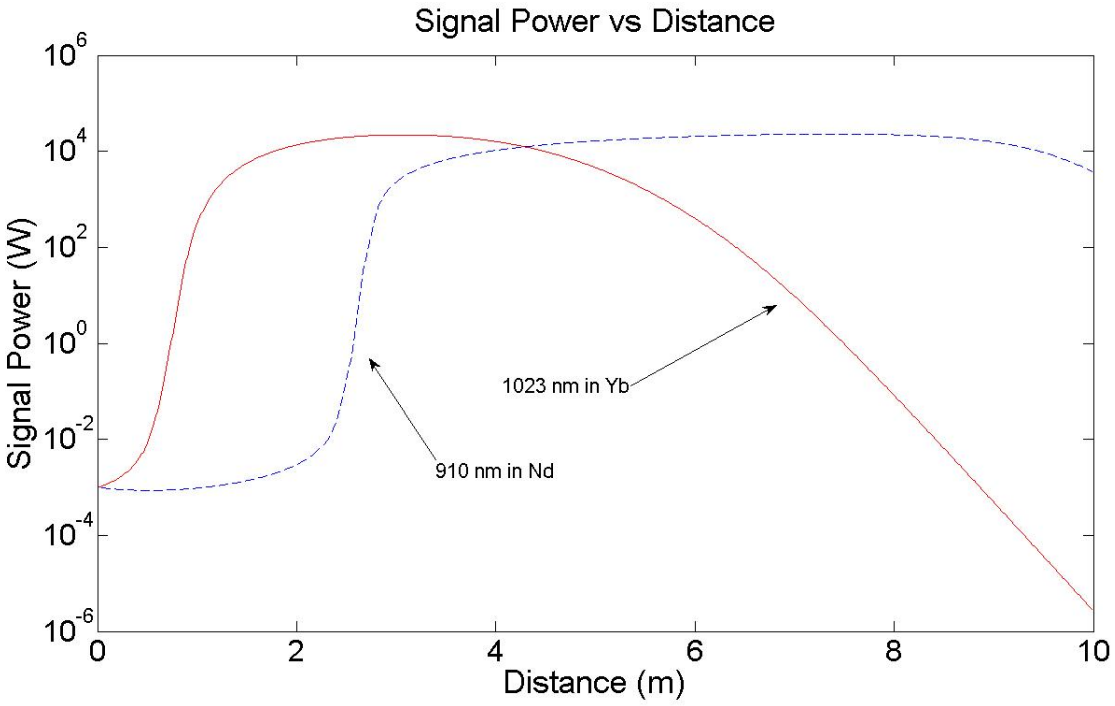


Figure 71: Comparison between 910 nm Signal in Nd and 1023 nm Signal in Yb

of these wavelengths. Both configurations exhibit periods of explosive signal growth near the beginning of the fiber, remain steady for some distance, and then become attenuated later. The 910 nm signal in Nd grows more quickly because, in Yb, the 978 nm ASE is a significant impediment to signal gain during the first 2 meters of the fiber. Later, however, the 910 nm signal in Nd also becomes attenuated more quickly and earlier than the Yb signal. This is due to the larger absorption cross section in Nd at 910 nm than in Yb at 1023 nm. Despite these differences, there are significantly more similarities. These two choices mirror each other in behavior to a remarkable degree.

## 14.6 Diffraction Gratings

A method that has been proposed to limit the effect of ASE in Nd-doped devices is the insertion of periodically placed diffraction gratings. These gratings, created by subtle changes

in the index of refraction of the glass, diffract light of specified wavelength out of the fiber. In the case of neodymium, these gratings can be designed to severely limit the growth of 1060 nm ASE. Note that diffraction gratings can only be used in the case where the significant ASE band is not at the same wavelength as the signal. This is because the grating cannot distinguish between ASE and signal light: it will diffract all light of a specific wavelength out of the fiber.

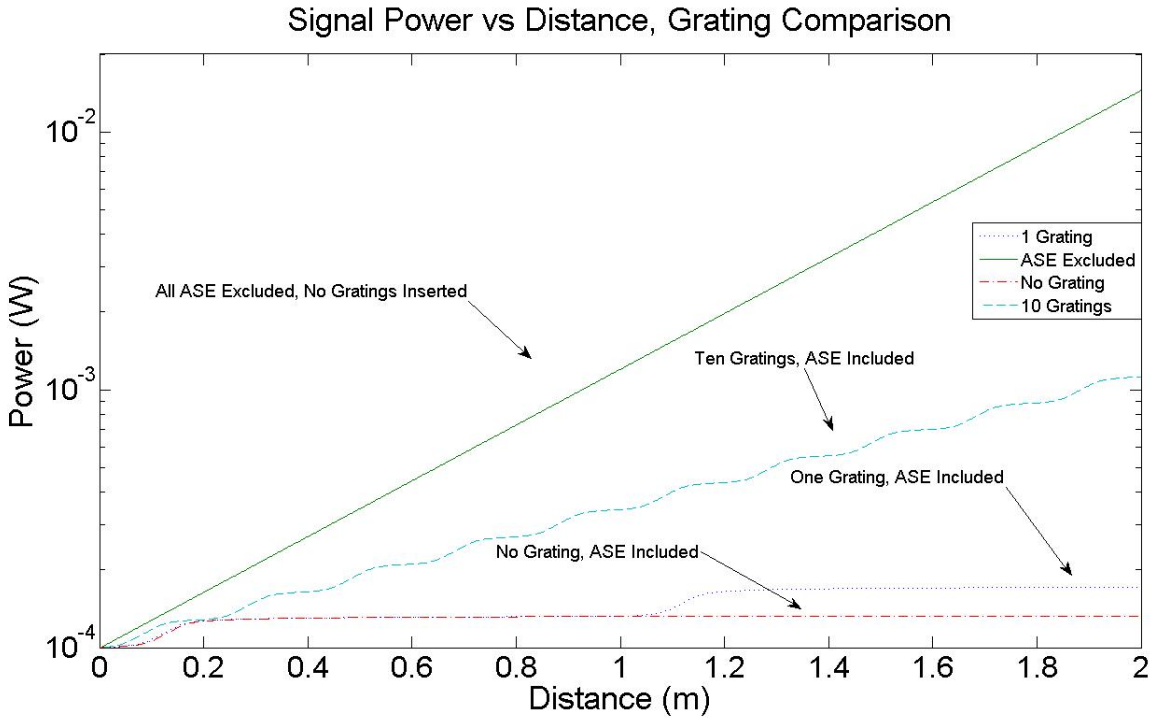


Figure 72: Signal Power vs Distance with Insertion of Diffraction Gratings, $P_p = 10^3$ W and $P_s = 10^{-4}$

In Figure 72 we investigate the effect of inserting these gratings in Nd-doped silica. The signal wavelength is chosen to be 1400 nm, with pumping at 808 nm, initial pump power of $10^3$ W, for a fiber length of 2 m. The initial signal is $10^{-4}$ W. The solid line represents the signal power as a function of distance with all ASE terms excluded. Also, the dash-dot line represents the signal power with no gratings and ASE included. These curves demonstrate

the significant effect of ASE on signal power, and also provide upper and lower bounds on the effectiveness of the diffraction gratings. We can see inclusion of one grating has a small effect on signal gain. The output signal is approximately 20 % larger when a single grating is included. On the other hand, a significant improvement is seen when gratings are placed every 20 cm. The output signal power in this configuration is much higher: 8.4 times larger than in the case with no gratings. However, it is also more than order of magnitude smaller than the ideal case (with no ASE at all). The inclusion of more gratings approaches the case without ASE at all. Therefore, we expect that greater gain would be achievable with more gratings. However, these diffraction gratings also add a scattering losses and a reflection coefficient that cannot be ignored; therefore, the optimum number of gratings cannot easily be determined.

## 14.7 Conclusions for the NDFA

We have seen that the Nd doped fiber amplifier has a wide and interesting spectrum. The 1060 nm four level transition is the strongest, with the highest emission cross section and no absorption. This is the famous Nd laser transition, used in many applications. When analyzing signal at other wavelengths in Nd, we saw that this same transition is also a source of significant and debilitating ASE. With signal at 1400 nm in Nd, this is an apparently insurmountable obstacle. Coupled with the ESA near 1300 nm, it is unlikely that the Nd doped fiber amplifier can be used as a source of light amplification near this telecommunications band without implementation of a method to limit the effect of ASE at 1060 nm. Finally, the choice of 910 nm signal can also suffer from the stringent requirements imposed by ASE at 1060 nm. Because of the nonzero absorption at this wavelength, achieving signal gain here is nearly impossible without ASE reduction. Without ASE, however, this transition behaves similarly to the 1023 nm signal in Yb that we saw earlier.

# 15 Conclusion

There have been many significant results discovered in this project due to the number of parameters that were investigated in this model. Among them, they include results in the basic derivation of the model as well as specific results from in depth experimentation with the model using varied parameters. The modeling of ASE was a particularly involved aspect of this project.

The equivalent bandwidth method was investigated as a potential approximation designed to improve the efficiency of more computationally intensive modeling. We have found that the approximation has a significant number of caveats that make its accurate application very case specific. In particular, the pure equivalent bandwidth method fails when applied to three level transitions or, to a lesser degree, four level transitions with broad linewidth. However, a more accurate method, while still keeping in the concept of the equivalent bandwidth method, is to implement a two bin method for three level transition cases such as the ytterbium doped fiber amplifier. In general, we have found the inaccuracies implicit in these approximations to be inadequate in many cases. Therefore, a more straightforward method of ASE computation was implemented that more closely followed the methods used in the published literature.

We also investigated the possibility of achieving signal gain at three different wavelengths in Yb: 978, 1023, and 1060 nm. In the case of signal wavelength of 978 nm, significant gain is achievable only in very short fiber lengths due to rapid reabsorption of signal power into the fiber. The 1060 nm option is appealing in that it is transparent to the fiber; however, its low absolute emission cross section makes it inefficient in converting pump energy to signal energy. Particularly since the Nd-doped fiber amplifier provides a dramatically greater potential for signal gain at 1060 nm, the Yb option is of little interest. Of most appeal is the 1023 nm choice for signal wavelength in Yb. The high emission cross section, coupled with

low absorption at this wavelength implies signal gain is readily achievable even for lower pump powers. In order to compete with ASE at 978 and 1023 nm, the fiber length must be chosen carefully to access optimum signal gain.

Finally, the Nd doped fiber amplifier has garnered increased attention in recent years because of the requirement for signal amplification near the 1300 nm telecommunications band. However, the immediate insurmountable problem of excited state absorption in our considered glass host effectively removes the possibility of achieving gain near 1300 nm. Instead, we examined the potential for signal gain near 1400 nm, outside the affected wavelength range. We demonstrated that, even in the absence of ESA, the monolithic ASE near 1060 nm is a serious impediment to signal gain. The large emission cross section of this four level transition implied that extremely high pump powers were required to achieve even moderate gain. We showed that through the implementation of selective gratings designed to limit ASE at 1060 nm, we were able to achieve significant gain compared to devices without this feature.

# References


[1] Richard S. Quimby, *Photonics and Lasers: An Introduction*, Wiley-Interscience, New Jersey, (2006).

[2] Michel J. F. Digonnet, *Rare-Earth-Doped Fiber Lasers and Amplifiers*, Marcel Dekker, New York, (1993).

[3] Anders Bjarklev, *Optical Fiber Amplifiers: Design and System Application*, Artech House, Boston, (1993).

[4] Rudiger Paschotta, *Ytterbium-Doped Fiber Amplifiers*, IEEE Journal of Quantum Electronics, Vol. 33, No. 7, July, (1993).

[5] Mikko Soderlund, *A Model of Erbium-Doped Fiber Amplifier Gain Dynamics*, Physica Scripta, Vol. T79, 149-151, (1999).

[6] Turan Erdogan, *Fiber Grating Spectra*, Journal of Lightwave Technology, Vol. 15, No. 8, August, (1997).

[7] Nicholas Verlinden, *The Excited State Absorption of Nd-Doped Silica Glass Fibers in the 1200-1500 nm Wavelength Range*, Worcester Polytechnic MS Thesis, July, (1998).

[8] Jonathan R. Armitage, *Three-level Fiber Laser Amplifier: A Theoretical Model*, Applied Optics, Vol. 27, No. 8, December, (1988).

[9] C. Henry Edwards, *Calculus. Early Transcendentals Version*, Prentice Hall, New York, (2002).

[10] Michel J. F. Digonnet, *Theoretical Analysis of Optical Fiber Laser Amplifiers and Oscillators*, Applied Optics, Vol. 24, No. 3, December, (1985).

[11] P. R. Morkel, *Theoretical Modeling of Erbium-Doped Fiber Amplifiers with Excited State Absorption*, Optical Society of America Optics, (1989).

[12] Michel J. F. Digonnet, *Closed-Form Expressions for the Gain in Three and Four-level Laser Fiber*, IEEE Journal of Quantum Electronics, Vol. 26, No. 10, July, (1990).

[13] A. A. M. Saleh, *Modeling of Gain in Erbium-Doped Fiber Amplifers*, IEEE Journal of Quantum Electronics, Vol. 2, No. 10, September, (1990).

[14] C. Randy Giles, *Modeling Erbium-Doped Fiber Amplifers*, IEEE Journal of Quantum Electronics, Vol. 9, No. 2, May, (1991).

[15] Athanasios Laliotis, *Model Signal an ASE Evloution in Erbium-Doped Amplifiers with the Method of Lines*, IEEE Journal of Quantum Electronics, Vol. 24, No. 3, March, (1990).

[16] Emmanuel Desurvire, *Amplification of Spontaneous Emission in Erbium Doped Single-Mode Fiber*, IEEE Journal of Quantum Electronics, Vol. 7, No. 5, May, (1989).

[17] Amos Hardy, *Signal Amplification in Strongly Pumped Fiber Amplifiers*, IEEE Journal of Quantum Electronics, Vol. 33, No. 3, March, (1997).

[18] W. J. Miniscalco, *1.3 micron Fluoride Fiber Laser*,Electron, Lett. 24:28-29 (1988).

[19] Y. Miyajima, *1.31-1.36 micron Optical Amplification in a Nd-Doped Fluorozirconate Fibre*,Electron, Lett. 26:194-195 (1988).

[20] T. Sugawa, *10 dB Gain and High Saturation power in a Nd-Doped Fluorozirconate Fibre Amplifier*,Electron, Lett. 24:28-29 (1988).

[21] Y. Ohishi, *Pr-Doped Fluoride Fiber Amplifier Operating at 1.31 microns*,Electron, Lett. 24:28-29 (1988).

[22] Y. Ohishi, *Recent progress in 1.3 micron fiber amplifiers*,Proc. Opt. Fiber Commun.. 2:27 (1996); TuG1.

[23] M. Yamada, *Gain Characteristics of Pr3+-doped fluoride fiber amplifier.*,Electron. Commun. Japan. 77 (Part 2):75 - 87 (1997)

[24] M. Yamada, *Gain vs wavelength of 1.3 micron-band fluoride fiber amplifier*, Institute of Electron., Inform. Commun. Eng., general spring conference (IEICE), 1994; c-395